

Role of Galectin-3 in Melanoma Progression

A

DISSERTATION

Thesis Submitted for a Doctoral degree in Human Biology
at the Faculty of Medicine Ludwig-Maximilians- University,
Munich, Germany

Alexandra Anastasia Mourad-Zeidan, B.S., Diplom Biol. M.S.

Munich, Germany

2008

Aus dem Institut für Immunologie
der Ludwig-Maximilians-Universität München
Vorstand: Prof. Thomas Brocker

Role of Galectin-3 in Melanoma Progression

Dissertation

zum Erwerb des Doktorgrades der Humanbiologie
an der Medizinischen Fakultät der
Ludwig-Maximilians-Universität zu München

vorgelegt von

Alexandra Anastasia Mourad-Zeidan, B.S., Diplom Biol. M.S

aus

München, Deutschland

Jahr

2008

**Mit Genehmigung der Medizinischen Fakultät
der Universität München**

Berichterstatter: **Prof. Judith P. Johnson**

Mitberichterstatter: **Priv. Doz. Dr. Barbara Mayer**
Prof. Dr. Dolores J. Schendel

**Mitbetreuung durch den
promovierten Mitarbeiter:**

Dekan: **Prof. Dr. med. Dr. h.c. M. Reiser, FACR, FRCR**

**Tag der mündlichen
Prüfung:** **12. 12. 2008**

Dedication

To my wonderful son,
Joseph Adrian Zeidan,
a present of God.

Table of Contents

Dedication	iii
Table of Contents	iv
List of Figures	ix
List of Tables	xii
Chapter I:	1
1. Introduction.....	1
1. 1 Melanoma Incidence and Risk Factors	1
1.1.1 Stages and Diagnosis of Melanoma Development	2
1.1.2 Common cutaneous melanomas	4
1.1.3 Therapy for metastatic melanoma.....	5
1.1.4 Molecular changes associated with melanoma progression	7
1.1.4.1 Inactivation of tumor suppressors INK4A/ARF, p53, PTEN and activating mutations in BRAF and N-Ras in melanoma.....	8
1.1.4.2 Melanoma Progression from RGP to VGP	11
1.1.4.5 Matrix Metalloproteinases (MMP)	16
1.1.4.6 Angiogenic factors	16

1.2 Galectin-3.....	18
1.2.1 Gal-3 intracellular functions	19
1.2.2 Gal-3 extracellular functions.....	23
Specific Aims.....	26
Chapter II:	27
2. Materials and Methods.....	27
2.1 Cell Lines and Culture Conditions.....	27
2.2 Three-dimensional Type-I Collagen Gels.....	28
2.3 Animals	29
2.4 Cell Preparation for Injection.....	29
2.5 Injection and Monitoring of Tumor Cells.....	30
2.6 In Vitro Proliferation Assay.....	31
2.7 Antibodies.....	31
2.8 Protein Extraction	32
2.9 Western Immunoblot Analysis	33
2.9 Expression Constructs.....	34
2.10 Transient Transfections and Luciferase Activity Assays.....	36

2.11 Stable Transfection with small hairpin RNA Lentivirus Expression Vectors	36
2.11.1 shRNA expression vector construction.....	36
2.11.2 Cell sorting with Flow Cytofluorometry.....	37
2.11.3 Recombinant lentivirus production.....	38
2.11.4 Target cell transduction.....	42
2.12 Zymography.....	42
2.13 Invasion Assay through Matrigel.....	43
2.14 RNA Extraction	43
2.15 RT-PCR.....	44
2.16 Tissue Microarray (TMA).....	44
2.17 Immunohistochemical Analysis.....	47
2.18 Immunofluorescence Staining	48
2.19 In situ Terminal dUTP Nick End Labeling (TUNEL) Assay	49
2.20 Enzyme-Linked Immunosorbent (ELISA) Assay.....	50
2.21 cDNA Microarray Analysis	51
2.22 Chromatin Immunoprecipitation (ChIP) Assay.....	51
2.23 Densitometric Quantification.....	53

2.24 Statistical Analysis.....	53
Chapter III:.....	55
3. RESULTS	55
<u>3.1 Specific Aim I:</u>	55
3.1.1. Pattern of Gal-3 expression during melanoma progression.....	55
3.1.1.1 Tissue microarray analysis.....	55
<u>3.2 Specific Aim II:</u>	67
3.2.1 Effect of Gal-3 shRNA on tumor growth and metastasis in vivo.....	67
3.2.1.1 Expression of Gal-3 in melanoma cell lines	67
3.2.1.3 Effect of Gal-3 downregulation on tumor growth in vivo	70
3.2.1.4 Effect of Gal-3 downregulation on metastasis in vivo.....	76
3.2.1.5 Effect of Gal-3 downregulation on in vivo cell proliferation, microvessel density (MVD) and apoptosis	80
<u>3.3 Specific Aim III:</u>	87
3.3.1 Identification of novel Gal-3 downstream target genes by Gal-3 small hairpin RNA	87
3.3.1.1 Determining novel genes possibly regulated by Gal-3 via a cDNA microarray analysis	87

3.3.1.2 Validation of target genes after Gal-3 shRNA knockdown in highly metastatic melanoma cell lines	90
3.2 Effect of Gal-3 shRNA on VE-Cadherin (CDH5) expression and function.....	92
3.3 Effect of Gal-3 shRNA on IL-8 expression	99
3.3.2.1 Effect of Gal-3 downregulation on the MMP-2 expression.....	103
3.3.2.2 Effect of Gal-3 downregulation on the in vitro tumor cell invasion.....	107
Chapter IV:.....	110
4. Discussion	110
Summary	131
Zusammenfassung.....	134
List of Abbreviations	137
References.....	146
Acknowledgement	164

List of Figures

<i>Figure 1 Schematic of molecular changes associated with the progression of human melanoma.....</i>	<i>9</i>
<i>Figure 2 Vasculogenic mimicry observation in 3-D collagenase culture.</i>	<i>15</i>
<i>Figure 3 Galectin subunit types.....</i>	<i>20</i>
<i>Figure 4 Gal-3 intracellular and extracellular ligands and related functions.....</i>	<i>22</i>
<i>Figure 5 Schematic of Lentiviral production.....</i>	<i>39</i>
<i>Figure 6 pLV-THM vector construct.</i>	<i>40</i>
<i>Figure 7 Forward and reverse target oligo sequences for direct cloning of the shRNA into the pLV-THM lentiviral vector.</i>	<i>41</i>
<i>Figure 8 Three progression tissue microarray blocks of melanocytic lesions.</i>	<i>46</i>
<i>Figure 9 Gal-3 expression in benign nevi (BN), dysplastic nevi (DN), melanoma (MM), and metastatic melanoma (MMM).</i>	<i>57</i>
<i>Figure 10 Gal-3 expression in primary and metastatic melanoma.</i>	<i>61</i>
<i>Figure 11 Gal-3 expression subclassified into sun-exposed areas in primary melanoma.....</i>	<i>62</i>
<i>Figure 12 Gal-3 expression in different types of metastatic lesions.....</i>	<i>64</i>

<i>Figure 13 Disease free survival analysis and nuclear / cytoplasmic ratio of Gal-3 expression</i>	65
<i>Figure 14 Gal-3 expression in melanoma cell lines.</i>	68
<i>Figure 15 Immunofluorescence staining for Gal-3 expression in low to high metastatic cell lines.</i>	69
<i>Figure 16 Gal-3 protein expression following downregulation with short hairpin RNA using lentiviral delivery.</i>	71
<i>Figure 17 Effect of Gal-3 knockdown on tumor growth in vivo after s.c. injection.</i> .	72
<i>Figure 18 Luciferase Imaging with IVIS technology in vivo of the luciferase-labeled C8161 tumor cells after s.c. injection.</i>	73
<i>Figure 19 Luciferase Imaging with IVIS technology in vivo of the Luciferase-labeled C8161 tumor cells after i.v. injection.</i>	78
<i>Figure 20 Immunohistochemical staining of in vivo s.c. tumors for H&E, Gal-3, cell proliferation (PCNA), apoptosis (TUNEL), microvessel density (MVD), IL-8 and MMP-2 expression.</i>	82
<i>Figure 21 Quantitative measurement of cell proliferation (PCNA), apoptosis (TUNEL) and microvessel density.</i>	83
<i>Figure 22 Western Blot validation of novel downstream targets of Gal-3 after cDNA microanalysis.</i>	91
<i>Figure 23 Analysis of the CDH5 promoter activity after Gal-3 knockdown.</i>	93

Figure 24 Chip analysis of CDH5 transcription binding site for EGR1..... 94

List of Tables

<i>Table 1 Melanocytic Lesions included in the tissue microarray</i>	<i>56</i>
<i>Table 2 Cytoplasmic and Nuclear Expression Levels of Gal-3.</i>	<i>59</i>
<i>Table 3 Luciferase light absorbance data of Gal-3 shRNA versus NT shRNA tumor cells after s.c. injection.</i>	<i>75</i>
<i>Table 4 Mouse lung melanoma metastasis model after i.v. injection of Gal-3 shRNA and NT shRNA C8161 tumor cells.</i>	<i>77</i>
<i>Table 5 Luciferase light absorbance data of Gal-3 shRNA versus NT shRNA tumor cells after i.v. injection.</i>	<i>79</i>
<i>Table 6 List of down- and upregulated genes after Gal-3 knockdown identified after cDNA microarray analysis.</i>	<i>89</i>

Chapter I:

1. Introduction

1. 1 Melanoma Incidence and Risk Factors

The increase in incidence of melanoma over the past thirty years is higher than any other cancer, with annual incidences reaching 3–7% among fair-skinned populations (Hall et al. 1999; Brochez & Naeyaert 2000; Jean & Bar-Eli 2000; Ries LAG 2003; Jemal et al. 2007). Although part of this increase may be due to heightened awareness or changes in diagnostic criteria, there also seems to be an actual increase in disease incidence itself (Dennis 1999). An estimated 60,000 new cases of melanoma are diagnosed each year with more than 8,000 annual deaths in the United States; about one in 75 persons will develop this cancer in their lifetime (Chatelain et al. 1999; Jemal et al. 2007). Patient survival can be high, if the disease is diagnosed in early, non-metastatic stages, but later stages and particularly those associated with distant metastasis to the brain, lung or bone lead directly to short-term survival (Motzkin et al. 1992; O'Day et al. 2002). Despite the increased worldwide incidence of melanoma, the underlying biology of this disease is still not well understood.

Risk factors for melanoma are numerous. Genetic predisposition and exposure to factors in the environment represent, as for most cancers, the most serious risk factors in human melanoma. About 5-12% of all cases of melanoma originate in patients with a strong family history of this malignancy (Haluska & Hodi 1998; Goldstein & Tucker 2001). Environmental exposure to factors such as UV, as found in patients with a history of severe sunburns, represent a major cause of melanoma and, understandably, areas with high UV exposure such as the upper body show the greatest incidence of lesions (Holman

et al. 1983; Elwood & Jopson 1997; Jhappan et al. 2003). Data suggest that patients with a familial history of melanoma who sustained childhood sunburns are at critical risk to develop melanoma (Veierod et al. 2003), as genetically predisposed melanomagenesis could be promoted by exposure to burning doses of UV radiation in this group (Holman et al. 1983; Whiteman et al. 2001).

The link between UV radiation and development of melanoma has been heavily studied and early inquiries as to mechanism revealed associations between UV exposure and the occurrence of activating N-Ras mutations in lesions present on sun-exposed skin (van 't Veer et al. 1989). Significant data to understand the effect of UV radiation of the development and progression of melanoma has been gathered from the use of mouse models of this disease (Kusewitt & Ley 1996; Chin et al. 1998; Ley 2002). The mouse currently represents the best available animal model in cutaneous malignant melanoma and exposure of mice to UV radiation clearly induces the formation of primary lesions (Romerdahl et al. 1988; Romerdahl et al. 1989). Incidence and outgrowth of melanocytic lesions is enhanced when melanoma cells are transplanted by injection into the skin of UV-irradiated mice (Donawho & Kripke 1991; Donawho et al. 1994), indicating a role for immune surveillance.

1.1.1 Stages and Diagnosis of Melanoma Development

Development of melanoma occurs through a series of discrete clinically and histologically transformative stages. Pigment-producing cells derived from the neural crest called melanocytes are localized along the dermal-epidermal border as individual cells and, in the first stage of melanoma progression, these cells give rise to the formation of melanocytic nevi (Clark et al. 1984; Friedman & Heilman 2002). These nevi represent focal proliferation of benign cells, each of which may or may not progress further. These

nevi represent a risk factor on their own, as approximately 25% of melanomas originate directly from these preexisting nevi (Bevona et al. 2003). Second-stage transformation is associated with the formation of dysplastic lesions formed by abnormal cell growth, called hyperplasia, and atypical differentiation of these cells. Dysplastic lesions, known as melanoma precursors, can form out of benign lesions or form as normal nevic tissue (Clark et al. 1984). The presence of dysplastic nevi is an indication of high-risk development of primary melanoma (Garbe et al. 1994a, b; Titus-Ernstoff et al. 2005). Stage III of melanoma progression is known as the radial growth phase (RGP) where primary tumors spread superficially but are unable to compromise the surrounding stroma and cannot yet metastasize (Clark et al. 1984). Left untreated, melanoma in the RGP will likely enter the last step of melanoma tumor progression, known as the vertical growth phase (VGP). Once melanoma enters the VGP, it acquires metastatic potential, is able to invade surrounding stroma, and proliferates vertically through the epidermal layers, leading ultimately to the appearance of regional and distant metastases (Clark et al. 1984).

Through a distinct biopsy, which analyzes excised tissues from the epidermis, dermis, and subcutaneous layers of the skin, an estimation of the depth of penetration of the melanoma is made possible by microscopy. The lesion is described by Clark's level (involvement of skin structures) and Breslow's depth (measured in millimeters) (Balch et al. 2001a; Balch et al. 2001b). Clark Level I includes all tumors considered that are localized above the basement membrane of the skin (malignant melanoma in situ). The invaded tumor into the papillary dermis, which extends around the skin appendages, is described as Clark Level II. Clark Level III sets the standard for a tumor progression into the interface between papillary and reticular dermis. The Clark Level IV describes the tumor between the layers of collagen of reticular dermis. Tumor invasion from the subcutaneous tissue into the lower layers of the dermis in accomplishment of metastases

formation are specified as Clark Level V (Balch et al. 2001a; Balch et al. 2001b). Furthermore, melanoma staging is made upon the Clark Levels and Breslow thickness, which further defines the measurement of the depth of invasion by measuring the tumor thickness in millimeters (thin: < 0.75 mm depth of invasion; intermediate: 0.76 - 3.99 mm depth of invasion; thick: > 4 mm depth of invasion) (Breslow 1970). The different stages of melanoma are set upon those classifications (Balch et al. 2001a; Balch et al. 2001b; Greene 2002).

1.1.2 Common cutaneous melanomas

There are different forms of melanoma, some of which produce melanin and appear dark in color, whereas others are amelanotic and light in color. The melanin producing types of melanoma belong to the superficial spreading melanoma (SSM), nodular melanoma, acral lentiginous melanoma, and lentigo maligna melanoma groups. Approximately 70% of melanomas are considered cutaneous melanoma SSM, this disease evolves from a precursor lesion, usually a dysplastic nevus, otherwise it arises in previously normal skin. This form of melanoma is most common in Caucasians, is often diagnosed on the backside in males or on the lower limbs in females, on sun-exposed skin and particularly on areas of intermittent sun exposure (Newell et al. 1988; Brochez & Naeyaert 2000). Nodular melanoma, a type of lesion that exclusively grows in the vertical direction, accounts for 5% of melanomas. It has no known precursor, and is described as a small black, or, if amelanotic, pink nodule lesion, which enlarges with tendency of bleeding (Bondi & Clark 1980; Feibleman et al. 1980). It is found primarily on the trunk or limbs of male patients with older age (Barnhill & Mihm 1993; Cox et al. 1996). The Acral-lentiginous melanoma (ALM) is mostly localized on non-hair bearing surfaces of the body which are likely exposed to sunlight, and usually involves glabrous

skin and adjacent skin of the digits, palms and soles (Feibleman et al. 1980; Sondergaard & Olsen 1980; Paladugu et al. 1983; Slingluff et al. 1990; Wells et al. 1992; Barnhill & Mihm 1993; Boyd & Rapini 1994; Cascinelli et al. 1994; Perniciaro 1997; Reed & Martin 1997). It represents only 5% of all melanomas and predominantly afflicts Asian, Hispanic and African populations (MacKie 1985; Kato et al. 1996; Chen et al. 1999; Barnhill RL 2004; Luk et al. 2004; Curtin et al. 2005). Lentigo maligna accounts 4-15% of all cutaneous melanoma, which is defined as a melanoma in situ and consists of malignant cells without ability of invasiveness (Clark & Mihm 1969). It is common in the elder population on visceral high sun exposed skin areas, like the face and forearms (Clark & Mihm 1969; Koh et al. 1984; McGovern et al. 1986; Cox et al. 1996; Flotte & Mihm 1999; Crowson AN 2001).

1.1.3 Therapy for metastatic melanoma

Standard therapy for metastatic disease is systemic chemotherapy with agents such as the alkylating agent dacarbazine (DTIC) or cisplatin (Mandic et al. 2001). Dacarbazine (5-3, 3- dimethyltriazeno-imidazole-4- carboxamide) is the primary chemotherapeutical drug used for Stage IV melanomas and is administered parenterally. After undergoing metabolic changes in the liver through interaction with cytochrome P₄₅₀ to its active metabolite 5-(3-methyl-1-triazeno)-imidazole-4-carboxamide, DTIC spontaneously exerts to the major metabolite 5-aminoimidazole-4-carboxamide. Half of it is secreted through the kidneys into the urine (Carter & Friedman 1972). This alkylating drug then binds to the DNA, eliciting a clinical response rate of 22% (Bellett et al. 1976). But metastatic melanoma has a well-known resistance to chemotherapy, which often hinders effective treatment of this disease (Lev et al. 2004; Melnikova & Bar-Eli 2006). Lev et al. generated dacarbazine-resistant cell lines to analyze the role of DTIC in

metastasis and tumor growth *in vivo* and its long term effects. These were generated in the primary cutaneous melanoma cell lines MeWo and SB2 through repeated exposure to increasing concentrations of dacarbazine (Lev et al. 2004). In nude mice, these dacarbazine-resistant cell lines displayed signs of exhibited increased tumor growth and metastatic behavior. In comparison to the parental counterparts, *in vivo* tumors produced by SB2-D and MeWo-D were found to have more MMP-2, VEGF, IL-8, and microvessel density (CD31), as well as high levels of phosphorylation in the protein kinases ERK, RAF and MEK (Lev et al. 2004).

These results suggest a substantial danger with decarbazine treatment in that a more aggressive melanoma phenotype could be selected in melanoma patients treated with the drug. However, using a combination treatment of either MEK inhibitors or anti-VEGF/IL-8, may increase the therapeutic effects of dacarbazine.

Cisplatin treatment of melanoma cells has been shown to induce ERK activation. Additionally, increased cisplatin resistance occurred in human melanoma cells via overexpression of mutant N-ras (and subsequent activation of MAPKs). This resulted in inhibition of cell death by inducing overexpression of the anti-apoptotic protein bcl-2 (Jansen et al. 1997; Borner et al. 1999). However, studies using the ERK inhibitor PD 98059 only resulted in sensitization of melanoma cells to cisplatin treatment in a limited number of cell lines (Mandic et al. 2001).

When using MAPK inhibitors to sensitize cells to chemotherapeutic drugs, one of the issues to bear in mind is that apoptosis effector proteins such as Apaf-1, are frequently lost in metastatic melanomas (Soengas et al. 2001). This could result in chemoresistant in cells even if survival signals are abrogated.

Immunotherapy with Interleukin-2 (IL-2) or interferon is also used, alone or in combination with chemotherapy, but the overall success of these therapies in melanoma

has been limited to date, around 10-15% (Atkins 2006; Atkins et al. 2006; Kirkwood et al. 2006; Sondak et al. 2006; Tagawa et al. 2006).

Combination therapies, known as biochemotherapy, of biological effectors (IL-2 and Interferon alpha) with chemotherapeutic reagents (cisplatin, vinblastin, and DTIC) are used currently (Buzaid et al. 1994c; Buzaid & Legha 1994; Buzaid et al. 1994a, b; Legha et al. 1996; Atkins 1997; Legha 1997; Legha et al. 1997; Legha et al. 1998) and have produced a striking response rate in the range of 69% (Legha et al. 1996).

Alternative approaches have evaluated vaccination against key antigens driving melanoma invasion and metastasis with mixed results. These approaches are currently in the experimental phase (Kirkwood et al. 2006; Sondak et al. 2006; Leslie et al. 2007). The most current therapeutic vaccine for melanoma is the polyvalent allogeneic whole-cell vaccine (PACV). It is derived from three different allogeneic melanoma cell lines and used in combination with an immune adjuvant (Detox-PC). PACV is designed to target multiple antigens and has shown a 5-year survival rate compared to historical use of vaccines (39% versus 19%) (Hsueh et al. 2002).

Melanoma is highly radioresistant (Ang et al. 1990; Ang et al. 1994; Geara & Ang 1996; Amozorrutia-Alegria et al. 2002; Ballo et al. 2002b; Ballo et al. 2002a; Ballo & Ang 2003, 2004; Ballo et al. 2004; Ballo et al. 2005; Ballo et al. 2006). Radiation therapy is only successfully used in primary treatment of ocular, nodular and lentigo maligna melanoma (Harwood & Lawson 1982; Tsang et al. 1994; Schmid-Wendtner et al. 2000).

1.1.4 Molecular changes associated with melanoma progression

The progression of melanocytic nevi to the vertical growth phase (VGP) and the formation of distant metastases involve many genetic and molecular changes, the

mediating mechanisms are largely undefined. Involved in the initiation and progression of malignant melanoma are tumor suppressor genes (p16 INK4a/p14ARF, PTEN and p53), transcription factors (CREB/ ATF-1, AP-2), oncogenes (BRAF, NRAS), tyrosine kinases (c-kit, PDGF receptors), cell adhesion molecules (E-cadherin) and Matrix Metalloproteinases (MMP-2) (Carr & Mackie 1994; Jafari et al. 1995; Reed et al. 1995; Weiss et al. 1995; Barnhill et al. 1996; Bar-Eli 1999b; Hofmann et al. 1999; Bar-Eli 2001; Deichmann et al. 2002; Shen et al. 2003; Tsao et al. 2004). These genetic alterations are summarized in Figure 1.

1.1.4.1 Inactivation of tumor suppressors INK4A/ARF, p53, PTEN and activating mutations in BRAF and N-Ras in melanoma

In approximately 20-30% of familial melanoma and 15-30% of sporadic melanomas, an inactivation of the INK4a/ARF melanoma susceptibility locus has been identified (Haluska & Hodi 1998). Two independent *bona fide* tumor suppressor proteins are encoded by the INK4a/ARF locus, where one functions as a growth inhibitor (cyclin dependent kinase (CDK) inhibitor p16^{INK4a}) and the other one as an effector of cellular senescence (p53 activator p14^{ARF} (mouse p19^{Arf})). A similar frequency of deletions and

LOH (loss of heterozygosity) alterations in matched primary or metastatic melanoma have been reported by many (Chang et al. 1997; Talve et al. 1997; Cachia et al. 2000; Palmieri et al. 2000; Straume et al. 2000; Vuhahula et al. 2000; Pollock et al. 2001; Pavey et al. 2002; Ghiorzo et al. 2004).

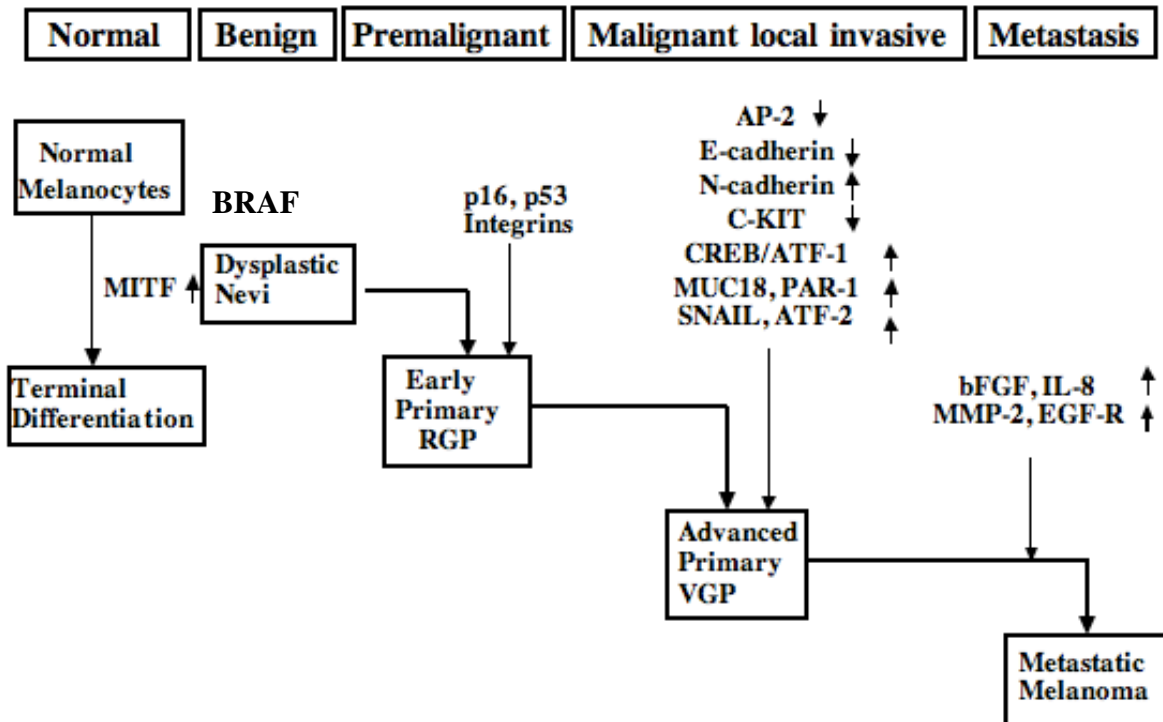


Figure 1 Schematic of molecular changes associated with the progression of human melanoma.

Activating mutations in BRAF or N-Ras are early events in melanoma. Abnormalities in the p16INK4A/ARF gene also occur early during melanoma development. Changes in E-cadherin, c-KIT, MUC18, and integrin $\alpha\beta 3$ expression occur during the transition from early primary radial growth phase (RGP) to the malignant stage of vertical growth phase (VGP). Genes, important for angiogenesis are upregulated with higher metastatic potential of melanoma, including VEGF, bFGF, MMP-2, and IL-8 (Melnikova & Bar-Eli 2006)

The latent, short-lived transcription factor and tumor suppressor protein, p53 (Harris & Hollstein 1993), activates proteins important in mechanisms of DNA repair, cell cycle, and/or programmed cell death. Conversely, p53 can also repress the transcriptional activation of genes important to cell growth and survival (Ko & Prives 1996; Levine 1997; Jin & Levine 2001; Sherr & McCormick 2002). p53 mutations have been found to be present in approximately 10-30% of cultured human melanoma cell lines (Volkenandt et al. 1991; Weiss et al. 1993; Albino et al. 1994; Montano et al. 1994), and analysis of melanoma tumor tissues have revealed a 0-25% frequency of p53 mutation (Albino et al. 1994; Lubbe et al. 1994; Sparrow et al. 1995; Hartmann et al. 1996; Papp et al. 1996). Patients with UV induced melanoma and defective DNA repair show a 60% high mutation rate in p53 (Spatz et al. 2001), which reveals that p53 is important in the UV induction which leads to apoptosis in melanoma (Zhang 2006). Furthermore, p53-stabilizers have proven to significantly induce UVB-induced apoptosis (Luu & Li 2002). Overall, p53 has a low frequency of mutations in human melanoma.

Another alteration that occurs early in melanoma progression affects the tumor suppressor PTEN (*phosphatase and tensin homolog*), inactivation of which occurs in approximately 40% of both primary and metastatic lesions (Rodolfo et al. 2004). The tumor suppressor PTEN activates throughout a lipid phosphatase the PI3K/AKT pathway and regulates G1 progression and apoptosis, whereas by protein phosphatase activity PTEN inhibits MAPK signaling (Wu et al. 2003). Loss of PTEN has been observed within 5-15% of melanoma specimens/metastases and in 30-40% in established melanoma cell lines (Guldberg et al. 1997; Teng et al. 1997). Subsequent AKT activation as a result of loss of PTEN may be an early marker for malignant progression of melanoma. Activation of AKT has numerous downstream effects that may be critical to malignant progression such as upregulation of nuclear factor kappa B (NFκB) leading to

control of the cell cycle, inflammatory and survival cytokine signaling downstream (Dhawan et al. 2002).

Global molecular profiling of cancer recently revealed oncogenic somatic mutations in the BRAF gene in approximately 66% of primary sporadic human melanomas, compared to lower rates of BRAF mutation in other cancers (Pollock et al. 1996; Brose et al. 2002; Davies et al. 2002; Rajagopalan et al. 2002; Cohen et al. 2003; Dong et al. 2003; Gorden et al. 2003; Weber et al. 2003; Xu et al. 2003). An estimated 70-80% of the total mutations were identified as a V600E (formerly recognized as V599E) (exon 15) single phosphomimetic substitution in the kinase activation-domain, whereas mutations in NRAF are fairly uncommon in nevi (5.10%) (Brose et al. 2002; Davies et al. 2002). A serine/threonine kinase encoded by the BRAF gene activates ERK/MAPK cascade signaling upon phosphorylation by Ras, which leads to the key influence of cell growth and proliferation downstream (Lenormand et al. 1993; Treisman 1994; Davies et al. 2002; Rajagopalan et al. 2002). An interesting observation by Omholt et al. obtained through sequencing of BRAF mutations in exon 11 and exon 15 as well as N-Ras mutations in codon 61 in both primary melanoma and corresponding distant metastases in over 70 patients, revealed that they arise early during melanoma pathogenesis and are preserved throughout tumor progression, indicating they are a key pathological event (Omholt et al. 2003).

1.1.4.2 Melanoma Progression from RGP to VGP

Conversion to a metastatic phenotype is a multistep process that requires cells to acquire an invasive phenotype, to survive in the lymph/blood, and be able to produce tumors in a new environment. This complex conversion requires the recruitment of adhesion molecules, matrix-degrading enzymes, motility factors and cytokines, growth

factors, together with their receptors to achieve an aggressive profile. Previous study of metastatic conversion of melanoma has revealed key changes, which involve the downregulation of E-cadherin, and coordinate upregulation of adhesion proteins N-cadherin, upregulation of the melanoma cellular adhesion molecule (MCAM) and protease-activated receptor-1 (PAR-1). Additionally, activation of matrix metalloproteinases such as Matrix-Metalloproteinase 2 (MMP-2), and upregulation of Epidermal Growth Factor Receptor (EGFR), Basic Fibroblast Growth Factor (bFGF) and Interleukin-8 are thought to contribute to this process (Bar-Eli 2001) (Figure 1).

The contact region between endothelial cells acts as a permeability barrier to solute and control the passage of cells through the endothelium. Several categories of junctional complexes have been found between endothelial cells. These include tight junctions, adherens junctions, and gap junctions (Dejana et al. 1995; Lampugnani et al. 1997). The family of cadherin proteins is comprised of Ca^{2+} -dependent cell adhesion molecules whose primary function is to facilitate intracellular communications and heterotypic/homotypic adhesion, enabling the formation of cell-cell adherens junctions (Vleminckx & Kemler 1999). The different members of the Cadherin family are E (epithelial)-Cadherin, N (neuronal)-Cadherin, P (placental)-Cadherin, and VE (vascular endothelial)-Cadherin.

1.1.4.2.1 E-Cadherin

E-cadherin, now considered a natural metastasis suppressor, is characteristically lost in a majority of carcinomas and represents a primary step in melanoma metastatic conversion (Guilford 1999; Timar et al. 2001). As melanoma progresses, cells lose functional E-cadherin through deregulation and loss of expression. Loss of the transcription factor AP-2 during melanoma progression leads to reduced expression of E-

cadherin, and this reduced expression directly correlates with expression of adhesion receptors associated with cell invasion, such as MCAM/MUC18, and with loss of keratinocyte-mediated regulation of cell growth. (Valyi-Nagy et al. 1993; Shih et al. 1994; Danen et al. 1996; Hsu et al. 1996; Huang et al. 1998; Jean et al. 1998; Hsu et al. 2000b; Gershenwald et al. 2001) .

Conversely, reduced expression of E-cadherin in melanoma cells directly correlates with increased expression of the cell adhesion molecule N-cadherin (Tang et al. 1994; Hsu et al. 1996; Hsu et al. 2000b). The strategic expression of N-cadherin facilitates melanoma cell homophilic adhesion, as well as the formation of gap-junctions with stromal fibroblast and endothelial cells that similarly express N-cadherin. Migration of melanoma cells, over dermal fibroblasts, is further promoted by the expression of N-cadherin (Li et al. 2001).

1.1.4.2.2 VE-Cadherin and vasculogenic mimicry

Vascular endothelial cadherin (VE- Cadherin), also known as cadherin-5 (CDH5) or CD144, is Ca^{2+} - dependent and largely found in the endothelial adherens junctions (Breviario et al. 1995; Lampugnani et al. 1997). Only endothelial cells express VE-Cadherin, which is enhanced through the cells homotypic cellular contacts (Lampugnani et al. 1992; Ayalon et al. 1994). The extracellular region of VE-cadherin, like the classical cadherins, contains five cadherin motifs. In a Ca^{2+} -dependent manner, VE-cadherin can mediate cell–cell adhesion by homophilic binding. However, in comparison to other cadherins, VE-cadherin does not have a HAV (His-Ala-Val) motif, and there is relatively low homology in its cytoplasmic domain compared to other cadherins (Suzuki et al. 1991). Although both N- and P-cadherins have been detected in endothelial cells (Liaw et al. 1990; Ayalon et al. 1994), they show a more scattered distribution on the cell

surface and seem to be eliminated from the cell–cell contact region (Salomon et al. 1992). Studies with both chimeric proteins and truncation mutations demonstrate that the cytoplasmic domain of VE-cadherin contains a membrane proximal region responsible for exclusion of N-cadherin from endothelial contact sites, despite the fact that the cytoplasmic domains of both cadherins can bind plakoglobin, α - and β -catenins equally well (Lampugnani et al. 1995; Navarro et al. 1998).

Mouse knockout models have demonstrated experimentally that loss of VE-Cadherin or expression of a truncated VE-Cadherin is embryonic lethal. Midgestational death is associated with severe vascular defects, and embryos display endothelial apoptosis and dysregulated cell survival signaling (Carmeliet et al. 1999; Gory-Faure et al. 1999). In melanoma, it was recently shown that VE-Cadherin is strongly expressed in highly aggressive cells, but is expressed at undetectable levels in poorly aggressive melanotic cells, demonstrating that aggressive melanoma, as a strategy, mimics endothelial cells to form vasculogenic, patterned networks in a 3-dimensional environment (Hendrix et al. 2001; Seftor et al. 2002; Hendrix et al. 2003a) (Figure 2). However, how VE-Cadherin is regulated by melanoma cells is unknown.

Vasculogenic Mimicry by Aggressive Melanoma Tumor Cells

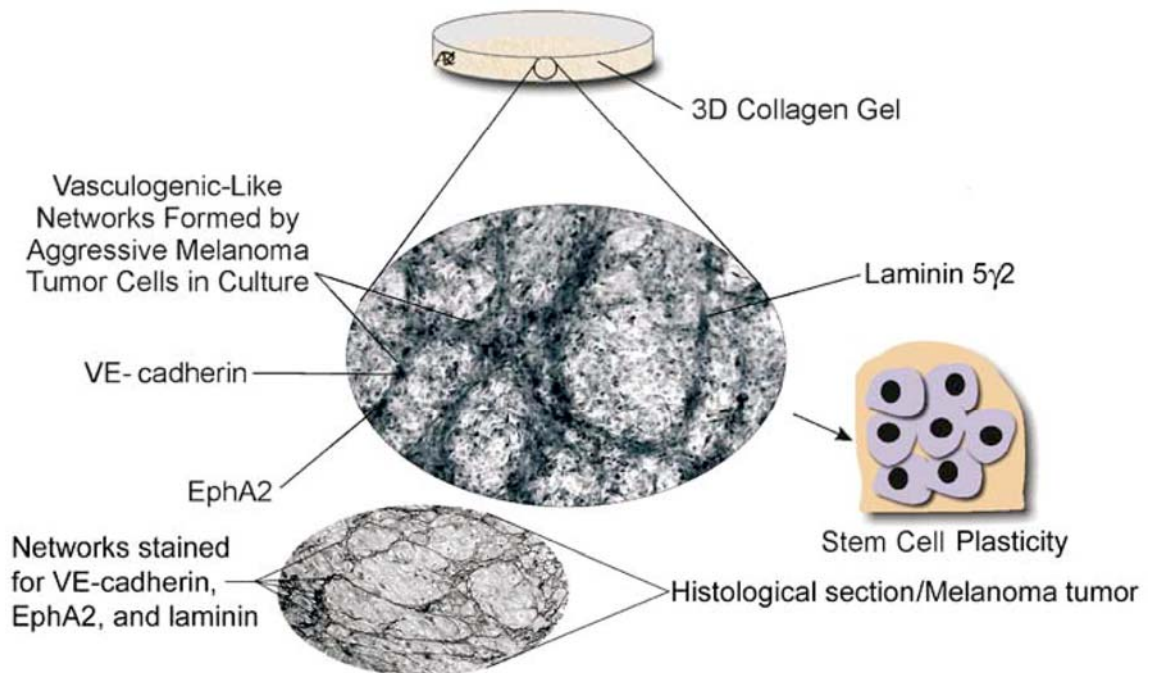


Figure 2 Vasculogenic mimicry observation in 3-D collagenase culture.

The formation of patterned, vasculogenic-like networks in three-dimensional culture reflect the patterned networks seen in a histological section from a patient's aggressive melanoma tumor Plasticity of human melanoma cells (Hendrix et al. 2003a).

1.1.4.5 Matrix Metalloproteinases (MMP)

The ability of tumor cells to invade requires the presence of matrix-degrading enzymes. These include: the cysteine proteinases (cathepsin B, L), the serine-protease family (cathepsin G, elastase, plasmin and uPA), and the matrix metalloproteinases (matrilysins, gelatinases, and stromelysins) (Duffy 1996). In malignant melanoma, transcriptional upregulation of MMP2 expression has been reported and involves the transcription factors activator protein 2 (AP-2) and cAMP response element-binding protein (CREB) with downregulation of AP-2 and increased activity of CREB (Gershenwald et al. 2001). MMP-2 is a 72 kDa type IV collagenase also known as gelatinase A. Pro-MMP-2 activation occurs through proteolytic cleavage of the N-terminal pro-peptide, which results in a 64-kDa intermediate, that is further processed to a 62-kDa active form (Strongin et al. 1993) and this process requires two MT1-MMP molecules. The first MT1-MMP molecule recruits to the cell surface and serves as a surface receptor for the TIMP2-pro-MMP-2 complex (Strongin et al. 1995). The second MT1-MMP molecule proteolytically activates MMP-2 through cleavage of MMP-2 and degrades extracellular matrix components (*e.g.* fibronectin, collagen types I, II, and III; vitronectin and laminins 1 and 5) (Strongin et al. 1995; Egeblad & Werb 2002).

1.1.4.6 Angiogenic factors

Angiogenesis, the formation of vascular networks, represents a sustaining factor in the growth and survival of primary and metastatic tumors. Angiogenic factors are secreted in large amounts by melanoma cells to encourage angiogenic growth (Potgens et al. 1995; Claffey et al. 1996; Oku et al. 1998; Rofstad & Danielsen 1998). Angiogenic factors include vascular endothelial growth factor (VEGF), Interleukin 8 (IL-8) (Singh et

al. 1994; Luca et al. 1997; Kunz et al. 1999), platelet-derived endothelial cell growth factor, PD-ECGF (Leyva et al. 1984; Asgari et al. 1999), and basic fibroblast growth factor, bFGF (Halaban et al. 1988; Becker et al. 1989; Wang & Becker 1997).

VEGF, also known as vascular permeability factor, is a strong specific mitogen for endothelial cells and may also stimulate endothelial cell migration and reorganization (Dvorak et al. 1995; Ferrara 2000). The thymidine phosphorylase and gliostatin, PD-ECGF stimulates endothelial cell mitogenesis and chemotaxis *in vitro* and is strongly angiogenic *in vivo*, possibly through modulation of nucleotide metabolism (Griffiths & Stratford 1997). BFGF, which belongs to the family of heparin-binding growth factors, is a multifunctional protein having a well-established key role in tumor angiogenesis (Slavin 1995; Ellis & Fidler 1996; Bikfalvi et al. 1997).

A potent angiogenic factor *in vitro* and *in vivo*, is IL-8, which belongs to the superfamily of CXC chemokines (chemotactic cytokines), and functions as a multifunctional cytokine and acts as an autocrine growth factor for melanoma cells (Koch et al. 1992; Schadendorf et al. 1993; Bar-Eli 1999a). Interleukin 8 (IL-8), or CXCL8, belongs to the chemokine group, which consists of the CX3C, CXC, CC, and C families of small peptides (Schroder & Christophers 1986; Walz et al. 1987). A wide range of cells can produce IL-8 including: keratinocytes, lymphocytes, fibroblasts, endothelial cells, hepatocytes and monocytes (Oppenheim et al. 1991). A critical role is played by chemokines in immune and inflammatory reactions by promoting chemotactic migration of leukocytes. A positive correlation has been shown between disease progression and the expression of IL-8 (Nurnberg et al. 1999; Kunz et al. 2000) (Singh et al. 1994; Scheibenbogen et al. 1995; Singh et al. 1995; Singh et al. 1999; Ugurel et al. 2001). Furthermore it has been reported in human melanoma specimens a concomitant upregulation of one of two putative IL-8 receptors (Varney et al. 2006). CXCR1 and

CXCR2 are two types of 7-transmembrane spanning G-protein-coupled receptors that can mediate the effects of IL-8 with CXCR1 being a selective receptor for IL-8 (Miller & Krangel 1992; Chuntharapai & Kim 1995; Addison et al. 2000).

1.1.4.6.1 Interleukin-8 and carcinogenesis

It has been reported that melanoma cells produce IL-8, which has been primarily explained as an important role of chemokines in autocrine and paracrine regulation of tumor cell proliferation, angiogenesis, invasion and metastatic dissemination (Strieter 2001). IL-8 exhibits potent angiogenic activities both *in vitro* and *in vivo*, and also acts as an autocrine growth factor for melanoma cells (Koch et al. 1992; Schadendorf et al. 1993; Bar-Eli 1999a). In addition to melanoma cells, both receptors of IL-8, called CXCR1 and CXCR2, are found expressed on fibroblasts, keratinocytes, and endothelial cells (Horuk et al. 1993; Moser et al. 1993). CXCR1 has been shown to be ubiquitously expressed in human melanoma specimens from different Clark levels. However, CXCR2 is expressed frequently in higher grade melanoma tumors and metastases. This suggests an association between expression of CXCR2 and IL-8 with vessel density in metastasis and advanced lesions (Varney et al. 2006).

1.2 Galectin-3

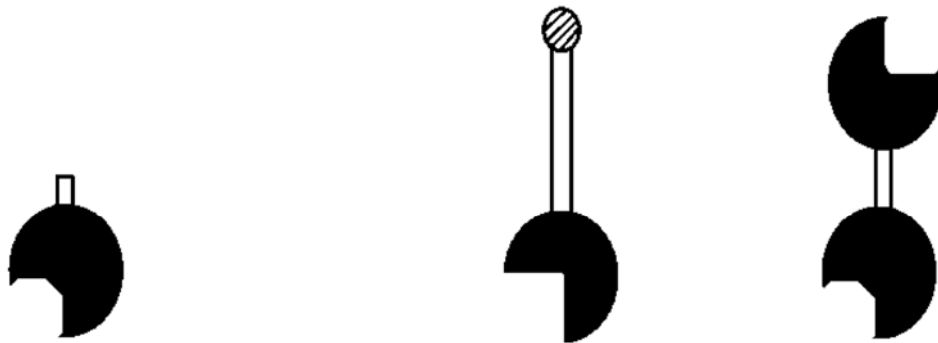
Galectins, a family of carbohydrate-binding proteins, have a high affinity for β -galactoside-containing glycoconjugates and the acid sequences of their carbohydrate recognition domains (CRD) are evolutionary conserved (Shimura et al. 2005; Dunic et al. 2006). In higher vertebrates, fifteen members of the galectin family have been identified

so far. They contain either one CRD (proto and chimera types) or two CRD (proto and tandem repeat types) (Cooper 2002). Some examples of the prototype galectins are Gal-1, -2, -5, -7, -10, -11, -13, -14, and -15. They are all homodimers except Gal-5 and -7 which are monomers. In addition they are four tandem-repeat type galectins: Gal-4, -6, -8, -9, and -12. Three major groups have currently been described. Gal-3 belongs to the chimera type, which contains 12 amino acids, for cellular targeting, in the NH₂-terminal domain, a substrate for matrix metalloproteinases (Clark et al. 1984) which contains a proline and glycine rich sequence, and for binding to the carbohydrates, a CRD region in the COOH-terminal domain (Figure 3) (Gong et al. 1999; Cooper 2002; Nakahara et al. 2005)

Gal-3 appears to play a part in several different physiological and pathophysiological conditions. These include: immune reactions, development, metastasis, and neoplastic transformation. It can interact with both intra- and extracellular proteins, which may explain its broad range of functions (Xu et al. 2000; Ellerhorst et al. 2002; Nakahara et al. 2005; Domic et al. 2006).

1.2.1 Gal-3 intracellular functions

As a pre-mRNA splicing factor, Gal-3 acts intracellularly (Dagher et al. 1995). This has been correlated with the Sm epitopes of the small nuclear ribonucleoprotein complexes in speckled structures and the non-small nuclear ribonucleoprotein splicing factor SC35 (Vyakarnam et al. 1998). Further confirmation was shown by association and co-localization in the nucleus with Gal-3 and single-stranded DNA and RNA. This occurred by way of high affinity to poly (A) ribonucleotide homopolymers (Wang et al. 1995). In motor neuron containing complexes, the ability of Gal-3 to associate with Gemin4



Galectins-1, -2, -5,
-7, -10, -13, -14,
GRIFIN, HSPC159,
PP13, PPL13, OVGAL11

Galectin-3

Galectins-4,-6,
-8,-9, and -12

Figure 3 Galectin subunit types.

The CRDs are shown filled and other parts of the peptide open or hatched. The mono CRD galectins can occur as monomers or dimers, or in case of Gal-3 as higher order oligomers (Cooper 2002).

increases their survival and strengthens their function for pre-mRNA splicing (Park et al. 2001). Furthermore, Gal-3 regulates through downregulation of cyclins A and E and upregulation of p21 and p27 cyclin inhibitors and hypophosphorylation of Rb protein the G1 or G2/M arrest (Kim et al. 1999). Therefore, Gal-3 is important not only in RNA processing, but also in cell replication and death (Iacobini et al. 2003) (Figure 4). In addition, enforced expression of Gal-3 in epithelial cells rendered them more resistant to apoptotic stimuli (Yang et al. 1996; Akahani et al. 1997; Kim et al. 1999; Lin et al. 2000; Yoshii et al. 2002).

Indeed, Gal-3 contains the anti-death Asp-Trp-Gly-Arg (NWGR) motif that is conserved in the Bcl-2 homology domain (BH1) of the Bcl-2 family (Yang et al. 1996; Akahani et al. 1997; Kim et al. 1999; Hsu et al. 2000a; Lin et al. 2000; Tsujimoto & Shimizu 2000; Yoshii et al. 2002). Nakahara et al. revealed the controversy of the role of Gal-3 as intracellularly an antiapoptotic and /or extracellularly as a proapoptotic factor in various cell types (Iacobini et al. 2003; Nakahara et al. 2005) (Figure 4). Gal-3 has also been reported to be an anti-apoptotic molecule, which is able to inhibit T-cell apoptosis induced by Fas. Additionally Gal-3 was able to inhibit apoptosis that had been induced by geneistein, cisplatin, staurosporine and anoikis (apoptosis induced by loss of cell anchorage) in epithelial cells (Yang et al. 1996; Akahani et al. 1997; Kim et al. 1999; Lin et al. 2000; Yoshii et al. 2002).

It is on one hand found intracellularly in the nucleus and cytoplasm or secreted via non-classical pathway outside of the cell and on the other hand being found on the cell surface or in the extracellular space (Dumic et al. 2006). In Gal-3 knockout mice, anti-apoptotic activity has also been noted. Compared to normal control mice, macrophages from the Gal-3 knockout mice were more sensitive to apoptosis (Hsu et al. 2000).

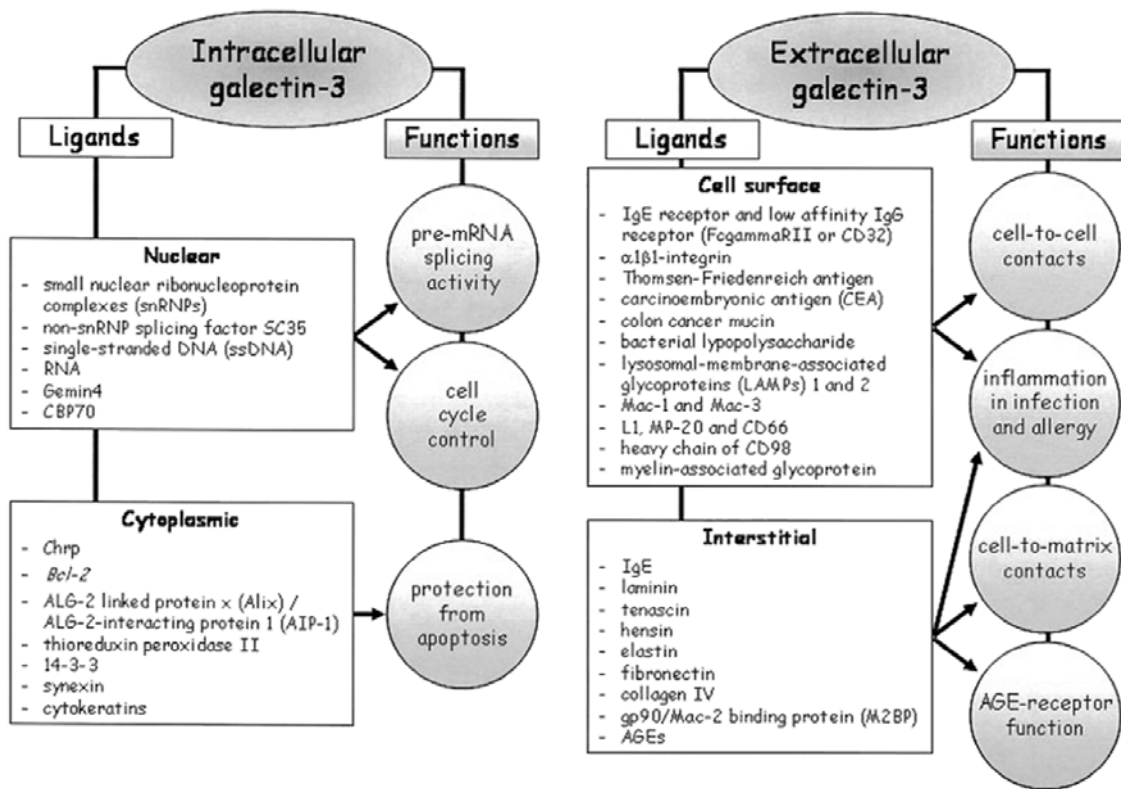


Figure 4 Gal-3 intracellular and extracellular ligands and related functions.

Intracellularly Gal-3 binds to nuclear expressed proteins that affect the pre-mRNA splicing activity and cell cycle control. Through its binding to cytoplasmic proteins like BCL-2 it serves as an antiapoptotic molecule. Extracellularly, Gal-3 functions in cell-cell adhesion and cell to matrix contacts through binding with cell surface and interstitial expressed proteins. Therefore it gained also its ability to act as an apoptotic molecule (Iacobini et al. 2003).

The ability to resist apoptosis is essential for cancer cell survival and shares an important role in tumor progression.

1.2.2 Gal-3 extracellular functions

The list of known Gal-3 ligands, which includes Mac-2 BP (Inohara et al. 1996), Fibronectin and laminin (Sato & Hughes 1992; Warfield et al. 1997) (Figure 4), was recently expanded to include Mgat5-modified N-glycans. Mgat5 is important for fibronectin matrix remodeling in tumor cells (Lagana et al. 2006). Golgi generate Mgat5, which are present on mature glycoproteins and other N-glycosylated cell surface signaling receptors (Henrick et al. 1998; Perillo et al. 1998; Barboni et al. 2000; Yu et al. 2002). The binding of Gal-3 to Mgat5-modified N-glycans induces $\alpha_5\beta_1$ - integrin activation, which enhances fibronectin (FN) fibrillogenesis and FN-dependent tumor cell spreading and motility (Reiske et al. 1999; Ilic et al. 2004; Clark et al. 2005).

Gal-3 can bind both integrins and receptor tyrosine kinases which contribute via signaling to adhesion remodeling (Fukumori et al. 2003). Focal adhesion kinase (FAK) is activated through Gal-3 stimulation and integrins are exchanged to substratum. This results in microfilament turnover, the activation of the phosphatidylinositol 3-kinase (PI3K), and recruitment of integrins and translocation to fibrillar adhesions. Gal-3 binding has been proposed to control the movement along actin stress fibers through translocation rate of fibrillar adhesion, as well as, FN polymerization and FN fibril stretching (Lagana et al. 2006). The cleavage of the laminin $5\gamma_2$ chain results from the activation of MMP-2, which is itself activated through PI3K initiation downstream of FAK (Hendrix et al. 2003a) (see section 1.1.4.2.2).

Ochieng et al. report that Gal-3 is also a substrate for MMP-2 and MMP-9. Cleavage of Gal-3 by MMP, results in two fragments: a 9 kDa fragment with the amino

terminal end and a 22 kDa fragment with carbohydrate recognition domain (Ochieng et al. 1994). This 22 kDa fragment binds 1.5 -2 times more tightly to glycoconjugates but fails to self-associate (Ochieng et al. 1998). Tumor aggressiveness has been shown to be associated with increased expression of MMP, more specifically MMP-2. The ability of MMP-2 to cleave Gal-3 may therefore have a role in tumor metastasis (Zucker et al. 2000).

Gal-3 has been shown to be a receptor for advanced glycosylation end product (AGE) binding proteins. These include RAGE (receptor for advanced glycosylation end products), the AGE-receptor complex p60, p90, and the macrophage scavenger receptor type I and II. Gal-3 has a high-affinity binding for AGEs in astrocytes, macrophages, and endothelial cells. In the mesangium and endothelium, tissues that are targets of diabetic vascular complications, Gal-3 is weakly expressed but with aging it is induced by the diabetic milieu. Therefore, in target tissue injuries, the overexpression of Gal-3 may be important for pathogenic events (Pricci et al. 2000).

Recent experiments using Gal-3 null mice gave evidence of Gal-3 acting as a pro-inflammatory protein (Colnot et al. 1998; Hsu et al. 2000a; Bernardes et al. 2006). Gal-3 showed an activating effect on NADPH oxidase (Almkvist et al. 2004), a downregulating effect on interleukin (IL)-5 expression in human eosinophils (Cortegano et al. 1998), on promotion of monocyte chemotaxis (Sano et al. 2000) and stimulation of superoxide production of neutrophils (Yamaoka et al. 1995). Further, extracellularly, Gal-3 acts as a de-adhesion molecule in the interaction of thymocytes and thymic microenvironmental cells (Villa-Verde et al. 2002), stimulate cell migration (Silva-Monteiro et al. 2007) and cell death (Stillman et al. 2006; Silva-Monteiro et al. 2007).

In LNCaP cells, which do not express Gal-3 constitutively, exogenous expression of Gal-3 is able to inhibit apoptosis induced by anticancer drugs, by stabilizing the

mitochondria. It also stimulates the phosphorylation of Ser (112) on Bcl-2-associated death (Bad) protein and down-regulates Bad expression after treatment with cis-diammine-dichloroplatinum. Translocation from the nucleus to the cytoplasm allows Gal-3 to be able to inhibit cytochrome c release and caspase-3 activation by inhibiting mitochondrial depolarization and damage (Fukumori et al. 2006). Fukumori et al. speculate that Gal-3 inhibits apoptosis induced by anticancer drugs through suppression of the mitochondrial apoptosis pathway and regulation of Bad protein. The ability to improve the efficacy of chemotherapy anticancer drugs could be achieved by targeting Gal-3 in prostate cancer.

Gal-3 is widely spread among different types of cells and tissues including epithelial and endothelial cells (Glinsky et al. 2001; Lin et al. 2002; Mengwasser et al. 2002; Khaldoyanidi et al. 2003) activated macrophages (Dong & Hughes 1997; Kim et al. 2003) and dendritic cells (Swarte et al. 1998; Vray et al. 2004). A previous study on a small series of melanocytic lesions (Mollenhauer et al. 2003), revealed that some nevi and melanomas express Gal-3.

Gal-3 plays an important role in tumor cell adhesion, proliferation, differentiation, angiogenesis, and metastasis (Nakahara et al. 2005) in multiple tumors (Xu et al. 2000; Ellerhorst et al. 2002). However, the exact mode of action of how Gal-3 contributes to melanoma growth and metastasis remains unknown. The studies reported here are aim to fill this gap. To that end I propose the following Specific Aims:

Specific Aims

- 1. Pattern of Gal-3 expression during melanoma progression**
- 2. Effect of Gal-3 shRNA on tumor growth and metastasis**
- 3. Identification of Gal-3 downstream target genes by Gal-3 shRNA**

Chapter II:

2. Materials and Methods

2.1 Cell Lines and Culture Conditions

The highly metastatic A375SM human melanoma cell line was established from pooled lung metastases produced by A375-P cells injected intravenously (i.v.) into nude mice (Li et al. 1989). A375-P is a human melanoma cell line, which was established in culture from a lymph node metastasis of a melanoma patient (Kozlowski et al. 1984).

The human melanoma cell line WM266-4, purchased from ATCC, is tumorigenic and metastatic in nude mice (Luca et al. 1995). The human melanoma MeWo cell line was established in culture from a lymph node metastasis of a melanoma patient and was kindly provided to us by Dr. S. Ferrone (New York Medical College, New York, NY).

In nude mice, MeWo cells are tumorigenic and have low metastatic potential (Ishikawa et al. 1988). The SB-2 cell line was isolated from a primary cutaneous lesion and was a gift of Dr. B. Giovanella (St. Joseph's Hospital, Houston, Texas). In nude mice, SB-2 cells are poorly tumorigenic and nonmetastatic (Luca et al. 1993; Singh et al. 1995). The cell lines DX-3, DM-4, TXM-40, -18, -1 and TXM-13 are low to intermittent metastatic melanoma cells. The highly metastatic melanoma cell line C8161 was obtained from Dr. Welch (Department of Pathology, University of Alabama at Birmingham, Birmingham, AL, USA) and maintained in DMEM/F12 (BRL-GIBCO Life Technologies, Rockville, MD) containing 5% FBS. The C8161 cell line containing a luciferase plasmid construct was kindly provided by Dr. Vladislava Melnikova.

Through injection of melanoma cell lines into the tail vein of mice the definition for low (0-10 metastasis), intermediate (10-50 metastasis) and highly metastatic (50>200 metastasis) cell lines was made upon the numbers of metastasis formed in the lungs.

All human melanoma cell lines were maintained in culture as adherent monolayers in Eagle's minimal essential medium (MEM) supplemented with 10% fetal bovine serum (HyClone, Logan Utah), 20mM HEPES buffer (Invitrogen, Carlsbad, CA), 100 mM of sodium pyruvate (BRL-GIBCO LifeTechnologies, Rockville, MD), 10 mM non-essential amino acids (Invitrogen, Carlsbad, CA), 100 U/ml penicillin (Invitrogen, Carlsbad, CA), 100µg /ml streptomycin (Invitrogen, Carlsbad, CA) and 2mM L-glutamine (BRL-GIBCO LifeTechnologies, Rockville, MD).

Human embryonal kidney (HEK) cells 293T (Invitrogen, Carlsbad, CA) were cultured in DMEM supplemented with 10% FBS. All cells were mycoplasma free and kept in a humidified chamber at 37° C in 5% CO₂.

2.2 Three-dimensional Type-I Collagen Gels

250 µl of type I collagen (average 3 mg/ml; Collaborative Biomedical) were coated onto 24 well plates to create a three-dimensional type I collagen gel as described (Maniotis et al. 1999; Hendrix et al. 2003a) (Figure 2). 25×10^4 melanoma cells were plated on top of the collagenase layer in 3ml medium containing 5% FBS and left to grow in culture for four weeks until they form networks in 3-D manner. Live cells were then photographed unstained using an inverted brightfield Leica microscope, which was attached to an Optronics Camera, and the pictures were analyzed with Optimas program.

2.3 Animals

Female athymic BALB/c nude mice were obtained from the Animal Production Area of the National Cancer Institute, Frederick Cancer Research Institute (Frederick, MD, USA). The mice were housed in laminar flow cabinets under specific pathogen-free conditions and used at eight weeks of age. Animals were maintained in facilities approved by the American Association for Accreditation of Laboratory Animal Care and in accordance with current regulations and standards of the US Department of Agriculture, Department of Health and Human Services, National Institutes of Health, and institutional regulations. Their use in these experiments was approved by the Institutional Animal Care and Use Committee (IACUC).

If the largest dimension of a tumor reached 1.5 cm, the mice were considered moribund and sacrificed as designated by IACUC. Moribund mice were sacrificed in a CO₂ chamber. The date of natural death or sacrifice was recorded.

2.4 Cell Preparation for Injection

To prepare tumor cells for inoculation, we harvested cells in the exponential growth phase by brief exposure to 0.25% trypsin, 0.2% EDTA solution (w/v). The flask was sharply tapped to dislodge the cells, and supplementary medium was added. The cell suspension was pipetted to produce a single-cell suspension. Then, the cells were washed and resuspended in Ca²⁺- and Mg²⁺- free HBSS (Hank's Balanced Salt Solution) to the desired cell concentration. Cell viability was determined by Trypan blue exclusion, and only single-cell suspensions of more than 90% viability were used.

2.5 Injection and Monitoring of Tumor Cells

Subcutaneous (s.c.) tumors were produced by injecting 2.5×10^5 tumor cells in 0.2 ml HBSS into the right flank. Growth of subcutaneous tumors was monitored by daily examination of the mice and three weekly measurements of tumors with calipers. Through measurement of the long (a) and short diameter (b) of the tumors the tumor growth in cm^3 was evaluated by using following formula: $a \times (b)^2 / 2$. The mice were killed 47 days after injection or as soon as they reached 1.5 cm^3 tumor volume, and tumors were processed in paraffin and in OCT for hematoxylin and eosin and immunohistochemical staining. Tumor growth was compared among the parental and transfected cells using the Student's t-test.

To determine metastatic potential, 1×10^6 C8161 tumor cells in 0.2ml HBSS were injected into the tail vein using a 25G5/8 needle. The injected tumor cells go through the tail vein to the inferior vena cava where they enter the right chamber of the heart and finally arrive at the pulmonary capillary bed via the pulmonary artery. The tumor cells colonize the lung and form lung metastasis. 35 days after i.v. tumor injection mice were sacrificed and their lungs were harvested and fixed in Bouin's solution, where the number of surface tumor nodules was counted and recorded. Data are given as number of metastatic nodules per mouse.

Since the C8161 tumor cells contain a luciferase expression plasmid the tumors were additionally monitored with IVIS 100 Imaging System (Xenogen), which measured the bioluminescence of the luciferase labeled tumor cells within the tumor and provides measurement of the tumor volume using Living Images Program (Ramachandran et al. 2007). The IVIS 100 Imaging System is attached to a XG18-Gas Anesthesia System (Xenogen) for anesthetizing the mice prior to measurement and to a CCD Array Scientific Camera (Spectral Instruments, Inc.) for taking pictures capturing the bioluminescence of

the tumor cells within the live mice. The substrate luciferin (150mg /mouse), was kindly provided by Dr. Logsdon, Department of Cancer Biology, University of Texas MD Anderson Cancer Center, Houston, Texas. Luciferin was injected 12 minutes prior to measurement, and the tumors showed a peak of bioilluminescence (relative light intensity) at around 12 minutes after intraperitoneal injection of the substrate.

2.6 In Vitro Proliferation Assay

Ninety-six-well plates containing 1500 cells/well from parental control, non-targeting shRNA, and shRNA Gal-3 knockdown melanoma cells were cultured for five days in normal growth medium. Cell growth was analyzed by MTT-assay, which determines relative cell numbers based on the conversion of MTT to formazan in viable cells. MTT (40 µg/ml) was added to each well and incubated for two hours. The medium was removed and 100 µl of dimethyl sulfoxide (DMSO) was added to lyse the cells and solubilize the formazan. Absorbance at 570 nm was determined using a microplate reader. This procedure was repeated each day for five days to determine the proliferation rate of the cells before and after Gal-3 knockdown.

2.7 Antibodies

The polyclonal anti-human antibody to Gal-3 used in Western Blot (1:1000 dilution) and immunohistochemical staining (1:400 dilution) analyses was kindly provided by Dr. Avraham Raz, PhD, Karmanos Cancer Institute, Wayne State University, Detroit, MI, USA.

The following primary antibodies were also used: goat polyclonal anti-VE-Cadherin antibody (C-19; 1:200 dilution; Santa Cruz Biotechnology), mouse IgG1 anti-Fibronectin antibody (Fibronectin 610077; 1:5000 dilution; BD Biosciences Pharmingen), rabbit anti-

Sphingolipid Receptor Edg1/S1P1 antibody (1ug/ml; GeneTex, Inc.), rabbit anti-human MMP-2 (MMP-2-AP1; 1:400; Chemicon), rabbit anti-human EGR1 (200µg / 0.1ml; 2 ug for CHIP; Santa Cruz Biotechnology), rabbit anti-actin (1:1000 dilution; Sigma); mouse anti-human PCNA (PC10; 1:50 dilution; Dako), rabbit anti-human IL-8 (1:25 dilution; Biosource International), rat anti-mouse m-CD31 (PECAM-1; 1:500 dilution; Pharmingen), rabbit anti-mouse Immunglobulin (IgG) Alexa 488 (1:400 dilution; green fluorescent; Jackson Immuno Research, West Grove, PA), rabbit anti-mouse Ig Alexa 594 (1:400; red fluorescent; Jackson Immuno Research, West Grove, PA). The following secondary antibodies were used: donkey anti-goat IgG (1:1000 dilution; Santa Cruz Biotechnology), goat anti-rabbit IgG Horseredish Peroxidase (HRP) (1:200; Jackson Immunoresearch, West Grove, PA), goat anti-rat IgG HRP (1:200; Jackson Immunoresearch, West Grove, PA), rat anti-mouse IgG2a HRP (1: 200; Serotec/ Harlan Bioproducts), anti-rabbit IgG Cy3 (1:600 dilution; red fluorescent; Jackson Immunoresearch, West Grove, PA), anti-rabbit Cytochrom (1:1000 dilution; green fluorescent; Jackson Immunoresearch, West Grove, PA), donkey anti-rabbit IgG HRP (1:1000 dilution; GE Healthcare UK limited) and sheep anti-mouse IgG HRP (1:1000 dilution; GE Healthcare UK limited).

2.8 Protein Extraction

Total protein extracts were prepared by seeding cells onto 100 mm culture dishes in normal growth medium and growing to 70-80% cell confluence. Cells were washed in cold PBS and lysed in 500 µl of Triton lysis buffer (25 mM Tris-HCL, pH 7.5, 150 mM NaCl, 1% Triton X-100, 5mM EDTA) containing protease inhibitors (1mM phenylmethyl-sulfonyl fluoride, 20 µM leupetin, 0.15 unit/ml aprotinin, 1 mM Na₃VO₄, and 10 mM NaF) for 20 minutes on ice. Proteins were extracted for 30 minutes on ice

and collected by centrifugation at 11,000 X g at 4°C for 15 minutes. The supernatant was transferred to a clean tube and protein concentration was determined using Bradford reagent (Bio-Rad Laboratories, Hercules, CA) according to the manufacturer's instruction.

2.9 Western Immunoblot Analysis

Proteins of total cell extracts were separated by 10% and 13% SDS-polyacrylamide gel electrophoresis under reducing conditions in a BioRad Mini Protean III gel apparatus (BioRad, Hercules, CA). The proteins were electrophoretically transferred to an Immobilon P membrane (Millipore Corp., Bedford, MA) using the Criterion Blotter transfer system (BioRad laboratories, Hercules, CA) in 2,5 mM transfer buffer (10xTBS, Methanol and H₂O). The membranes were washed in TBS (10mM Tris-HCl, pH 8 containing 150 mM NaCl) and blocked with 5% nonfat milk in TBS overnight at 4°C.

The membranes were then probed with the chosen antibody in TBS for 2 hours at room temperature at given dilutions (see section 2.7). The primary antibodies were incubated on the same membrane after cutting the membrane in half. The unbound primary antibody was removed by washing the membrane with TTBS (0.1% Tween 20, TBS) followed by two hours room temperature incubation with horseradish peroxidase-conjugated secondary antibody at given dilutions (see section 2.7) in 0.5% nonfat milk in TTBS.

After stripping the membranes at 80°C for 25 minutes in stripping buffer (0.2 M Glycine (pH 2.5), 0.05% Tween 20) the membranes were again blocked for 30 minutes and then incubated with anti-actin antibody overnight.

Immunoreactive proteins were detected by enhanced chemiluminescence per manufacturer's instructions (ECL detection system) (Amersham Pharmacia Biotech, Arlington Heights, IL) and chemiluminescence signals were captured on Kodak Bio-MAX MR X-ray films.

2.9 Expression Constructs

pcDNA3.1 (Invitrogen, Carlsbad, CA) is a mammalian cell expression construct in which expression is driven by the CMV promoter and provides neomycin resistance. The pbkCMV-Gal-3 construct containing the human Gal-3 open reading frame gene sequence was kindly provided by Dr. Avraham Raz.

The CDH5 promoter reporter construct was amplified from genomic DNA extracted from C8161 cells and used for PCR template cloning for the CDH5 promoter (-515nt upstream to +24nt downstream of the transcription initiation site) with following primers (Kn2863 forward primer: 5'-**GGGTACCAGCCAGCCAGCCCTCACAAA** GG-3'; H3-24 reverse primer: 3'-**CCCAAGCTTTGTCCGTCCAGGGCTGAGCGTGA** GTG-5'). The CDH promoter reporter construct was amplified by PCR in the same reaction as follows: an initial denaturation for two minutes at 94°C; followed by 30 cycles of denaturation at 94°C for 10 seconds, annealing at 50°C for 30 seconds, and extension at 72°C for one minute. A final elongation step was carried out at 72°C for ten minutes.

After amplification the PCR product was purified with QIAquick PCR Purification Kit (Qiagen, Valencia, CA) and the vector was digested with KpnI and Hind III. On the 5'-end the KpnI site (shown bold) was incorporated into the 5' end of the forward primer and HindIII was incorporated into downstream of the 3' reverse primer sequence (shown bold).

After digestion of the PCR product with KpnI and Hind III, the resulting fragment was ligated to the pGL3-basic vector (Promega, Madison, WI) using the same two enzyme sites located at the multiple cloning site of the vector. The inserted promoter was confirmed by sequencing with the use of GP₂ Primer (5'-TTTATGTTTTTGGCGTCTTCA-3'), which showed 100% homology with the corresponding sequence, which was downloaded from the NCBI human genomic sequencing program.

For construction of the IL-8 promoter reporter construct, the pGL2-basic plasmid (Promega, Madison, WI) was used as the backbone. The human IL-8 promoter region - 133+44 is as follows: AGTGTGATGACTCAGGTTTGCCCTGAGGGGATGGGCC ATCA GTTGCAAATCGTGGAATTTCTCTGACATAATGAAAAGATGAGGGTG CATAAGTTCTCTAGTAGGGTGATGATATAAAAAGCCACCGGAGCACTCCATA AGGCACAACTTTCAGAGACAGCAGAGCACACAAGCTT. It was put upstream of the open reading frame of the luciferase gene as previously described (Huang et al. 2000) using following primers (IL8-1741 forward primer: 5'-CCCACATTACTCAGAAA GTTACTCC-3' and IL8-2455 reverse primer: 3'-GATGGTTCCTTCCGGTGGTTT CTTC-5').

The EGR-1 sequence was amplified from cDNA which was obtained by reverse transcription from the melanoma A375SM cell line using following primers (EGR-1 forward primer: 5'-GGAATTCCATATGGCCGCGGCCAAGGCCGAGATGC-3' and EGR-1 reverse primer: 3'-CCCAAGCTTTTAGCAAATTTCAATTGTCCTGGGAG-5'). The EGR-1 cDNA was cloned into pcDNA3.1 expression vector with N-terminal HA-flag and c-myc tags using NdeI and HindIII Restrictionenzymes.

2.10 Transient Transfections and Luciferase Activity Assays

Transient transfections were performed using Lipofectamine 2000 (Invitrogen, Carlsbad, CA) according to the manufacturer's instructions. A total of 25×10^3 cells /well in a 24-well plate were transfected with 0.5 μg of the basic pGL3 expression vector with no promoter or enhancer sequence (pGL3-Basic containing firefly luciferase) or with 0.5 μg of the pGL3-CDH5 or pGL2-IL-8 above described luciferase expression constructs. For each transfection, 30 ng of promoter derived *Renilla* luciferase reporter pRL-CMV (Promega, Madison, WI) was included. Transfection was performed by addition of 1.0 μg of the expression constructs or empty vector to the DNA solutions for transfection. After six hours of incubation, the transfection medium was replaced with serum-containing growth medium. After 72 hours of incubation period, the cells were harvested and lysed, and luciferase activity was assayed using a dual luciferase reporter assay system (Promega, Madison, WI) as instructed by the manufacturer. The luminescence of *Renilla* (relative light intensity 1×10^6) was measured with the LUMIstar reader (BMG Labtech) and it was evaluated with the LUMIstar-Galaxy program.

A comparison of the *renilla* luciferase activity (actin promoter) and the firefly luciferase activity (CDH5 or IL-8 promoter) normalizes for differences in transfection efficiency between different cell lines. Luciferase units were calculated using the following formula: (firefly luciferase units/*Renilla* luciferase units).

2.11 Stable Transfection with small hairpin RNA Lentivirus Expression Vectors

2.11.1 shRNA expression vector construction

The pLV-THM vector was provided by Didier Trono and used as the backbone construct for the shRNA expression vector in order to knock down Gal-3. The pLV-THM

vector is a HIV-based lentivirus vector, which is 11,085 bp long and expresses the green fluorescence protein GFP under the Efl-alpha promoter. The H1 polymerase III promoter was used to drive the shRNA expression. Directly downstream of the H1 promoter one MluI and one ClaI site, which are unique sites, are used for insertion of the specially designed DNA fragments as described below (Figure 6 and 7). For retrieving the insert, two complementary oligos were synthesized, which allowed for direct cloning of the annealed shRNA into the lentiviral vector, which was designed as depicted in Figure 7. After annealing procedure, the resulting double stranded DNA revealed two sticky ends (one at the ClaI and one at the MluI site). Those ends were then ligated to the pLV-THM vector, which was cut by ClaI and MluI. For direct cloning of the shRNA into the pLV-THM lentiviral vector the shRNA must be designed with following oligos as described by Didier Trono (www.tronolab.com) (Figure 7). The resulting construct pLVTH-A3 was designed to provide stable delivery of the shRNA expression cassette targeting the following sequence of Gal-3 cDNA: 5'-CGC GTC CCC GTA CAA TCA TCG GGT TAA ATT CAA GAG ATT CAA GAG ATT TAA CCC GAT GAT TGT ACT TTT TGG AAA T-3' (Figure 6). The same procedure was done for creating the nontargeting shRNA as the control shRNA by using specific primers described in Figure 7. The shRNA expression cassettes in the final construct were confirmed by DNA Sequencing.

The GFP expression cassette, which is located between two LTR sites in the vector, was used for cell sorting of the positive expressing shRNA knockdown cells.

2.11.2 Cell sorting with Flow Cytometry

Cells were grown to approximately 90-100% confluency, trypsinized into PBS with 2% FBS and spun down at 1000 rpm for three to five minutes. They were washed with 10 ml PBS containing 2% FBS once and then the cell pellet was resuspended with

0.5 to 1 ml PBS containing 2% FBS into 15 ml tubes and sent for cell sorting with GFP. The top 70% of GFP positive cells were collected into 15 ml tubes with 5 ml growth medium and enriched for further experimental assays *in vitro* and *in vivo*.

2.11.3 Recombinant lentivirus production

For virus production the lentivirus vector pLVTH-A3, PAX2 packaging plasmid (containing gag and pol genes of HIV) and pMD2G-VSVG envelope plasmid (containing vesicular stomatitis viral glycoprotein expressing vector) were cotransfected into HEK293T packaging cells with standard procedure of phosphate-calcium precipitation. In brief the HEK 293 FT cells were seeded into 10 cm dishes one day before transfection. When the cells reached a confluency of 50%, the transfection mixture, prepared as described below, was added to the cells in a dropwise manner. 500 µl water solution of 20µg pLVTH-A3 vector, 15 µg PAX2 and 6 µg pMD2G-VSVG plasmid were combined with 500µl 2xHBS and then mixed with 50µl of 2.5 M CaCl₂. The virus transfection mixture was incubated for 20 minutes at room temperature prior to adding it to the cells. Twelve hours after discarding the medium containing virus transfection mixture, the 293 FT cells were washed once with PBS and then normal growth medium was added overnight. After 24 hours the virus was harvested by collecting the virus containing medium, which was centrifuged at 4000 rpm for five minutes. The supernatant was collected and filtered through a 0.45µM low protein-binding filter (Whatman, Clifton, NJ). The filtered medium is ready to be used to transduce the target cells (Figure 5).

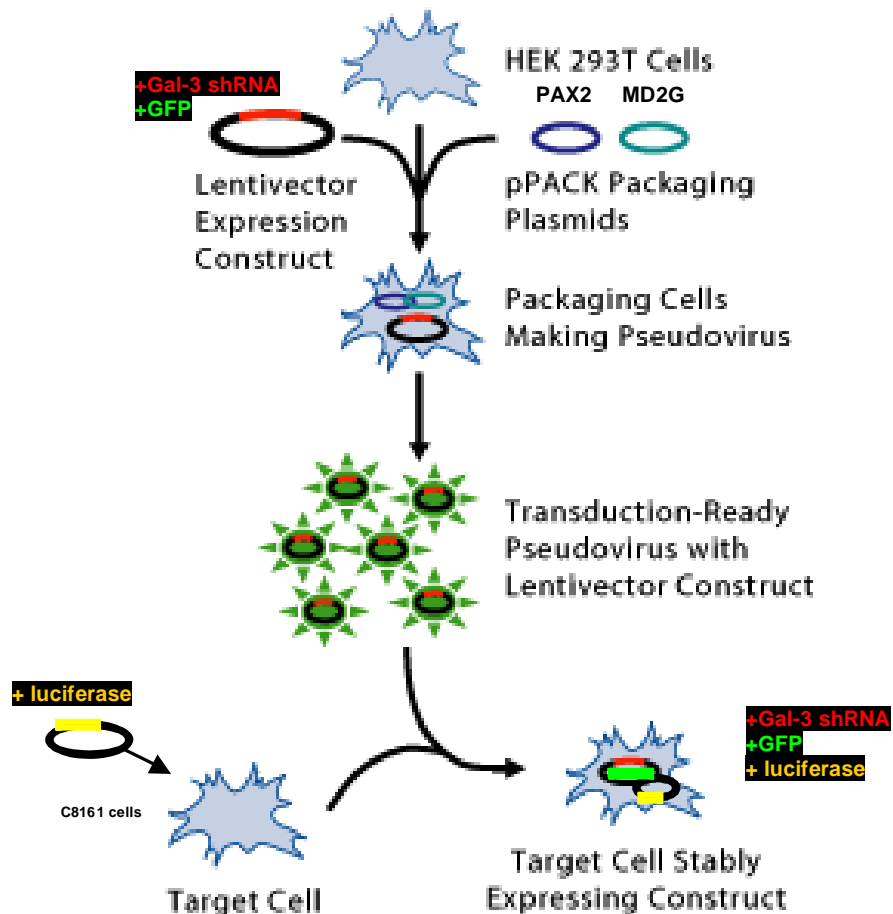


Figure 5 Schematic of Lentiviral production.

After transfection of the Gal-3 shRNA construct, which is green-fluorescent protein (GFP) labeled, together with the packaging plasmids PAX2 and MDG2 into the 293 T cells, the packaging cells produced pseudovirus. After virus production the melanoma cell line C8161, which contains a luciferase plasmid construct are transduced with the pseudovirus and grown in culture. The GFP⁺ cells were sorted with FACS and amplified in cell culture. The stable transfected cells were further used in vitro and in vivo (www.systembio.com).

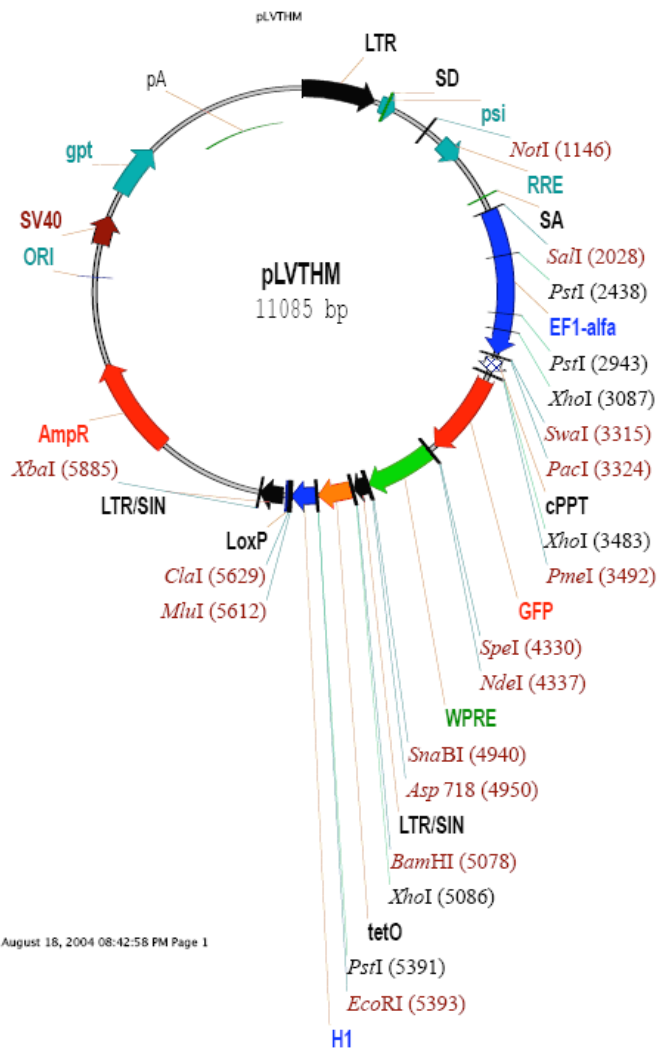


Figure 6 pLV-THM vector construct.

The pLV-THM vector was provided by Didier Trono. The pLV-THM vector is 11085 bp long and expresses the green fluorescence protein GFP and the H1 promoter. The shRNAs were cloned into the vector as described in the text. The resulting construct pLVTH-A3 was designed through stable delivery of the shRNA expression cassette targeting the Gal-3 cDNA sequence.

MluI 19 nt sense siRNA loop 19 nt antisense siRNA stop ClaI
CGCGTCCCC NNNNNNNNNNNNNNNNNNN TTCAAGAGA NNNNNNNNNNNNNNNNNNN TTTTT GGAAAT
AGGGG NNNNNNNNNNNNNNNNNNN AAGTTCTCT NNNNNNNNNNNNNNNNNNN AAAAA CCTTAGC

Forward oligo (67 nt):

cggtccccGTACAATCATCGGGTTAAATTtcaagagaTTTAACCCGATGATTGTACTT ttttggaat

Reverse oligo (65 nt):

CGATTCCAAAAGTACAATCATCGGGTTAAATTTCTCTTGATTTAACCCGATGATTGTACTT GGGGA

**Target sequence for Gal-3 shRNA : 5'-CGC GTC CCC GTA CAA TCA TCG GGT
TAA ATT CAA GAG ATT CAA GAG ATT TAA CCC GAT GAT TGT ACT TTT
TGG AAA T-3'**

Sense: GTACAATCATCGGGTTAAATT

Antisense: TTTAACCCGATGATTGTACTT

Target sequence for NT shRNA : NNAGATTAGTCTCCATCAATA

Sense: AGATTAGTCTCCATCAATATT

Antisense: TATTGATGGAGACTAATCTTT

Figure 7 Forward and reverse target oligo sequences for direct cloning of the shRNA into the pLV-THM lentiviral vector.

For direct cloning of the shRNA into the pLV-THM lentiviral vector the shRNA for Gal-3 and nontargeting (NT) shRNA must be designed with above described oligos as described by Didier Trono (www.tronolab.com).

2.11.4 Target cell transduction

The C8161 cells were seeded into a 6-well plate one day before the infection so that at the day of the infection the cell confluency would be reached about 20-30%. After removal of the medium and replacement with 1ml of the virus stock solution, polybrene was added to a final concentration of 3 µg /ml. Twenty-four hours later the infection mixture was removed and replaced with growth medium. The cells were grown and enriched to be GFP sorted with FACS analysis (see section 2.11.2). Top 70% GFP positive cells were collected, enriched and characterized for their knockdown effects via *in vitro* and *in vivo* functional assays.

2.12 Zymography

MMP-2 activity was determined on substrate-impregnated gels (Luca et al. 1997) with minor modifications. Approximately 5×10^3 melanoma cells were plated in 6-well dishes and allowed to attach for 24 hours, then the 10%FBS in normal growth medium (cMEM) was removed and replaced with serum-free medium overnight. The supernatant was collected, the volume was adjusted to the cell number, and the supernatant (total of 60 µl) was loaded on gelatin-impregnated (1mg/ml: Sigma, St. Louis, MO) SDS-8% polyacrylamide gels and separated under nonreducing conditions. As a positive control, 10% FBS in CMEM and as negative control serum-free medium was employed. Plates were shaken for one hour in 2.5% Triton X-100 (Fisher Scientific, Fair Lawn, New Jersey) to remove all the SDS from the gels. Plates were then removed and the gels were incubated for 16 hours at 37°C in 50mM Tris, 0.2 M NaCl, 5 mM CaCl₂, and 0.002% Brij 35 (w/v) at pH 7.6. At the end of the incubation, the gels were stained with 0.5% Comassie G 250 (Bio-Rad, Hercules, CA) in methanol/acetic acid/H₂O (30:10:60). The

intensity of the various bands was determined through quantification of a scanned image (Hp Scan Jet 5370C).

2.13 Invasion Assay through Matrigel

Invasion of highly metastatic melanoma cells was measured by plating the use of the Biocoat Matrigel invasion chambers (Becton-Dickinson) which were primed according to the manufacturer's directions. A solution of 5% FBS in DMEM medium was placed in the lower well to act as a chemoattractant and 2.5×10^3 cells in 500 μ l of serum-free medium were placed in the upper chamber of the Matrigel plate and incubated at 37°C for 22 hours. Cells on the lower surface of the filter were stained with Diff-Quick (American Scientific Products, McGraw Park, IL) and quantified with an image analyzer (Optimas 6.2) attached to an Olympus CK2 microscope. The data were expressed as the average number (\pm SD) of cells from 8 fields that migrated to the lower surface of the filter. Data was collected from two performed experiments.

2.14 RNA Extraction

Total RNA was extracted using Trizol Reagent (Invitrogen, Carlsbad, CA) according to the manufacturer's instructions. Briefly, cells were grown to 70-80% confluency, washed with PBS, and lysed in Trizol reagent. Proteins and DNA were extracted in 0.2 volumes of chloroform. RNA was precipitated from aqueous phase with an equal volume of isopropanol, washed with 75% ethanol, and resuspended in DEPC-treated water. RNA concentration was determined by measuring the absorbance at 260 nm in an UV/Visible Spectrophotometer Ultrospec 3000 pro (Amersham Pharmacia Biotech, Cambridge, England).

2.15 RT-PCR

One microgram of total RNA was reverse-primed with an oligo poly-dT primer and extended with MMLV reverse transcriptase (Clonotech, Palo Alto, CA). Using the Clonotech Advantage cDNA PCR kit (Clonotech, Palo Alto, CA), the PCR was performed using a 50 µl reaction mixture containing 1X PCR buffer, 5µl cDNA, 0.2mM dNTP, and 2.5 Units of Taq polymerase. For quantitation of IL-8, cDNA was amplified by PCR using specific primers for IL-8 (sense, 5'-CTT CTA GGA CAA GAG CCA GGA AGA AAC CAC-3' and antisense, 5'- GTC CAG ACA GAG CTC TCT TCC ATC AGA AAG -3') and the housekeeping gene glyceraldehydes-3-phosphate dehydrogenase (GAPDH) (sense, 5'-GAG CCA CAT CGC TCA GAC-3' and antisense, 5'-CTT CTC ATG GTT CAC ACC C-3') was amplified as a control comparison. IL-8 and GAPDH cDNAs were amplified by PCR in the same reaction as follows: an initial denaturation for two minutes at 94°C; followed by 30 cycles of denaturation at 94°C for 30 seconds, annealing at 61°C for 45 seconds, and extension at 72°C for two minutes. A final elongation step was carried out at 72°C for seven minutes. The reaction products were separated on a 1% agarose gel and visualised after ethidium bromide staining under UV illumination.

2.16 Tissue Microarray (TMA)

Tissue microarrays were constructed utilizing a total of 89 clinical samples of melanocytic lesions including benign nevi (BN, 17 cases), dysplastic nevi (DN, 18 cases), melanoma in situ (superficial spreading, nodular, acral, and lentigo malignant melanoma) (MM, 23 cases), and metastatic malignant melanoma to subcutaneous tissue, lymph node, visceral organs (MMM, 31 cases). This progressive melanoma TMA was constructed by Dr. Victor Prieto from the Department of Pathology at the University of Texas MD

Anderson Cancer Center, Houston, Texas (Table 2). The specimens consisted of small biopsies or excisions of original patient lesions. The University of Texas MD Anderson Cancer Center Institutional Review Board approved the study.

For tissue microarray construction, hematoxylin and eosin-stained sections were reviewed from each block to define the selective areas. Either 0.6 mm (punch biopsies of benign and dysplastic nevi cases) or 1.0 mm (excision specimens) cylindrical cores of tissue were punched out from donor blocks to preserve the original tissue block. The selected tissue cores were inserted in a standard 4.5 x 2 x 1 cm recipient block using a manual tissue arrayer (Beecher Instruments, Silver Spring, MD) with an edge-to-edge distance of 0.1 or 0.15 mm. At least two tissue cores were taken for each case for a total of 187 cores in three tissue microarrays to control for sample variability (Figure 8). Two same control cases (one BN and one MM) were included in all three blocks as an inter-block control. Serial 5- μ m-thick sections of all three blocks were cut, and one standard hematoxylin and eosin-stained slide was examined to verify the presence of diagnostic lesional cells (Shen et al. 2003).

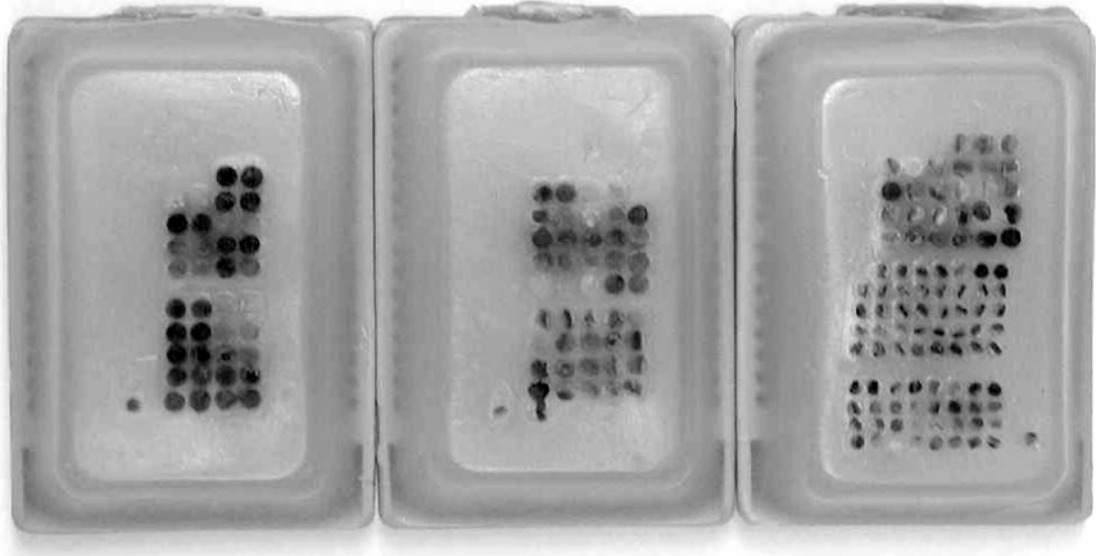


Figure 8 Three progression tissue microarray blocks of melanocytic lesions.

The three blocks were cut in 5- μ m-thick serial sections, provided from the Department of Pathology, University of Texas MD Anderson Cancer Center, Houston, Texas.

2.17 Immunohistochemical Analysis

Tumor tissue was fixed in 10% formalin (Fisher Scientific) for paraffin embedding or frozen in Optimal Cutting Temperature compound (Miles Laboratories, Elkhart, IN) in liquid nitrogen. Routine immunohistochemical staining protocols were used to detect α -Gal-3, IL-8 and MMP-2. The Gal-3 antibody staining was optimized using tissue sections before application to tissue microarray sections. Antigen retrieval was found to be unnecessary under the experimental conditions used. Tissues were washed three times for three minutes with PBS (Phosphate Balanced Saline) and treated with 3% H₂O₂ in methanol for 12 minutes to block endogenous peroxidase activity, followed by blocking solution (1% normal goat serum and 5% normal horse serum in PBS) for 15 minutes at room temperature. Gal-3 was detected by an overnight incubation with an anti- α -Gal-3 polyclonal antibody diluted 1:400 in blocking solution. Gal-3 immunoreactivity was detected using a horseradish-peroxidase conjugated goat anti- rabbit antibody (1:200; Jackson Immuno Research).

Two TMAs have been stained using two different chromogens, one with 3, 3'-Diaminobenzidine Tetra Hydrochloride (DAB) (brown; Open Biosystems, Huntsville, Alabama) and the other one with 3 Amino-Ethylcarbazole (RomulanAEC) (red; Biocare medical, Walnut Creek, CA) in order to avoid false-positive signal due to melanin (brown). They were counterstained with light hematoxylin for 10 seconds and Universal Mount (Research Genetics, Huntsville, AL) was used for mounting according to the supplier's instructions. Tissue Microarrays were examined under light microscopy and positive immunoreactivity was detected as a brown-reddish / red staining. The percentage of positive cells and the intensity of staining were recorded in a semiquantitative scale following a previously published method (Shen et al. 2003): 0 = 0-5% cells; 1 = 6-25%; 2 = 26-75%; 3 = >75%. The intensity of expression was

categorized into negative (0), weak (1), moderate (2), or strong (3). Lesions were considered positive when more than 25% of the cells expressed Gal-3, regardless the intensity of labeling. This cut-off was selected because it likely reflects clinically significant information, meaning that at least a quarter of the cells in the lesion will express the marker (Shen et al. 2003).

Further paraffin-embedded tumors were used to identify proliferating cell nuclear antigen (PCNA)-positive cells (ie, proliferating cells). For this reaction, the average measurement of the intensity of the staining was quantitated from 10 areas of each sample. Staining intensity was calculated with an image analyzer and the Optimas Image Analysis software (Bioscan, Edmonds, WA). For assessment of blood microvessel density, consecutive 5- μ m frozen tissue sections were cut, fixed in acetone, and stained with antibodies to CD-31/PECAM-1 (PharMingen, San Diego, CA), as described (Bruns et al. 2000). Seven tumors per group were stained for CD31 and pictures were taken of four fields of each slide with a Nikon Microphot-FX brightfield microscope equipped with a three-chip-charged coupled device (CCD) color video camera (Model DXC990, Sony Corp., Tokyo, Japan). Digital images were captured using Optimas Image Analysis software (Media Cybernetics, Silver Spring, MD).

2.18 Immunofluorescence Staining

Cells were fixed with acetone on the slides and stained for Gal-3. Immunofluorescence detection of Gal-3 expression was performed with polyclonal rabbit anti-Gal-3 and with a fluorescence marker anti-rabbit IgG Alexa 488 (1:400 dilution; green fluorescent) (Jackson Immunoresearch, West Grove, PA).

Immunofluorescence slides were counterstained with Hoechst stain and mounted using glycerol/PBS mounting media containing 0.1 M propyl gallate.

Images from H&E or immunohistochemically stained tissue microarray were collected using Zeiss photomicroscope (Carl Zeiss Inc., Thornwood, N.Y.) connected to a Sony Model DXC-960 MD Camera (Sony Corp., Tokyo, Japan). Images were acquired and analyzed using Optimas Image Analysis software (Media Cybernetics, Silver Spring, MD). Immunofluorescent microscopy was performed on a Zeiss Axioplan fluorescence microscope (Carl Zeiss Inc., Thornwood, N.Y.) equipped with 100W HBO mercury lamp and narrow bandpass excitation filters (Chrom Technology Corp, Brattleboro, VT) to individually select for green, red, and blue fluorescence. Images were captured with a cooled CCD Hamamatsu C5810 camera (Hamamatsu Photonics K.K., Bridgewater, NJ) and Optimas Image Analysis Software (Media Cybernetics, Silver Spring, MD) on a Dell computer (Round Rock, Texas). Composite photographs for publication were prepared using Adobe Photoshop software (Adobe Systems, Mountainview, CA).

2.19 In situ Terminal dUTP Nick End Labeling (TUNEL) Assay

Tissues were fixed in 10% buffered formalin solution and then embedded in paraffin. Thin sections (4 μm) were prepared, and the TUNEL assay was performed using a commercial kit according to the manufacturer's protocol (Promega). Briefly, tissue sections were deparaffinized and fixed at room temperature for five minutes in 4% paraformaldehyde. Cells were stripped of proteins by incubation for 10 minutes with 20 $\mu\text{g}/\text{ml}$ proteinase to increase permeability. The tissue sections were then permeabilized by incubating them with 0.5% Triton X-100 in Phosphate buffered Saline (PBS) for five minutes at room temperature. After being rinsed twice with PBS for five minutes, the slides were incubated with terminal deoxynucleotidyl transferase buffer for 10 minutes. Terminal deoxynucleotidyl transferase and biotin 16 labeled dUTP were then added in a 1:200 dilution to the tissue sections, which were incubated in a humid atmosphere at 37°C

for 1 hour. During this time TdT catalyzes the incorporation of labeled dUTP into the 3'OH ends of fragmented DNA. The slides were washed three times with PBS for five minutes. Prolong solution (Molecular Probes, Eugene, OR) was used to mount the coverslips. Immunofluorescence microscopy (FITC-dUTP) was performed using a 40x objective (Zeiss Plan-Neofluar) on an epifluorescence microscope equipped with narrow bandpass excitation filters mounted on a filter wheel (Lud1 Electronic Products, Hawthorne, NY) to select for green fluorescence. Images were captured using a cooled charge-coupled device camera (photometrics, Tucson, AZ) and SmartCapture software (Digital Scientific, Cambridge, United Kingdom) on a Macintosh computer. Images were further processed using Adobe PhotoShop software (Adobe Systems, Mountain View, CA). Quantitation of TUNEL was determined using the incorporation of biotin-labeled dUTP and this was visualized by incubation with peroxidase-streptavidin (1:400 dilution; Dako) and conventional 3,3'-diaminobenzidine substrate. Results are presented as the mean of counted dead cells in one field \pm SD of four pictures taken of each slide from seven tumors per group.

2.20 Enzyme-Linked Immunosorbent (ELISA) Assay

Tumor cells (2×10^5) were plated in six-well plates. When the cultures reached 70% to 80% confluency, fresh medium was applied and collected after an additional 24 hour incubation period, then clarified of cells and cell debris by centrifugation. The cells were harvested with trypsin-ethylenediaminetetra-acetic acid and counted. The conditioned media samples were stored at -20°C for later analysis, or used immediately for measurement of IL-8, using quantitative immunometric sandwich ELISA, following the procedure recommended by the manufacturer (R&D Systems, Minneapolis, MN). IL-8 concentration was calculated as the average of the three wells and expressed as pg of IL-8 protein / μg protein.

2.21 cDNA Microarray Analysis

Microarray analysis was performed using a custom made Gene Chip[®] Array, human Genome U133 Plus 2.0 Array featuring a total of 37,000 different human genes (Affymetrix). The microarrays were produced in the microarray core facility of Codon Biosciences (www.codonbiosciences.com). Total RNA was isolated from NT shRNA and Gal-3 shRNA knockdown cells with the Clontech (Takara Bio Co.)-Advantage RT-for PCR Kit (Mountain View, CA) according to the manufacturer's instructions.

The data was analysed using the Affymetrix program (www.affymetrix.com). The raw data were normalized per spot and per chip with intensity-dependent (Lowess) normalization (percent of the data used for smoothing =10%). Low hybridization signals were removed to yield an average of 794 differently expressed genes between control and knockdown cells. A significance level of three fold in decreased or increased data was chosen to limit the number of false-positive results.

2.22 Chromatin Immunoprecipitation (ChIP) Assay

The ChIP assay was performed using the reagents provided in a ChIP-IT kit obtained from Active Motif (Carlsbad, CA, USA). Cells were plated at a density of 4×10^6 cells onto 15 cm dishes and were treated with 1% formaldehyde in fresh medium at 37°C for 10 minutes followed by the addition of 0.125M glycine. The medium was removed, and the cells were suspended in 1 ml ice cold PBS containing protease inhibitors. Cells were pelleted, resuspended in 200 μ l of SDS lysis buffer (1% SDS, 10 mM EDTA, and 50 mM Tris-HCL, pH 8.1) containing protease inhibitors and incubated for 10 minutes on ice. The DNA was sheared into 200-1000 bp fragments by homogenizing the pellet with 10 dounce hits and a following incubation with an

enzymatic shearing cocktail at 37°C for 10 minutes. An aliquot was substituted with NaCl and RNase and incubated for 1.5 hours at 42°C and the sheared control was loaded on a 2% agarose gel to confirm the shearing efficiency. The supernatant containing enzymatic sheared DNA was collected after centrifugation at 14000 rpm for 10 minutes at 4°C and then mixed with antibody directed to EGR-1 and IgG control and crosslinked to magnetic beads. An overnight incubation with agitation with the supershift antibody and the magnetic beads was performed. Before that step, 10 µl of the chromatin solutions were saved as control (Input DNA) for the total DNA amounts of each sample. After washing the magnetic beads with Chip buffer 1 and 2, the immune complexes were then eluted from the magnetic beads and proteins were reverse crosslinked in 5M NaCl and Chip buffer 2 at 65°C for 2.5 hours. Proteins were digested with 2 µl of Proteinase K at 37°C for one hour and extracted in Elution buffer and analyzed by PCR. The input DNA had to be purified by phenol/ chloroform extraction and ethanol precipitation using 20mg/ml glycogen as carrier. A 805-bp fragment spanning +2100 to -500 region of the CDH5 promoter was amplified by PCR using primer sequences 5'-CCC AGC CAC AAA GGA ACA ATA-3' and 5'-TGT GGG CTG AGG GAT GTT TCT GTT- 3' for detection of possible SP1, AP-2, NFkB and EGR-1 transcription binding. For the detection of CreB binding on the CDH5 promoter, the following primers were designed: 5'- AGC CTC CCT GTC ACC TTT AAA GTC C-3' and 5'- GCT GCA GCA TCA CAT TTA ACC CTC-3'. A 133-bp fragment spanning -133 +44 region of the IL-8 promoter was amplified by PCR using primer sequences 5'-AAG TGT GAT GAC TCA GGT TTG CCC-3' and 5'- ATG GTT CCT TCC GGT GGT TTC TTC-3'.

The PCR condition was the same for all primers and was subjected to initial denaturation step for 3 minutes at 94°C, followed by 35 cycles of denaturation for 20 seconds at 94°C, annealing at 55°C for 30 seconds and extension at 72°C for 30 seconds. Then reaction

was subjected to a final extension time of 10 min at 72°C. PCR products were analyzed on a 3% agarose gel containing ethidium bromide and visualized under UV light.

2.23 Densitometric Quantification

Images were captured in a Gel Doc 2000 System (Bio-Rad Laboratories, Hercules, CA) connected to a CCD camera. Densitometric reading of DNA fragments separated in agarose gels, were quantitated using Quantity One Software Version 4 for Windows (Bio-Rad Laboratories, Hercules, CA). Western Blot densitometric analysis was performed in the linear range of the film, using ImageJ program (downloaded from www.nih.gov). The densitometric data presented are relative to the actin loading control.

2.24 Statistical Analysis

The McNemar and Stuart-Maxwell tests were used to assess the intra-group association in the TMA studies. To perform a McNemar or Stuart-Maxwell test, the frequency table is required to be square (same number of rows and columns). Thus, in some of the evaluations performed, a frequency of 0.00001 was added in the corresponding cell of the row (level) or column that was not observed (i.e., zero count). Furthermore, since some of the levels had few samples within that level, consecutive levels (i.e., 2 and 3) of the variable were collapsed.

The Fisher's exact test was used to test the inter-group association between all the groups and pairs of groups in the TMA studies. Due to the various two-group comparisons performed, we used the Bonferroni correction to adjust the significance level for an individual test to maintain an overall significance level of 5%. For example, since seven two-group comparisons were performed, an individual significance level of 0.0071 ($0.05/7=0.0071$) was used. Statistical analysis was carried out using SAS[®] 8.02 (Cary

NC, USA). Disease-free survival and overall survival were analyzed with the Log-rank test using JMP[®] 5.1 Software (Cary NC, USA).

The Student's t-test was used to evaluate the *in vivo* data of the lung metastasis experiment between the parental, non-targeted shRNA and the Gal-3 shRNA groups. Given those data sets, each characterized by its mean, standard deviation, and number of data points, it is possible to determine whether the means are distinct, provided that the underlying distributions can be assumed to be normal.

The Mann Whitney U test was used for all *in vitro* and *in vivo* analysis, which is a non-parametric test for assessing whether two samples of observations come from the same distribution. The null hypothesis is that the two samples are drawn from a single population, and therefore that their probability distributions are equal. It requires the two samples to be independent, and the observations to be ordinal or continuous measurements, i.e. one can at least say, of any two observations, which is the greater.

Chapter III:

3. RESULTS

3.1 Specific Aim I:

3.1.1. Pattern of Gal-3 expression during melanoma progression

3.1.1.1 Tissue microarray analysis

In order to investigate the pattern of expression of Gal-3 in melanoma, a tissue microarray of melanocytic lesions was stained with an anti-Gal-3 antibody. The tissue microarray included 89 melanocytic lesions, which were included in three tissue microarray blocks (see Materials and Methods; Figure 8). The lesions were obtained from a broad spectrum of 17 cases of benign nevi (BN), 18 cases of dysplastic nevi (DN), 23 cases of Melanoma (MM) and 31 cases of metastatic melanoma. The lesions from the melanoma stage are subclassified into 10 cases of superficial spreading, 2 cases of nodular, 4 cases of acral lentiginous and 7 cases from Lentigo maligna. Within the metastatic melanoma lesion specimens were 9 cases of lymph node metastases, 12 of subcutaneous metastases and 10 visceral metastases (Table 1).

Immunohistochemical staining showed a highly predominant cytoplasmic staining of Gal-3 (Figure 9). Cytoplasmic and nuclear expression of Gal-3 was observed with levels of expression increasing from BN to DN to MM to MMM. A highly significant difference between these subgroups was detected with a p-value of $*p < 0.0001$ (percentages of melanocytic cells with cytoplasmic Gal-3) to $*p = 0.0073$ (intensity of cytoplasmic expression) with the exception of nuclear intensity, which showed only a trend to a level of 0.09 (Tables 2).

Melanocytic Lesions (included in the tissue microarrays)

Melanocytic Lesions	Cases (<i>n</i>)
Benign Nevi (BN)	17
Dysplastic Nevi (DN)	18
Melanoma (MM)	23
Superficial spreading	10
Nodular	2
Acral lentiginous	4
Lentigo maligna	7
Metastatic Melanoma (MMM)	31
Lymph node metastasis	9
Subcutaneous Metastasis	12
Visceral metastasis	10

Table 1 Melanocytic Lesions included in the tissue microarray

From the Department of Pathology of the University of Texas MD Anderson Cancer Center were following 89 cases of melanocytic lesions obtained in three tissue microarrays blocks (see Figure 8). Included were specimens from benign nevi (BN, 17 cases), dysplastic nevi (DN, 18 cases), melanoma in situ (superficial spreading, nodular, acral, and lentigo malignant melanoma) (MM, 23 cases), and metastatic malignant melanoma to subcutaneous tissue, lymph node, visceral organs (MMM, 31 cases).

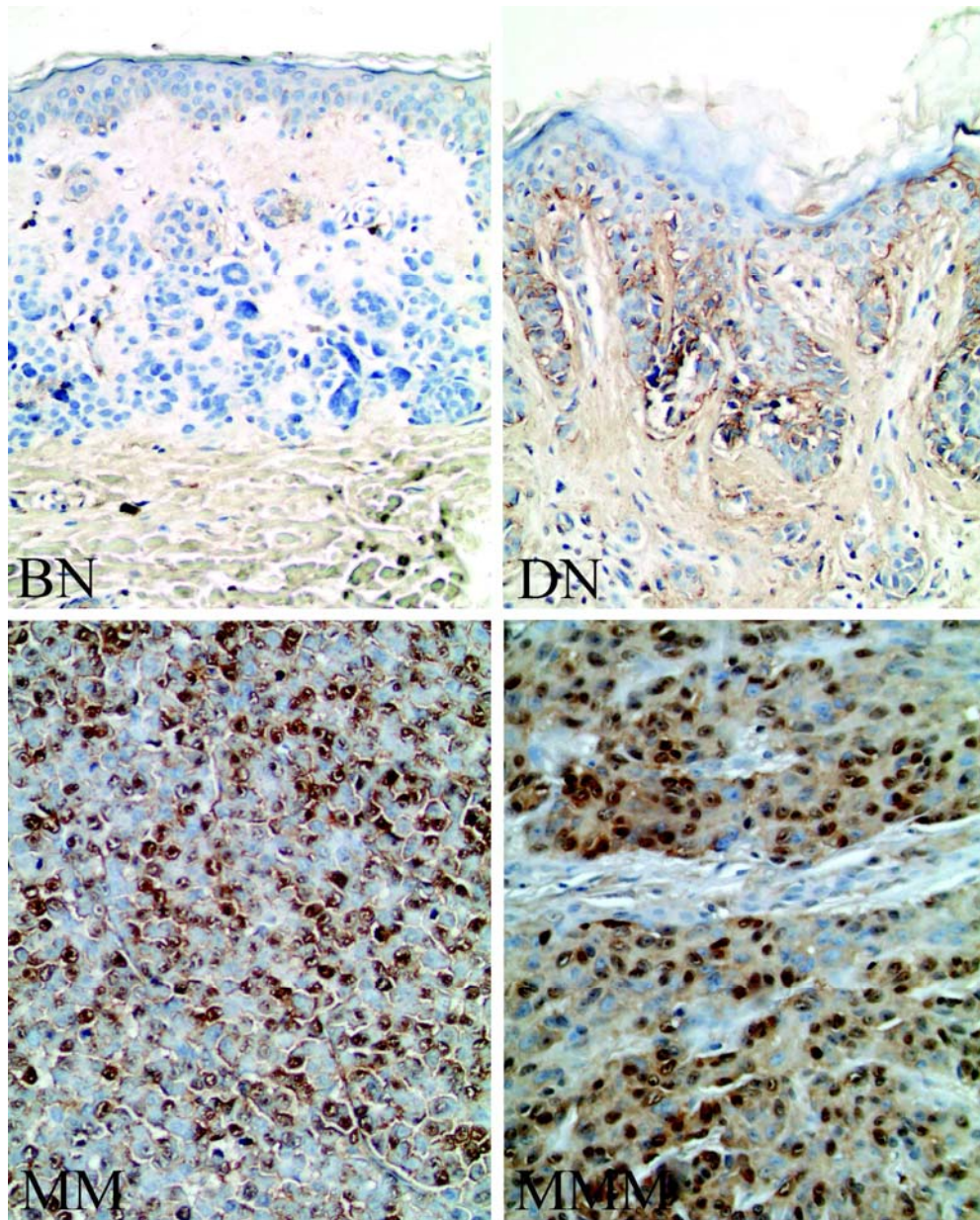


Figure 9 Gal-3 expression in benign nevi (BN), dysplastic nevi (DN), melanoma (MM), and metastatic melanoma (MMM).

Representative examples of immunohistochemical staining performed as described in section 2.17 are shown (40x magnification). Gal-3 expression is visualized as a brown precipitate. BN and DN expressed Gal-3 predominantly in the cytoplasm, whereas in MM and MMM Gal-3 expression was cytoplasmic and nuclear.

A. Intensity of Gal-3 Cytoplasmic Expression

Cytoplasmic Intensity Levels	Nevi		DN		MM		MMM		Total	<i>p-value*</i>
	<i>n</i>	%	<i>n</i>	%	<i>n</i>	%	<i>n</i>	%		
	0	1	5.9	0	0.0	3	11.5	3		
1	11	64.7	22	100.0	17	65.4	15	51.7	65	
2	5	29.4	0	0.0	6	23.1	10	34.5	21	
3	0	0.0	0	0.0	0	0.0	1	3.5	1	

**p-value from the Fisher's exact test*

B. Percent Cytoplasmic Expression

Cytoplasmic Intensity Levels	Nevi		DN		MM		MMM		Total	<i>p-value*</i>
	<i>n</i>	%	<i>n</i>	%	<i>n</i>	%	<i>n</i>	%		
	0	2	11.8	0	0.0	4	15.4	3		
1	6	35.3	20	90.9	8	30.8	4	13.8	38	
2	7	41.2	2	9.1	12	46.2	17	58.6	38	
3	2	11.8	0	0.0	2	7.7	5	17.2	9	

**p-value from the Fisher's exact test*

C. Intensity of Gal-3 Nuclear Expression

Nuclear Intensity Levels	Nevi		DN		MM		MMM		Total	<i>p-value*</i>
	<i>n</i>	%	<i>n</i>	%	<i>n</i>	%	<i>n</i>	%		
	0	10	58.8	14	63.6	12	46.2	14		
1	6	35.3	8	36.4	13	50.0	8	27.6	35	
2	1	5.9	0	0.0	1	3.8	7	24.1	9	
3	0	0.0	0	0.0	0	0.0	0	0.0	0	

**p-value from the Fisher's exact test*

D. Percent Nuclear Positive Cells

Nuclear Intensity Levels	Nevi		DN		MM		MMM		Total	<i>p-value*</i>
	<i>n</i>	%	<i>n</i>	%	<i>n</i>	%	<i>n</i>	%		
	0	11	64.7	19	86.4	13	50.0	14		
1	6	35.3	3	13.6	11	42.3	7	24.1	27	
2	0	0.0	0	0.0	2	7.7	8	27.6	10	
3	0	0.0	0	0.0	0	0.0	0	0.0	0	

**p-value from the Fisher's exact test*

Table 2 Cytoplasmic and Nuclear Expression Levels of Gal-3.

Benign nevi (BN), dysplastic nevi (DN), melanoma (MM), and metastatic melanoma (MMM). Intensity of expression was determined as described in section 2.17. Levels were defined in section 2.24. (A) Cytoplasmic intensity levels of Gal-3 expression; (B) Percentage of cytoplasmic Gal-3 positive cells among Benign nevi (BN), dysplastic nevi (DN), melanoma (MM), and metastatic melanoma (MMM); (C) Nuclear intensity levels of Gal-3 expression; (D) The comparison of nuclear percentage of Gal-3 expression.

A significant correlation between Gal-3 expression and the histologic subtype and localization of the melanoma was observed (Figures 10, 11). Gal-3 expression was subclassified into areas of high sun exposure (head and neck, arms), intermittent (trunk, legs) and acral (hands and feet). No Gal-3 expression in acral primary melanomas (n=4) was observed (Figure 10 top row). Lesions from the back (n=4) express Gal-3 only in the cytoplasm, whereas the scalp lesion shows a strong cytoplasmic and nuclear Gal-3 expression. Metastatic melanoma lesions stained for Gal-3 revealed that most subcutaneous metastases (n=12) expressed cytoplasmic Gal-3 as shown in Figure 10 (bottom row) and only one nuclear expression of Gal-3 shown in Figure 11. Also, metastases to the lung showed a highly predominantly cytoplasmic expression of Gal-3, whereas strong nuclear and cytoplasmic expression was observed in lymph node metastases.

Detection of cytoplasmic expression of Gal-3 in more than 50% (5/9) of sun-exposed lesions (head, neck and arms) was observed, whereas only three of these cases had nuclear expression of Gal-3. In intermittent sun exposed lesions, Gal-3 was expressed in 66% (6/9) in the cytoplasm. Overall, nuclear expression of Gal-3 was highly significant only in lesions on frequently sun-exposed areas (Figure 11).

It was observed, with respect to a possible relationship with Breslow thickness, that in thicker melanomas Gal-3 expression in the cytoplasm was increased, but this was not statistically significant (*p=0.15). Also no significant correlation of Gal-3 expression in the presence or absence of ulceration in primary melanomas was seen (data not shown).

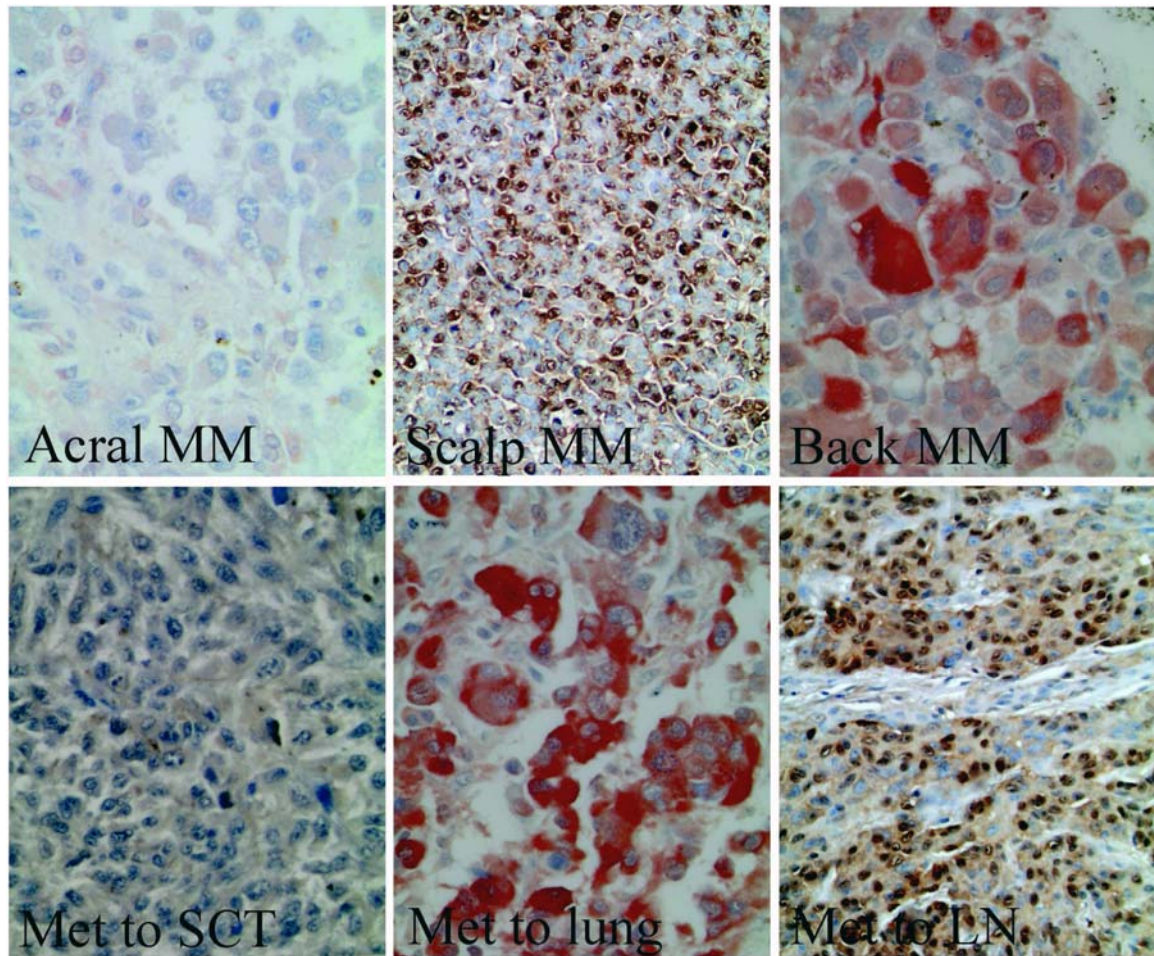


Figure 10 Gal-3 expression in primary and metastatic melanoma.

Representative examples of immunohistochemical staining performed as described in section 2.17 are shown. Gal-3 expression is visualized as a brown (DAB chromogen) or red (AEC chromogen) precipitate. The top row shows Gal-3 expression in primary melanomas (acral, scalp, back); the bottom row shows metastatic melanoma expression of Gal-3 (subcutaneous, lung, lymph node) (40x magnification).

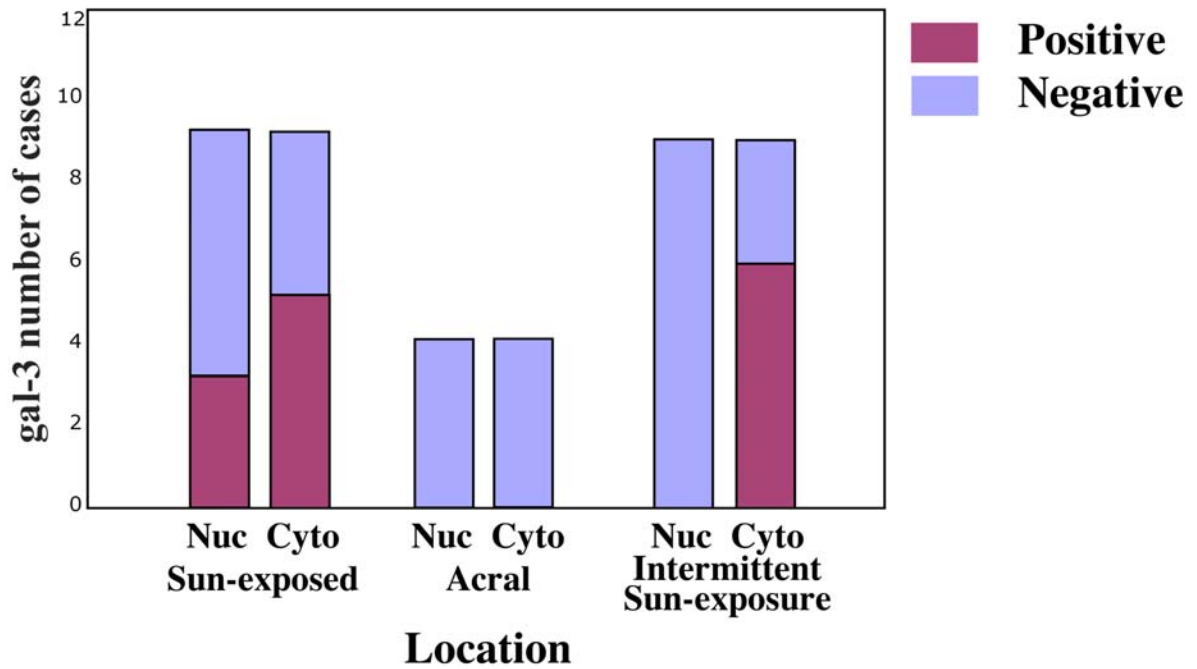


Figure 11 Gal-3 expression subclassified into sun-exposed areas in primary melanoma.

Areas of high sun exposure (head and neck, arms), intermittent (trunk, legs) and acral (hands and feet) are compared. No Gal-3 expression was seen in acral lesions.

Intermittently sun-exposed lesions showed cytoplasmic but not nuclear expression;

Nuclear expression was only seen in lesions of sun-exposed areas (*p=0.048 and

*p=0.038 for nuclear and cytoplasmic expression, respectively).

Figure 12 shows Gal-3 expression in different types of metastasis, which is statistically significant for both nuclear and cytoplasmic expression (*p=0.038 and *p=0.001, respectively). Cytoplasmic expression was seen in subcutaneous metastases (n=12) and only very rarely nuclear translocation of Gal-3 (Figures 10 and 12). A higher nuclear Gal-3 expression was detected in lymph node metastases (n=9). Visceral metastases (n=10) showed a slightly higher expression level in the nuclear than in the cytoplasm.

Patients with visceral metastatic lesions had a worse prognosis than those with subcutaneous metastasis or metastasis to the lymph node (*p<0.02) (data not shown). A statistically significant difference in Gal-3 expression between the subcutaneous, visceral and lymph node metastases was identified through analysis of the cytoplasmic level/ nuclear level (*p=0.01 and *p=0.008 for intensity and percentage ratios, respectively).

An almost significant association between disease-free survival and nuclear to cytoplasmic ratio of Gal-3 expression in patients with primary or metastatic lesions was observed (*p=0.09), as shown in Figure 13. Those patients, which had an equal or higher Gal-3 expression in the nucleus than the cytoplasm, displayed a worse prognosis than those with nuclear percentages lower than cytoplasmic.

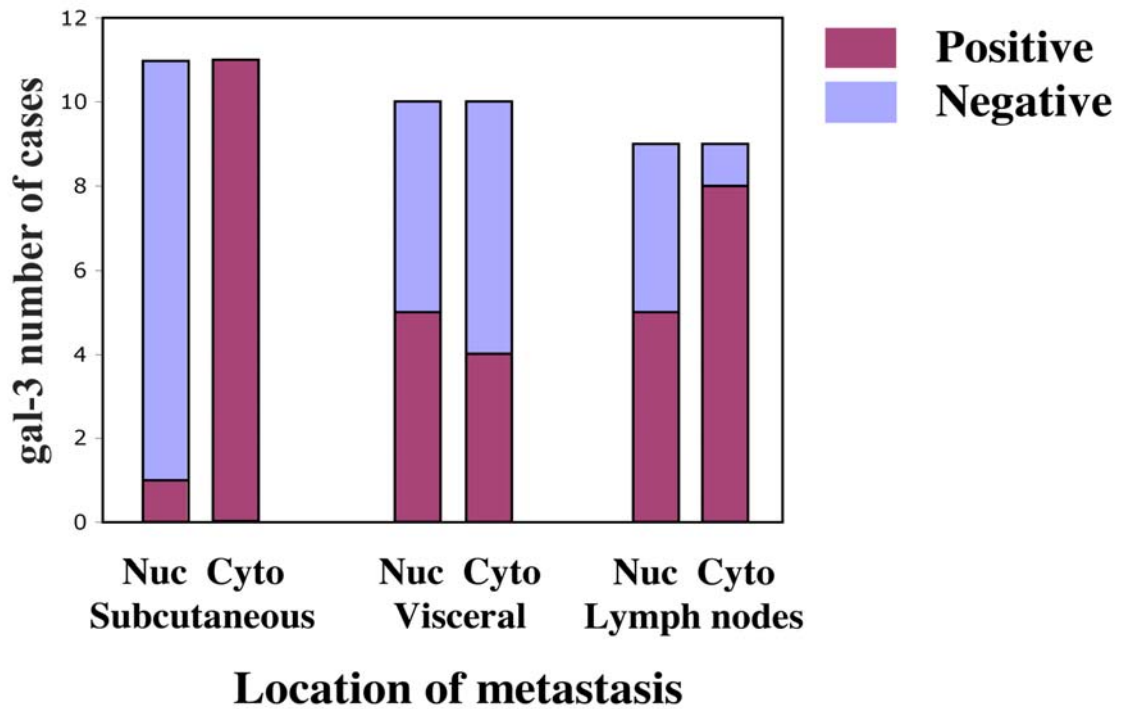


Figure 12 Gal-3 expression in different types of metastatic lesions.

Gal-3 in the subcutaneous lesions was expressed in the cytoplasm with rare nuclear expression. A higher nuclear expression was seen in lymph node metastases. The viscera expressed Gal-3 higher nuclear than cytoplasmic. The results were statistically significant when comparing nuclear and cytoplasmic expression in each group with each other (*p=0.038 and *p=0.001, respectively).

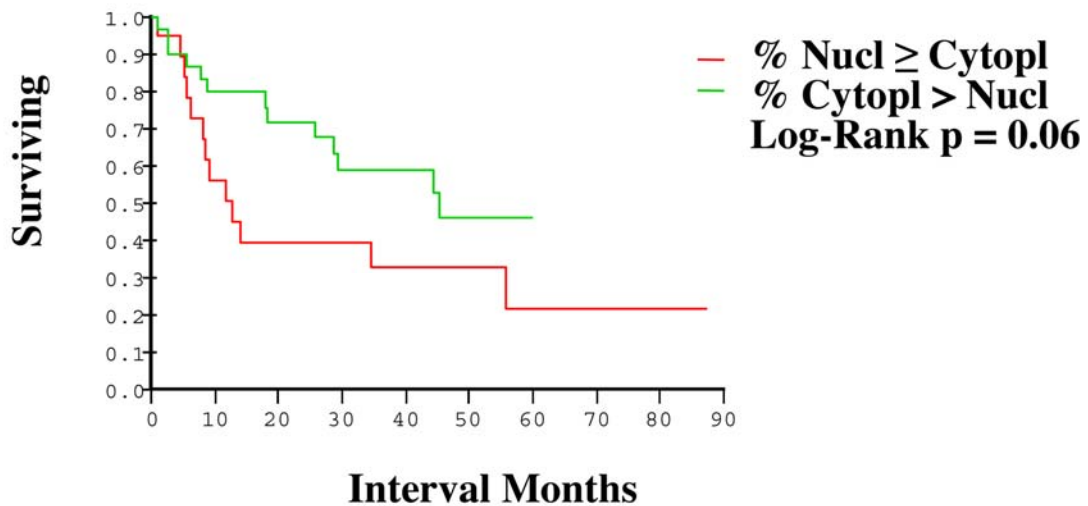


Figure 13 Disease free survival analysis and nuclear / cytoplasmic ratio of Gal-3 expression

Kaplan-Mayer survival analysis revealed a trend of worse prognosis for patients that had nuclear percentages higher than the cytoplasmic percentages. These differences approached statistical significance (*p=0.06). The ratio was calculated upon the number of cells expressing nuclear Gal-3 versus number of cells expressing Gal-3 in the cytoplasm.

In summary, the analysis of Gal-3 expression in melanocytic lesions revealed that:

- a) Cytoplasmic and nuclear expression levels of Gal-3 increase as lesions progress from the benign nevi to dysplastic nevi stages, as well as from the primary melanoma to metastatic melanoma stages.
- b) Tumors located on sun-exposed skin areas displayed high nuclear expression of Gal-3 and low cytoplasmic expression levels.
- c) Analysis of metastatic lesions revealed that subcutaneous metastases display only cytoplasmic expression of Gal-3, whereas lymph node metastases showed higher nuclear Gal-3 expression.
- d) Patients which had an equal or higher Gal-3 expression in the nucleus than in the cytoplasm experienced a worse prognosis than patients whose nuclear expression percentages were lower than cytoplasmic.

3.2 Specific Aim II:

3.2.1 Effect of Gal-3 shRNA on tumor growth and metastasis in vivo

3.2.1.1 Expression of Gal-3 in melanoma cell lines

After identifying Gal-3 as a marker of metastatic progression of melanoma by utilizing progression tissue microarray, Gal-3 expression in metastatic cell lines grown in vitro compared to non-metastatic cell lines was analysed by Western Blot, as shown in Figure 14 (see section 2.9). This confirmed that Gal-3 expression increases with increase in metastatic potential of melanoma cell lines. Low metastatic melanoma cell lines DM-4, DX-3 and TXM-40 showed less Gal-3 expression (Densitometric readings: 1, 2.8, and 1.6 respectively) than median metastatic melanoma cell lines (TXM-18= 4.8, TXM-1= 4.4, TXM-13= 5.1) or highly metastatic melanoma cells (MeWo= 4.7, WM2664= 4.8, A375SM= 4.0) with an exception of the highly metastatic C8161 cell line (Densitometric readings: 2.6).

The immunofluorescence stainings shown in Figure 15 reveal that the low metastatic cell line shows almost no Gal-3 staining (data not shown). The median metastatic cell line TXM-18 shows predominantly cytoplasmic staining of Gal-3. The highly metastatic cell line A375SM and WM2664 show, respectively, staining of Gal-3 mostly in the cytoplasm.

3.2.1.2 Stable downregulation of Gal-3 by lentiviral based shRNA

To delineate the role of Gal-3 on tumor growth and metastasis a shRNA knockdown for Gal-3 in C8161 spontaneous metastatic melanoma cells was created with lentiviral technology as described in sections 2.9 and 2.11. After transfection of the Gal-3 shRNA construct, which is green-fluorescent protein (GFP) labeled, together with the packaging plasmids PAX2 and MDG2 into the 293 T cells, the packaging cells start to

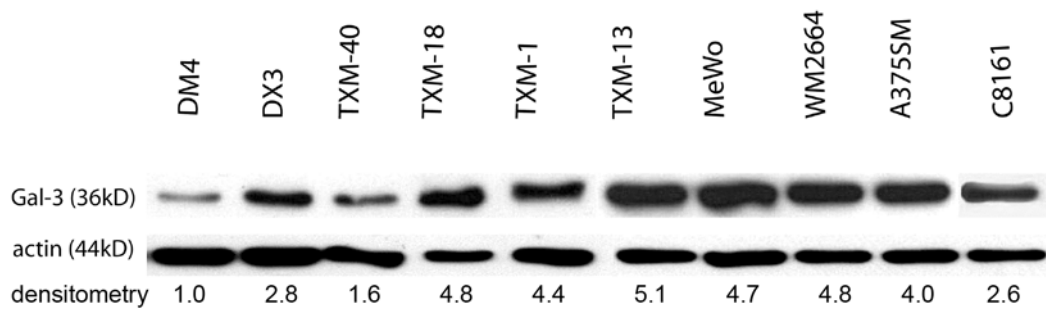


Figure 14 Gal-3 expression in melanoma cell lines.

Western Blot analysis revealed that Gal-3 expression directly correlates with the metastatic potential of cell lines in nude mice (low metastatic melanoma cell lines: DM-4, DX-3; median metastatic melanoma cell lines: TXM-40, TXM-18, TXM-1, TXM-13; highly metastatic melanoma cell lines: MeWo, WM2664, A375SM, C8161, metastatic potential was defined as described in section 2.1 10 ug of total cell lysate (section 2.8) were separated SDS-PAGE and transferred to a membrane as described in section 2.9. The membrane was stained with an antibody to Gal-3 and an antibody to actin as a control for protein loading.

The relative expression values for each cell line are shown underneath each lane (Densitometric analysis see section 2.23).

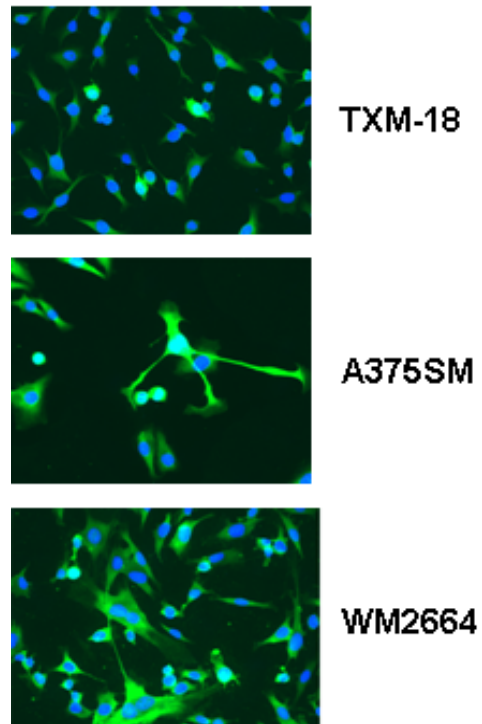


Figure 15 Immunofluorescence staining for Gal-3 expression in low to high metastatic cell lines.

Immunofluorescence staining was performed as described in section 2.18. The intermediate metastatic cell line TXM-18 shows cytoplasmic staining for Gal-3. The highly metastatic cell lines A375SM and WM2664 show mostly staining in the cytoplasm for Gal-3 (Gal-3 staining: Alexa 488 green; nuclei staining: Hoechst, blue).

produce pseudovirus. After virus production the melanoma cell line C8161, which contains a luciferase plasmid construct, were transduced with the pseudovirus and grown in culture and further used in all of the remaining experimental studies in this dissertation.

Gal-3 expression is three fold decreased in Gal-3 knockdown cells as compared to C8161 parental cells and cells transduced with non-targeting shRNA control vector (NT shRNA) (Densitometric readings: C8161 parental= 1, Nontargeting shRNA= 1.3, Gal-3 shRNA= 0.3; see section 2.23) (Figure 16).

3.2.1.3 Effect of Gal-3 downregulation on tumor growth in vivo

In order to monitor tumor growth capacity of the highly spontaneous metastatic C8161 cell line before and after Gal-3 knockdown, C8161 cells and C8161 Gal-3 shRNA cells were injected subcutaneously (s.c.) into nude mice and the tumor growth was monitored for 31 days as described in section 2.5. Gal-3 knockdown led to dramatic inhibition of tumor growth (t_{50}) by more than 40% (* $p < 0.01$), as shown in Figure 17. In the Gal-3 shRNA group, no increase in tumor volume was detected up until day 21. After day 21 tumors did grow, but at a significantly slower rate than the control NT shRNA group (* $p = 0.006$).

Tumors were additionally monitored with Luciferase imaging IVIS technology, which measures the light absorbance of the luciferase-labeled tumor cells within the tumor (see section 2.5). In Figure 18 and Table 3, the luciferase imaging of Gal-3 shRNA tumor cells versus NT shRNA control cells after 7, 14 and 27 days are shown. Comparing the tumor growth from day 7 with day 14 a 3.6 times reduction in the tumor volume of the Gal-3 knockdown cells ($131.52 \times 10^6 \pm \text{STD } 138.76$) compared to the

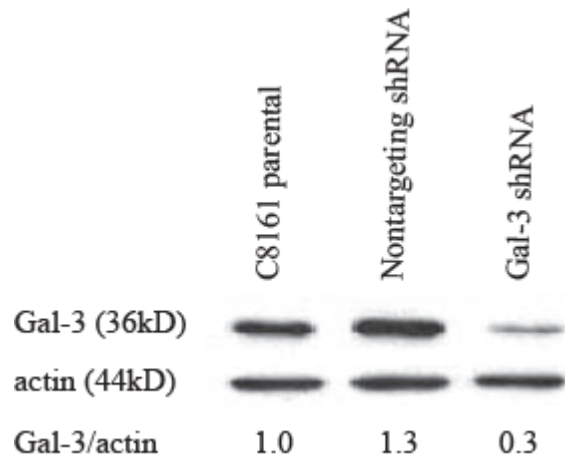


Figure 16 Gal-3 protein expression following downregulation with short hairpin RNA using lentiviral delivery.

20 ug of total cell lysate (section 2.8) were separated on a SDS-PAGE and transferred to a membrane as described in section 2.9. The membrane was stained with an antibody to Gal-3 and an antibody to actin as a control for protein loading. In comparison to the parental C8161 cell line and the non-targeting shRNA (NT shRNA), Gal-3 knockdown is 3 fold decreased (Densitometric readings: C8161 parental= 1, Nontargeting shRNA= 1.3, Gal-3 shRNA= 0.3; see section 2.23).

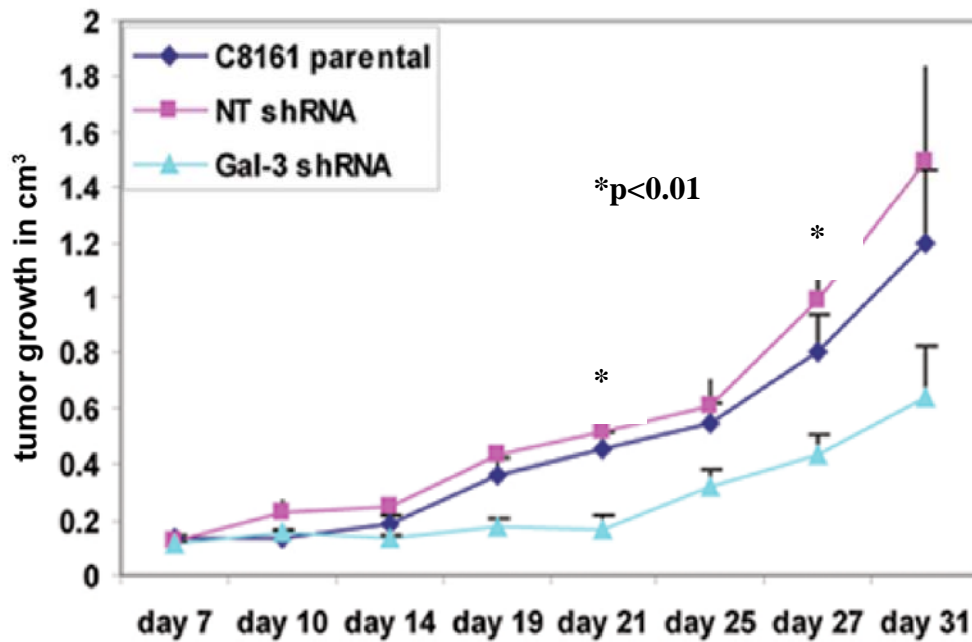


Figure 17 Effect of Gal-3 knockdown on tumor growth *in vivo* after s.c. injection.

Nude mice were injected with 2.5×10^5 C8161 tumor cells, Gal-3 shRNA expressing C8161 cells or control NT shRNA expressing C8161 cells (7 mice per group). Data are presented as mean tumor volume (cm³) with \pm STD. Downregulation of Gal-3 expression led to a decrease in tumor growth (t_{50}) by more than 40% (* $p < 0.01$).

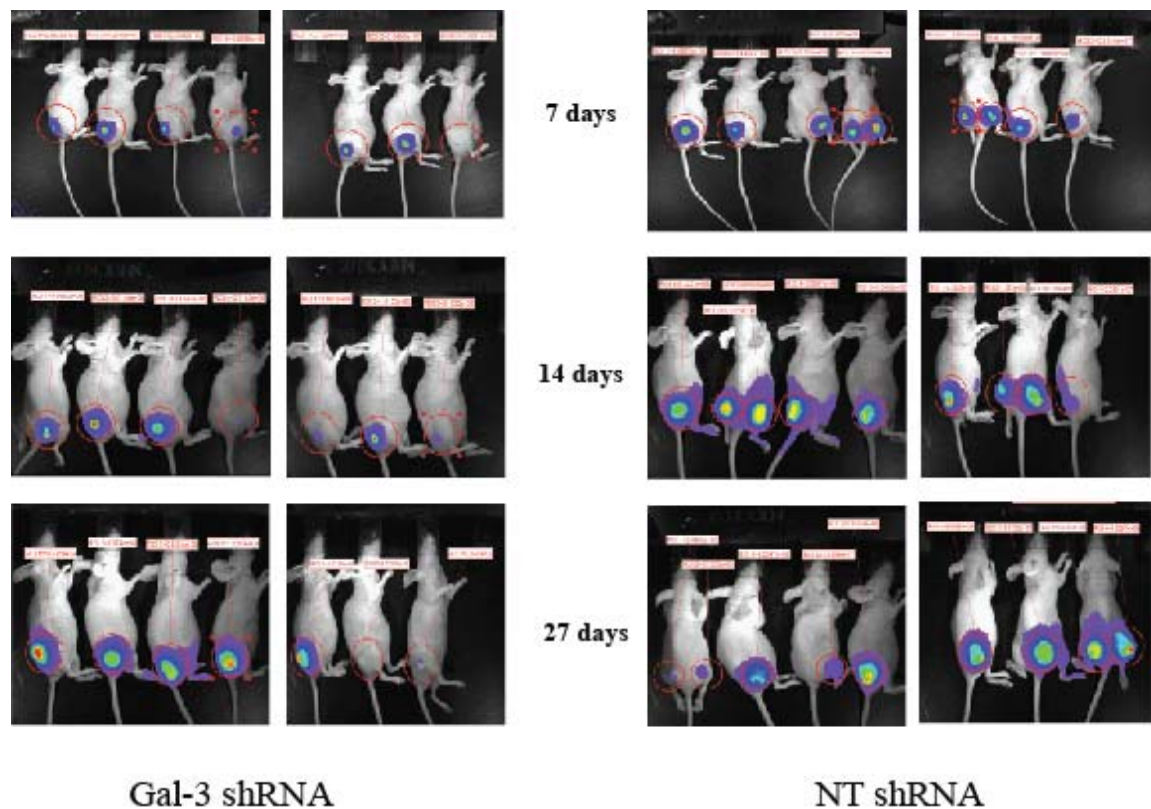


Figure 18 Luciferase Imaging with IVIS technology *in vivo* of the luciferase-labeled C8161 tumor cells after s.c. injection.

On the left side are the images taken from Gal-3 shRNA knockdown tumor cells compared to the NT shRNA tumor cells on the right side after 7, 14 and 27 days, respectively. A dramatic decrease in tumor size and light absorbance was detected after 27 days (Table 3).

	7 days	14 days	27 days
NT shRNA	465.57 x10 ⁶	428.45x10 ⁶	71.95x10 ⁶
	144.63x10 ⁶	192.2x10 ⁶	547.4x10 ⁶
	329.3x10 ⁶	720.3x10 ⁶	961.24x10 ⁶
	312.5x10 ⁶	22.39x10 ⁶	1657x10 ⁶
	467.49x10 ⁶	632.21x10 ⁶	1800x10 ⁶
	145.6x10 ⁶	533.75x10 ⁶	860.38x10 ⁶
	188.55x10 ⁶	865.69x10 ⁶	1378.8x10 ⁶
	115.84x10 ⁶	659.97x10 ⁶	984.17x10 ⁶
	51.814x10 ⁶	535.02x10 ⁶	1009.7x10 ⁶
Average	246.81x10⁶	509.99x10⁶	1030.07x10⁶
STD	152.86	263.34	535.55
Gal-3 shRNA	29.04x10 ⁶	4.17x10 ⁶	462.13x10 ⁶
	92.1x10 ⁶	101.53x10 ⁶	1.22x10 ⁶
	23.58x10 ⁶	3.18x10 ⁶	4.29x10 ⁶
	9.86x10 ⁶	196.52x10 ⁶	1048.5x10 ⁶
	27.29x10 ⁶	301.1x10 ⁶	837.4x10 ⁶
	56.48x10 ⁶	311.41x10 ⁶	953.24x10 ⁶
	0.79x10 ⁶	2.7x10 ⁶	1029.3x10 ⁶
Average	34.16x10⁶	131.52x10⁶	619.44x10⁶
STD	30.94	138.76	464.82

Table 3 Luciferase light absorbance data of Gal-3 shRNA versus NT shRNA tumor cells after s.c. injection.

This table represents the original data of the Luciferase absorbance \pm STD of the Gal-3 shRNA and NT shRNA groups after 7, 14, and 27 days. An almost 50% reduction of light intensity of the tumor cells between the Gal-3 shRNA group versus NT shRNA was detected after 27 days.

NT shRNA group ($509.99 \times 10^6 \pm \text{STD } 263.34$) was seen ($n=7$, respectively). An almost 50% reduction of the tumor cell light absorbance between the Gal-3 shRNA ($619.44 \times 10^6 \pm \text{STD } 464.82$) and the NT shRNA group ($1030.07 \times 10^6 \pm 535.55 \text{ STD}$) was seen after 27 days ($n=7$, respectively) (Table 3).

Table 3 shows the original measured light absorbance data to confirm the results described above.

3.2.1.4 Effect of Gal-3 downregulation on metastasis in vivo

The metastatic potential of C8161 cells was tested before and following Gal-3 knockdown using the mouse lung melanoma metastasis model. In this model tumor cells are injected intravenously (i.v.) and the formation of metastatic lesions in the lungs is monitored. Inhibition of Gal-3 expression in the C8161 cells led to a dramatic decrease in the number of melanoma lung metastases, as shown in Table 4. The median for C8161 NT shRNA cells was more than 200 metastases per mouse (Range 84->200, $n=6$), while for C8161 Gal-3 shRNA cells, the median was 22 metastases (Range 3-26, $n=8$). The incidence in both groups (number of mice developing metastases) remained at 100%.

The luciferase imaging after intravenous (i.v.) injection of Gal-3 shRNA tumor cells versus NT shRNA control cells after 14, 21, 27, 31, and 40 days is shown in Figure 19 and Table 5. An almost 90% reduction of the bioluminescence of the tumor cells between the Gal-3 shRNA and NT shRNA was observed at all time points except on day 14 (Gal-3 shRNA, $0.0 \times 10^5 \pm \text{STD } 0.0$; $n=8$; NT shRNA, $3.6 \times 10^6 \pm \text{STD } 4.6$; $n=6$). On day 21 the Gal-3 shRNA bioluminescence was $0.16 \times 10^5 \pm \text{STD } 0.189$ ($n=8$) compared to the NT shRNA group ($6.3 \times 10^6 \pm \text{STD } 11.2$; $n=6$). Also on day 31 the

Cell Line	Treatment	Median (No. of Metastasis)	Range (No. of Metastasis)	Incidence (No. of Mice)
C8161	NT shRNA	>200	9 → >200 (9, 89, >200, >200, >200, >200)	6 out of 6
	Gal-3 shRNA	22	3 → 46 (3, 9, 14, 22, 23, 27, 41, 46)	8 out of 8

Table 4 Mouse lung melanoma metastasis model after i.v. injection of Gal-3 shRNA and NT shRNA C8161 tumor cells.

Nude mice were injected with 1×10^6 tumor cells and the number of lung metastasis at day 36 was determined as described in section 2.5. Downregulation of Gal-3 resulted in an almost 90% decrease in the median number of metastasis when compared to non-targeting controls.

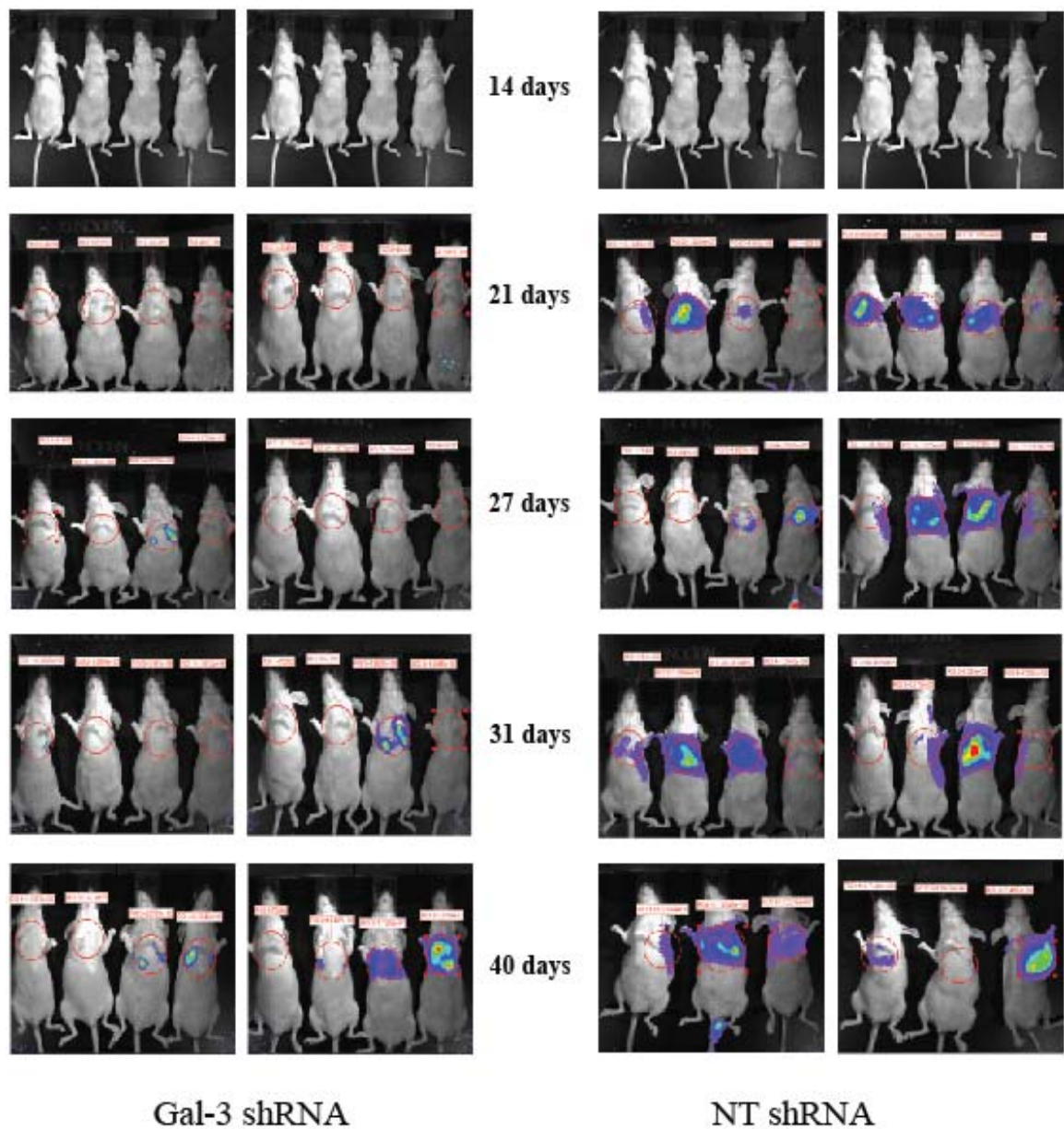


Figure 19 Luciferase Imaging with IVIS technology *in vivo* of the Luciferase-labeled C8161 tumor cells after i.v. injection.

On the left side are the images taken from Gal-3 shRNA knockdown cells compared to the NT shRNA cells on the right side after 14, 21, 27, 31, and 40 days, respectively. A marked decrease in tumor size and therefore bioluminescence was detected at all time points except on day 14.

	14 days	21 days	31 days	40 days
NT shRNA	0.31x10 ⁶	0x10 ⁶	0.64x10 ⁶	3.2x10 ⁶
	13.27x10 ⁶	0x10 ⁶	21.76x10 ⁶	112.5x10 ⁶
	0.44x10 ⁶	0.48x10 ⁶	8.7x10 ⁶	12.3x10 ⁶
	0x10 ⁶	1.59x10 ⁶	5.6x10 ⁶	9.7x10 ⁶
	6.65x10 ⁶	0.44x10 ⁶	182.1x10 ⁶	4.29x10 ⁶
	4.39x10 ⁶	17.5x10 ⁶	83.1x10 ⁶	748.5x10 ⁶
	3.83x10 ⁶	29.8x10 ⁶	1.8x10 ⁶	
	0x10 ⁶	0.49x10 ⁶	1375x10 ⁶	
Average	3.6x 10⁶	6.3x10⁶	43.4x10⁶	148.4x10⁶
STD	4.6	11.2	67.7	296.99
Gal-3 shRNA	0x10 ⁶	0x10 ⁶	0x10 ⁶	0.16x10 ⁶
	0x10 ⁶	0.13x10 ⁶	0x10 ⁶	0.18x10 ⁶
	0x10 ⁶	0.6x10 ⁶	1.61x10 ⁶	2.99x10 ⁶
	0x10 ⁶	0.1x10 ⁶	0.1x10 ⁶	3.59x10 ⁶
	0x10 ⁶	0.17x10 ⁶	0.33x10 ⁶	0x10 ⁶
	0x10 ⁶	0.138x10 ⁶	0.11x10 ⁶	1.54x10 ⁶
	0x10 ⁶	0x10 ⁶	0.21x10 ⁶	11.35x10 ⁶
	0x10 ⁶	0.15x10 ⁶	0.4x10 ⁶	70x10 ⁶
Average	0	0.16x10⁶	0.35x10⁶	11.26x10⁶
STD	0	0.189	0.53	24.16

Table 5 Luciferase light absorbance data of Gal-3 shRNA versus NT shRNA tumor cells after i.v. injection.

This table shows the original data of the Luciferase absorbance \pm STD of the Gal-3 shRNA and NT shRNA group after 14, 21, 27, 31, and 40 days. A near 90% reduction of light intensity of the tumor cells between the Gal-3 shRNA group versus NT shRNA was detected at each time point.

difference was 90% (Gal-3 shRNA, $0.35 \times 10^5 \pm$ STD 0.53; n=8; NT shRNA, $43.4 \times 10^6 \pm$ STD 67.7; n=6). A 13-fold decrease was observed after 40 days (Gal-3 shRNA, $11.26 \times 10^5 \pm$ STD 24.16; n=8; NT shRNA, $148.4 \times 10^6 \pm$ STD 296.99; n=6) (Table 5).

3.2.1.5 Effect of Gal-3 downregulation on in vivo cell proliferation, microvessel density (MVD) and apoptosis

In order to understand the mechanism of inhibition of tumor growth after Gal-3 knockdown tumor specimens were analyzed for the expression of markers of proliferation and angiogenesis. Hematoxylin and Eosin (H&E) staining revealed that Gal-3 shRNA tumor cells acquired a halo-like morphology, which appear with a nucleus surrounded with a swollen cytoplasm, as compared to parental or NT shRNA control tumors, which were more epithelioid (Figure 20, H&E). The significance of this morphological observation, however, is still unclear.

Immunohistochemical staining using an anti-Gal-3 antibody revealed very low Gal-3 expression levels in the Gal-3 shRNA tumors as compared to staining of tumors from the C8161 parental and NT shRNA ones (Figure 20, Gal-3). This confirmed that the Gal-3 knockdown was still effective in the tumor cells after 31 days *in vivo*.

Simultaneously, a strong 2.6-fold decrease in the percentage of proliferating (PCNA) positive cells was observed after Gal-3 knockdown compared to the C8161 parental and NT shRNA cell line (*p=0.003 C8161 parental, NT shRNA control versus Gal-3 shRNA tumors, respectively; Figure 20, 21A).

However, no difference in the *in vitro* cell proliferation was observed by MTT test (section 2.6, data not shown). In parallel with the decrease in the number of proliferating cells a dramatic increase in the number of apoptotic cells in the Gal-3 shRNA tumors compared to the C8161 parental and NT shRNA cell line was observed (Figure 20,

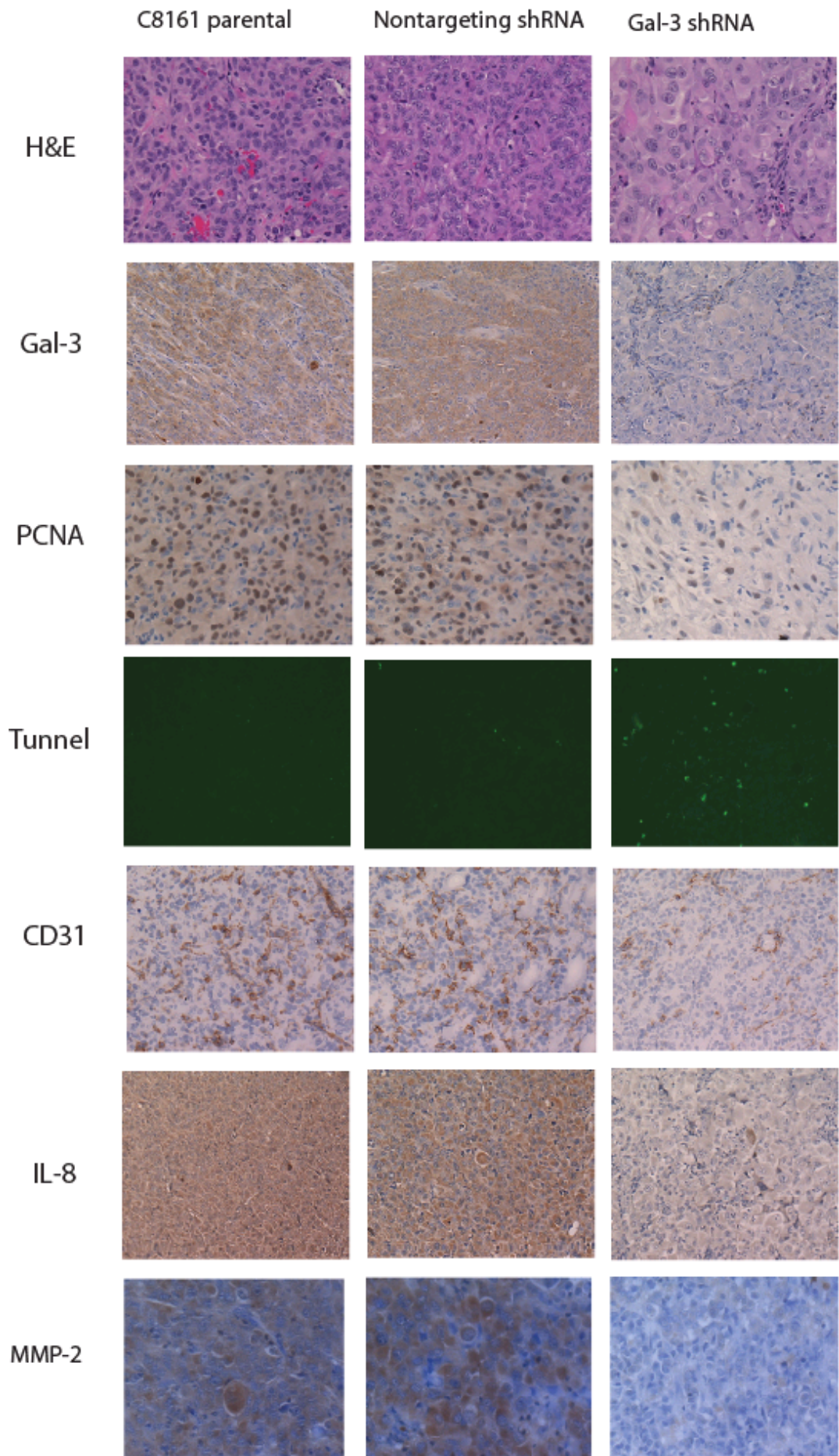


Figure 20 Immunohistochemical staining of *in vivo* s.c. tumors for H&E, Gal-3, cell proliferation (PCNA), apoptosis (TUNEL), microvessel density (MVD), IL-8 and MMP-2 expression.

From left to right: C8161 parental, NT shRNA, Gal-3 shRNA. Representative tumors are presented (20x Magnification). Immunohistochemistry was performed as described in section 2.17 with frozen or paraffin embedded tumors. Antigen positive cells are stained brown with the exception of the TUNEL assay in which the apoptotic cells fluorescence green.

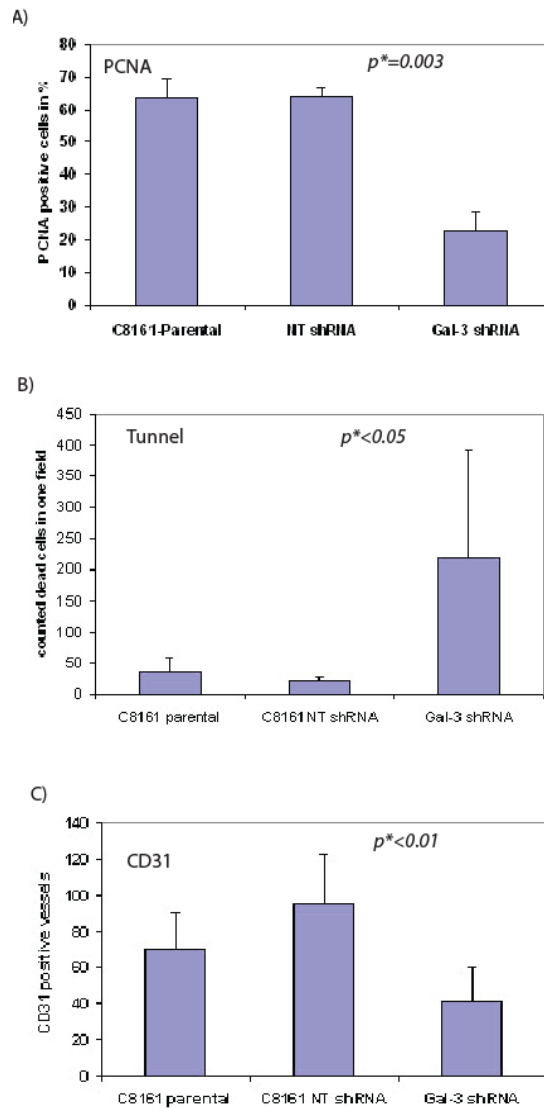


Figure 21 Quantitative measurement of cell proliferation (PCNA), apoptosis (TUNEL) and microvessel density.

A) Downregulation of Gal-3 resulted in a 2.6-fold decrease of proliferating cells in the Gal-3 shRNA tumors compared to C8161 parental and NT shRNA (* $p=0.003$). The percent of PCNA positive cells was determined as described in section 2.17 and is presented as the mean (7 tumors, respectively) +/- Standard Deviation (STD). B) TUNEL assay (see section 2.19) for apoptotic cells showed a marginally significant increase in apoptosis in Gal-3 shRNA tumor cells compared to C8161 parental and NT shRNA (* $p<0.05$). The data are presented as number of dead cells per field and the values

represent the mean and STD of 7 tumors respectively. C) MVD count of CD31 positive cells showed a highly significant downregulation of 2.3 fold in Gal-3 shRNA compared to NT shRNA and C8161 parental control (* $p < 0.01$). Differences in microvessel density between the C8161 parental group compared to Gal-3 shRNA tumor cells were not statistically significant. MVD was determined as described in section 2.17 and is presented as the mean number of CD31 positive vessels per slide of 4 fields +/- STD (n=7 tumors, respectively).

TUNEL). A 9 fold increase in apoptotic cells in the Gal-3 shRNA tumors versus NT shRNA was observed (* $p < 0.05$; in C8161 parental, NT shRNA control vs Gal-3 shRNA tumors respectively, Figure 20, 21 B).

For the tumor cell to be aggressive and invasive, it has to form vessels for additional blood and oxygen supply (Folkman & Klagsbrun 1987). This angiogenic activity in tumors has been analyzed through staining for the expression of the endothelial cell marker CD31. A notable decrease in microvessel density in Gal-3 shRNA tumors were observed as compared to the C8161 parental and NT shRNA tumor cells is shown in Figure 20 (CD31). Quantitative measurement of the CD31 positive vessels in the Gal-3 shRNA tumor specimens revealed a highly statistically significant decrease of 2.4 fold compared to NT shRNA (* $p < 0.01$, NT shRNA control and Gal-3 shRNA tumors, respectively, Figure 21A).

As can be seen from Figure 20, the Gal-3 knockdown tumors did not only show a reduction in Gal-3 expression. The expression levels of interleukin-8 (IL-8) and the matrix-metalloproteinase-2 (MMP-2) were also dramatically reduced in the Gal-3 knockdown tumors suggesting that Gal-3 may regulate the expression of other genes (see Specific Aim III).

Taken together, it can be concluded that:

- a) Gal-3 expression showed a significant correlation regarding cytoplasmic versus nuclear expression within a panel of melanoma cell lines with increased metastatic potential.
- b) Gal-3 shRNA knockdown led to a dramatic inhibition of tumor growth *in vivo*.
- c) Gal-3 shRNA knockdown inhibited also the formation of metastasis to the lung.

- d) A significant decrease in the proliferation and microvessel formation was observed in tumors after Gal-3 knockdown.
- e) A marked increase in apoptotic cells was also seen only after down regulation of Gal-3 in the tumors.

3.3 Specific Aim III:

3.3.1 Identification of novel Gal-3 downstream target genes by Gal-3 small hairpin RNA

3.3.1.1 Determining novel genes possibly regulated by Gal-3 via a cDNA microarray analysis

To further investigate the role of Gal-3 in melanoma metastasis, an Affymetrix cDNA array analysis was performed comparing C8161 melanoma cells following Gal-3 knockdown with the NTshRNA cells (see section 2.21). 794 genes, overall with differences in expression, were identified, of which 567 genes showed downregulation and 227 upregulation after Gal-3 knockdown. In the group of downregulated genes, the cDNA microarray analysis revealed that the Gal-3 knockdown had a dramatic effect on endothelial cell differentiation markers.

After analyzing the microarray data, a correlation between one group of genes was observed, which showed respectively a correlation with the endothelial and mesenchymal cell expression. These genes are emphasized as bold in Table 6, and include the Vascular Endothelial (VE)-Cadherin (CDH5), Interleukin-8 (IL-8), Fibronectin-1 (FN-1) and Endothelial Differentiation, Sphingolipid G-protein receptor-1 (EDG-1) (IL-8=12.96 fold; CDH5= 3.6 fold; FN= 9.6 fold and EDG1=4 fold downregulated). These genes were chosen for further study. The group of genes upregulated following knockdown of Gal-3 included protein fucosyltransferase (22.09 fold increase), NCOR-1 (21.16 fold increase), HGF agonistantagonist (10.89 fold increase), and WNTB2 (2.56 fold increase) (Table 6).

Downregulated genes

Gene	fold
Synaptotagmin 1	21.16
HSPC244	17.64
FGF13 (fibroblast growth factor 13)	16
PTPRC (protein tyrosine phosphatase, receptor type C)	14.44
Interleukin-8	12.96
Fibronectin 1	9.61
GPR49 (G-protein coupled receptor 49)	9
IFI27 (interferone, alpha- inducible protein 27)	8.41
GBP1 (guanylate binding protein 1)	5.76
Claudin-1	5.29
EDG1 (endothelial differentiation, sphingolipid G-protein coupled receptor, 1)	4
PTPRC (protein tyrosine phosphatase)	4
IGFBP7 (insulin-like growth factor binding protein 7)	3.61
SERPINE1	3.61
VE-Cadherin	3.61
IL1RAP (interleukin 1 receptor accessory protein)	3.24
BCL2A1 (BCL2-related protein A1)	3.24
GRO1 (guanylate binding protein 1)	2.89
CDC42 (CDC42 effector protein 3)	2.25
ADAMTS1 (disintegrin-like and metalloprotease (reprolysin type) with thrombospondin type 1)	2.25
Laminin	1.96
VEGF	1.69

Upregulated genes

Gene	fold
KIAA0958 (Protein fucosyltransferase 2)	22.09
NCOR1 (nuclear receptor corepressor isoform-2)	21.16
BRS3 (bombesin-like receptor-3)	13.69
HGF agonistantagonist	10.89
PILR(alpha) (Paired immunoglobulin-like receptor alpha)	7.29
WNT-2B	2.56
BCOR (BCL-6 corepressor short isoform)	2.56
TAX 40 (TAX interaction protein 40)	1.96
ITGB3 (platelet membrane glycoprotein IIIbeta)	1.69

Table 6 List of down- and upregulated genes after Gal-3 knockdown identified after cDNA microarray analysis.

The Affymetrix cDNA microarray analysis identified 794 genes, differentially expressed in Gal3 shRNA and NT shRNA tumor cells in which 567 genes showed downregulation and 227 upregulation after Gal-3 knockdown. Left panel shows the group of downregulated genes and the right panel the group of upregulated genes. The genes in bold type (Interleukin-8, Fibronectin-1, EDG-1, and VE-Cadherin (CDH5) were chosen for further study.

3.3.1.2 Validation of target genes after Gal-3 shRNA knockdown in highly metastatic melanoma cell lines

To further investigate the cDNA microarray analysis data, the downregulated genes CDH5, FN-1 and EDG-1 were validated by Western Blotting (Figure 22). The Gal-3 shRNA cells are three fold downregulated after Gal-3 knockdown compared to the parental cell line (Densitometric readings: C8161 parental= 1, Nontargeting shRNA= 1.3, Gal-3 shRNA= 0.3; see section 2.23; Figure 22, A). After Gal-3 knockdown a 2 fold decrease in the expression level of CDH5 was seen, comparing the parental with the Gal-3 shRNA knockdown cells (densitometric readings: C8161 parental= 1, Nontargeting shRNA= 1.9, Gal-3 shRNA= 0.5; see section 2.23; Figure 22,B). A 2.5 fold downregulation in the FN expression level compared to the C8161 parental cells was further observed (Densitometric readings: C8161 parental= 1, Nontargeting shRNA= 1.3, Gal-3 shRNA= 0.7; see section 2.23; Figure 22, D). The EDG-1 gene seems not to be drastically affected on the protein level by Gal-3 knockdown it only shows a 1.4 fold reduction in the level of expression compared to the parental cell line (Densitometric readings: C8161 parental= 1, Nontargeting shRNA= 1, Gal-3 shRNA= 0.4; see section 2.23; Figure 22, C).

Further immunohistochemical analysis will be performed on the genes described from the microarray analysis and Western Blot gels to confirm the results presented in section 3.3.1.1. All proteins except EDG-1 are highly downregulated in the Gal-3 knockdown cells.

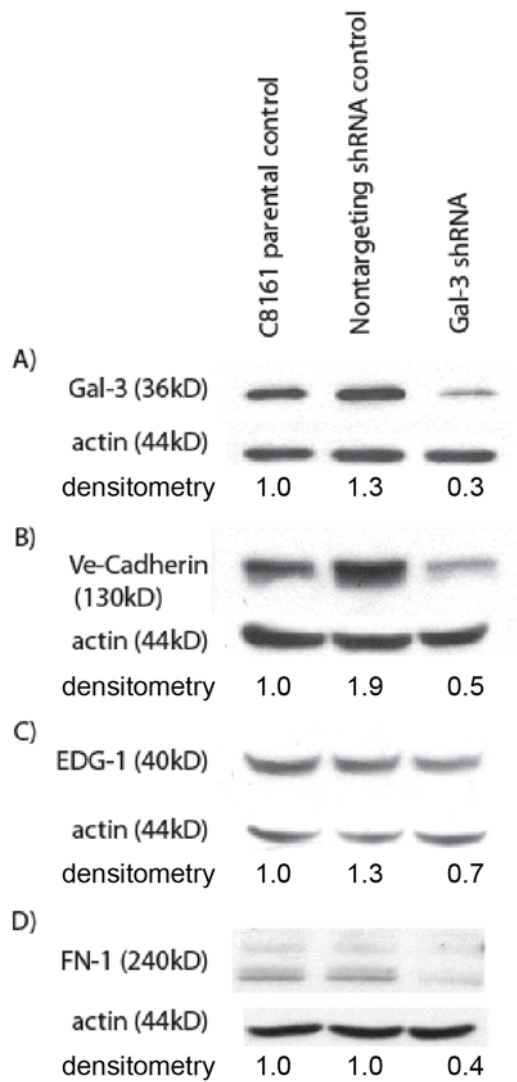


Figure 22 Western Blot validation of novel downstream targets of Gal-3 after cDNA microanalysis.

20 μ g of total cell lysate were separated on SDS-PAGE and transferred to a membrane as described in section 2.9. The membrane was then stained with the specific antibodies (Gal-3, CDH5, EDG1 and FN-1, see section 2.7) and with an antibody to actin as described in section 2.7. The protein expression relative to actin expression was obtained by densitometric analysis (see section 2.23).

3.2 Effect of Gal-3 shRNA on VE-Cadherin (CDH5) expression and function

To determine whether Gal-3 affected the expression of CDH5 on the transcriptional level, the activity of a CDH5 promoter reporter construct was evaluated in the Gal-3 shRNA and NTshRNA cells (see section 2.10). A slight difference with no statistical significance in the CDH5 promoter activity could be detected after transient transfection into Gal-3 knockdown compared to the NT shRNA control cells (*p=0.05, NT shRNA control and Gal-3 shRNA tumors, respectively, Figure 23).

To investigate which transcription factor binds to the CDH5 promoter, the promoter area of (-2300 to + 1000bp, relative to transcription start site for CDH5) was examined with the Genomatix program for possible interaction with transcription factors (see section 2.22). On the CDH5 promoter site upstream \pm 600 from the start sequence binding sites for SP-1, NFkB, EGR1 and Ap-2 transcription factors were found. The highest number of binding sites was identified for EGR-1 (5 binding sites on the CDH5 promoter).

The binding of the transcription factor EGR-1 to the CDH5 promoter was further investigated using chromatin immunoprecipitation assay (see section 2.22). An upregulation in the EGR-1 binding was observed in the Gal-3 shRNA cell line compared to the NT shRNA cells as seen in Figure 24.

Further a Western Blot analysis was performed after transiently overexpression of EGR-1 in the C8161 parental cell line, which showed a dramatic 3-4 fold decrease in the CDH5 protein expression level compared to the parental cells (Densitometric readings: C8161 parental= 1, Lipo 2000 control= 0.7, +1.2 μ g EGR-1= 0.2, +3.2 μ g EGR-1= 0.3; see section 2.23) (Figure 25).

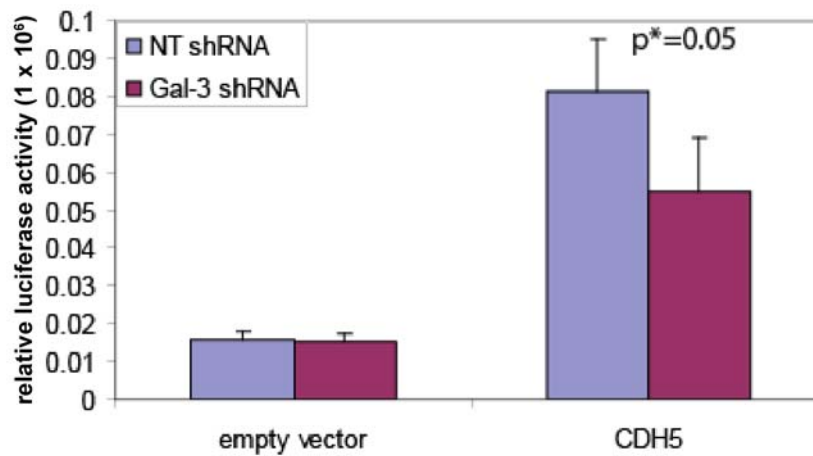


Figure 23 Analysis of the CDH5 promoter activity after Gal-3 knockdown.

Reporter activity was determined with the dual luciferase promoter analysis as described in section 2.10. Luciferase activity was measured at 72 hours after transfection of CDH5-pcDNA3.1 or pGL3 empty vector and is presented as the mean relative luciferase activity (firefly luciferase/renilla luciferase) of triplicates +/- STD.

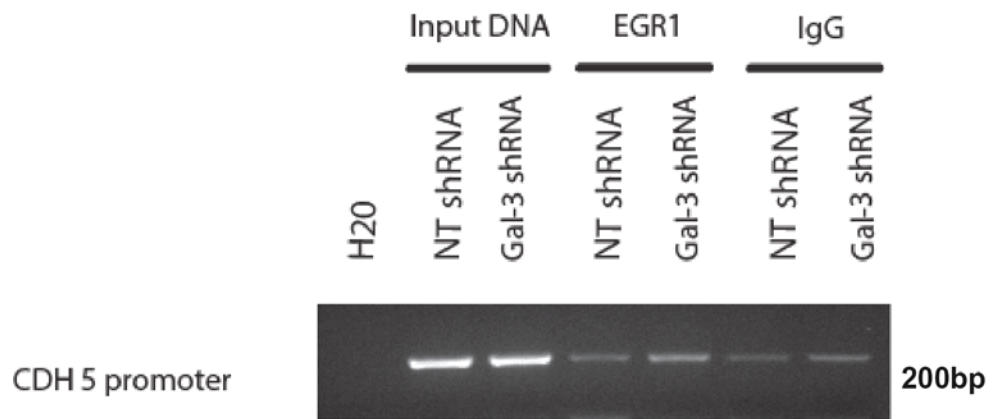


Figure 24 Chip analysis of CDH5 transcription binding site for EGR1.

PCR amplification of a 200 bp region of the CDH5 promoter, immunoprecipitated by anti EGR-1 antibody (lanes 4 and 5) or by control IgG (lanes 6 and 7) from Gal-3 shRNA knockdown cells and NT shRNA cells (see section 2.22).

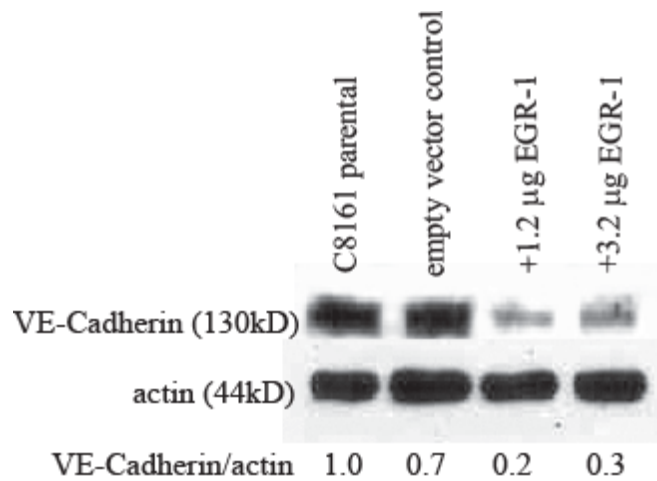


Figure 25 EGR-1 overexpression in C8161 parental cells influences VE-Cadherin expression

20 µg of total cell lysate were separated on SDS-PAGE and transferred to a membrane as described in section 2.9. The membrane was then stained with the specific antibody (CDH5, see section 2.7) and with an antibody to actin as described in section 2.7. The protein expression relative to actin expression was obtained by densitometric analysis (see section 2.23). After 48 hours transient transfection of EGR-1 into the C8161 parental cell line a 3-4 fold decrease in VE-Cadherin expression was observed (Densitometric readings: C8161 parental= 1, empty vector control= 0.7, +1.2 µg EGR-1= 0.2, +3.2 µg EGR-1= 0.3; see section 2.23).

On the transcriptional level of the CDH5 promoter a significant decrease was observed after transiently overexpression of EGR-1 compared to the C8161 parental cell line (*p=0.00394776, + 0.125 µg EGR-1;*p=0.00394776, + 0.25 µg EGR-1, compared to the VE-Cadherin promoter without EGR-1 transfection respectively, Figure 26).

CDH5 has been shown to be expressed by highly aggressive melanoma cells which results in the ability of the tumor cells to mimic endothelial cells and form embryonic-like, patterned, vasculogenic-like networks in 3-D cultures (Hendrix et al. 2001; Seftor et al. 2002; Hendrix et al. 2003b, a).

To further investigate a possible correlation between Gal-3 and CDH5 gene expression, a 3-dimensional type I collagen gel was created (see section 2.2, Figure 2) to observe the above described formation of patterned, vasculogenic-like networks. Only the highly metastatic melanoma cell lines C8161 parental and NT shRNA cells could form tube-like structures, as shown in Figure 27. The formation of vasculogenic mimicry could not be observed in metastatic melanoma cells after Gal-3 knockdown.

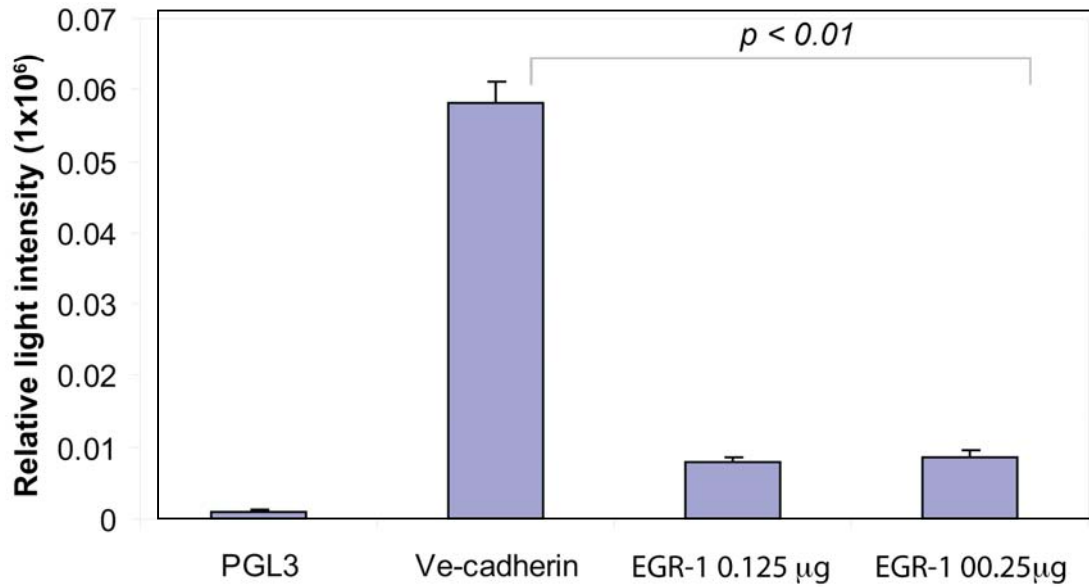


Figure 26 Analysis of the CDH5 promoter activity after EGR-1 transfection in C8161 parental cells.

Reporter activity was determined with the dual luciferase promoter analysis as described in section 2.10. Luciferase activity was measured at 72 hours after transfection of pGL3 empty vector and EGR-1 pcDNA3.1 (0.125 µg and 0.25 µg) is presented as the mean relative luciferase activity (firefly luciferase/renilla luciferase) of triplicates +/- STD.

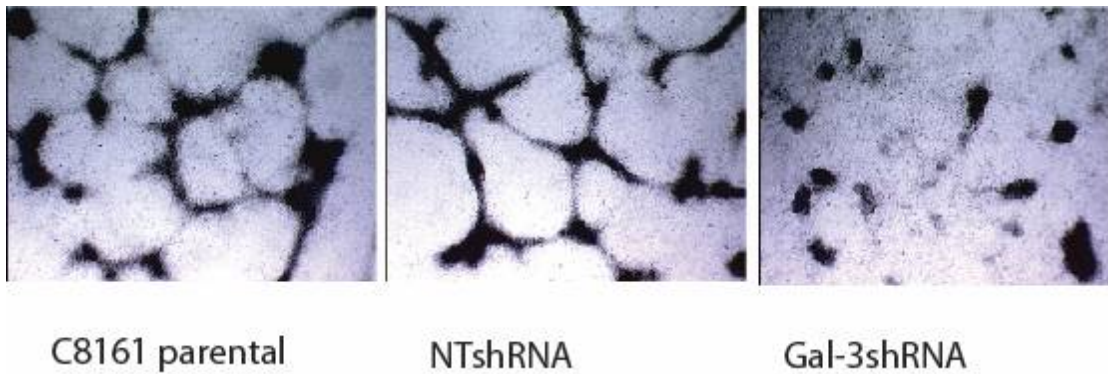


Figure 27 Formation of tube-like structures by melanoma cells before and after Gal-3 knockdown.

Cells were grown in collagen gels as described in section 2.2. In these photographs live unstained cells appear as vasculogenic networks and are black (20x Magnification). In a three dimensional type 1 collagen gel, highly metastatic melanoma cells showed the ability to form tube-like structures only in presence of Gal-3.

3.3 Effect of Gal-3 shRNA on IL-8 expression

IL-8 has been recently shown to act directly on vascular endothelial cells and to serve as a survival factor (Yoshida et al. 1997). To investigate the effect of Gal-3 knockdown on the angiogenic chemokine IL-8, immunohistochemical staining was conducted, which showed a marked decrease in the expression of IL-8 in the *in vivo* Gal-3 knockdown versus C8161 parental and NT shRNA tumors (Figure 20). With RT-PCR a 5 fold down regulation of IL-8 in the Gal-3 shRNA cells versus C8161 parental was also observed (Densitometric readings: C8161 parental= 1, Nontargeting shRNA= 0.6, Gal-3 shRNA= 0.2; see section 2.15 and 2.23; Figure 28).

The secretion of the chemokine into the supernatant by *in vitro* cultured cells before and after Gal-3 knockdown was determined using ELISA (see section 2.20). In the Gal-3 shRNA knockdown cells a highly significant, 3-fold decrease in IL-8 secretion was detected compared to the C8161 parental and NT shRNA cells respectively (* $p < 0.01$, NT shRNA control and Gal-3 shRNA tumors, respectively, Figure 29).

To determine whether Gal-3 was affecting the expression of IL-8 on the transcriptional level, the activity of an IL-8 promoter reporter construct was investigated using a dual promoter Luciferase analysis (see section 2.10). A marginally significant difference in promoter activity was detected in the Gal-3 shRNA cells compared to the NT shRNA control cells (* $p < 0.05$, NT shRNA control and Gal-3 shRNA tumors, respectively, Figure 30).

To further investigate the role of Gal-3 in regulating IL-8 on the transcriptional level, i.e. which transcription factors bind to the IL-8 promoter,

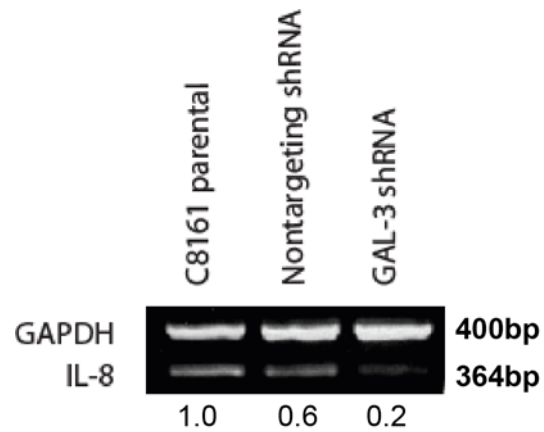


Figure 28 Validation of IL-8 downstream target gene of Gal-3 with RT-PCR.

RT-PCR analysis of IL-8 expression was performed as described (see section 2.15). A 5 fold down regulation of IL-8 was observed after Gal-3 knockdown compared to the parental (Densitometric readings: C8161 parental= 1, Nontargeting shRNA= 0.6, Gal-3 shRNA= 0.2; see section 2.23).

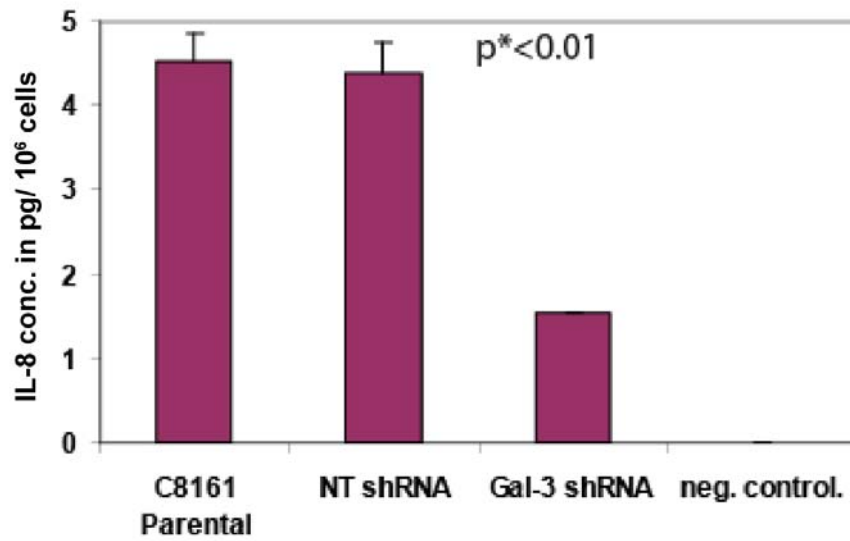


Figure 29 Quantitation of secreted IL-8 by melanoma cells before and after Gal-3 knockdown

Cells were cultured at 2×10^5 /ml for 24 hours and IL-8 in the supernatant was determined with an ELISA as described in section 2.20. The data are presented as mean and STD of duplicates. A highly significant downregulation in IL-8 secretion of 3 fold decrease was detected in the Gal-3 shRNA cells compared to C8161 parental and NT shRNA cells (* $p < 0.01$, NT shRNA control and Gal-3 shRNA).

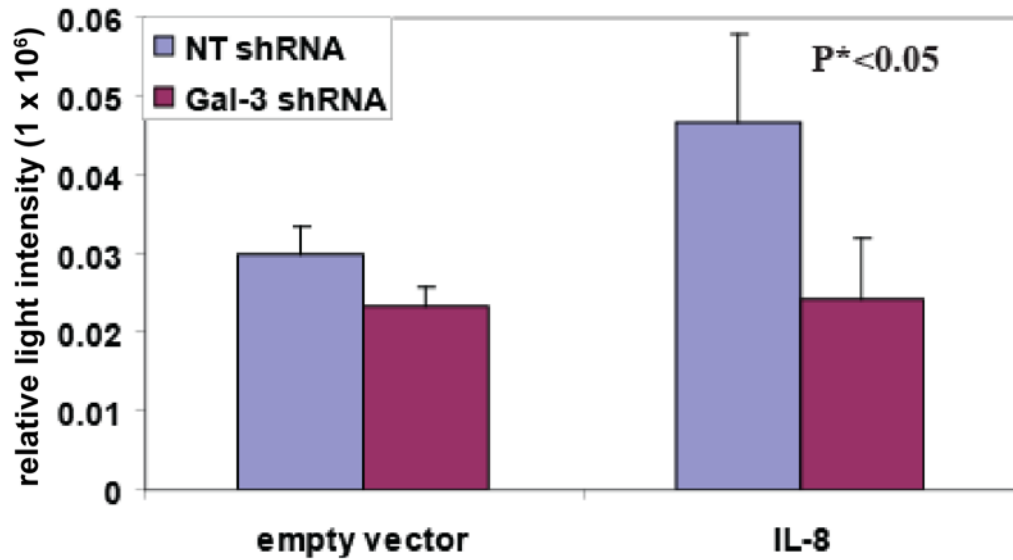


Figure 30 Activity of the IL-8 promoter after Gal-3 knockdown was determined with dual luciferase promoter analysis.

Luciferase activity was measured at 72 hours after transfection of pGL3-IL-8 or pGL3 empty vector and is presented as the mean relative luciferase activity (firefly luciferase/renilla luciferase) of 4 wells +/- STD (as described in section 2.10). A marginally significant decrease in IL-8 production was seen after Gal-3 knockdown (* $p < 0.05$, NT shRNA control and Gal-3 shRNA tumors, respectively).

the area from -133 to +44 bp (relative to transcription start site) on the IL-8 promoter was blasted with the Genomatix program for possible interaction with transcription factors (see section 2.22). On the IL-8 promoter, EGR1, NFkB, SP-1 and AP-2 transcription factor binding sites were detected. The binding of EGR1 to the IL-8 promoter was further investigated using chromatin immunoprecipitation (see section 2.22). An upregulation in the EGR-1 binding to the IL-8 promoter was observed only in the Gal-3 shRNA cell line compared to the NT shRNA cells, as seen in Figure 31.

3.3.2.1 Effect of Gal-3 downregulation on the MMP-2 expression

It has been shown by Luca et al. that metastatic melanoma cells producing IL-8 or primary cutaneous melanoma (IL-8-negative) transfected with the IL-8 gene displayed upregulation of Matrix Metalloproteinase-2 (MMP-2) expression and activity and increased invasiveness through Matrigel-coated filters (Luca et al. 1997). Immunohistochemical staining of *in vivo* Gal-3 shRNA tumor specimens versus C8161 parental and NT shRNA tumors indicated that MMP-2 expression was dramatically reduced in the Gal-3 knockdown cells (Figure 20).

To investigate further the association between Gal-3 knockdown and the downstream effect on MMP-2, a Western Blot analysis and a Zymography assay were performed on melanoma cells before and after Gal-3 knockdown (Figure 32 and 33). A three fold knockdown of the MMP-2 expression level in Gal-3 knockdown cells compared to the C8161 parental cells was observed in Figure 32 (Densitometric readings: C8161 parental= 1, Nontargeting shRNA= 0.9, Gal-3 shRNA= 0.3; see section 2.23). Also a 1.6 fold downregulation of MMP-2 activity as detected by Zymography analysis was observed after a 3 fold decrease in expression was seen in the Gal-3 shRNA cells versus the C8161

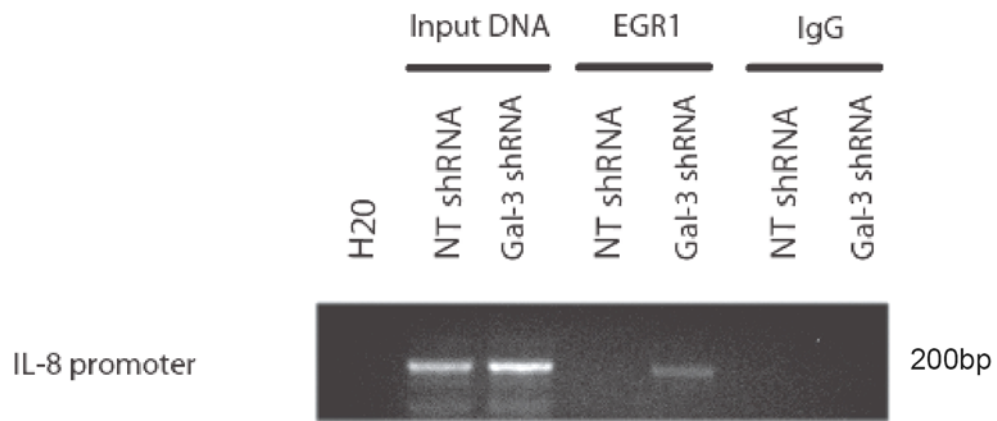


Figure 31 Chip analysis of IL-8 transcription binding site for EGR1.

PCR amplification of a 200 bp region of the IL-8 promoter, immunoprecipitated by anti EGR-1 antibody (lanes 4 and 5) or by control IgG (lanes 6 and 7) from Gal-3 shRNA knockdown cell line compared to the NT shRNA cells (see section 2.22).

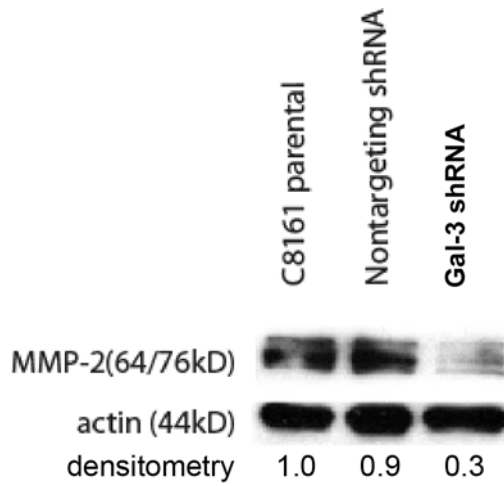


Figure 32 Detection of MMP-2 before and after Gal-3 knockdown with Western Blotting.

10 μ g of total cell lysate were separated on SDS-PAGE and transferred to a membrane as described in section 2.9. The membrane was then stained with the MMP-2 antibody (see section 2.7) and with an antibody to actin as described in section 2.7. The protein expression relative to actin expression was obtained by densitometric analysis (see section 2.23).

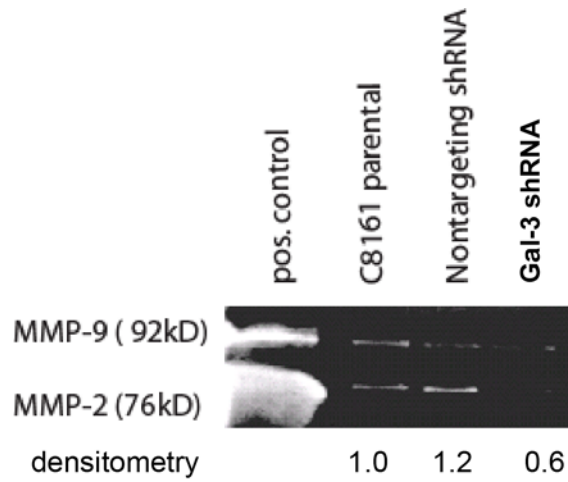


Figure 33 Zymography analysis of MMP-2 before and after Gal-3 knockdown.

MMP-2 and MMP-9 activity in the cell supernatants was determined on gelatin impregnated SDS-PAGE as described in section 2.12. The protein bands are visualized as gelatin-free areas in a Coomassie blue stained gel. A marked knockdown of MMP-2 activity could be detected in the Gal-3 knockdown cells versus C8161 parental or NT shRNA control cells (Densitometric readings: C8161 parental= 1, Nontargeting shRNA= 1.2, Gal-3 shRNA= 0.6; see section 2.23).

parental control cells (Densitometric readings: C8161 parental= 1, Nontargeting shRNA= 1.3, Gal-3 shRNA= 0.3).Gal-3 knockdown (Densitometric readings: C8161 parental= 1, Nontargeting shRNA= 1.2, Gal-3 shRNA= 0.6; see section 2.23; Figure 33).

3.3.2.2 *Effect of Gal-3 downregulation on the in vitro tumor cell invasion*

The activation of MMP-2 by IL-8 has been known to enhance the invasion of host stroma by tumor cells and increase angiogenesis and therefore the formation of metastasis (Luca et al. 1997).

Therefore, an invasion assay was conducted using matrigel-coated filters (see section 2.13; Figure 34). A decrease in invasion and expression of MMP-2 following transfection with shRNA has been observed, which showed a highly significant effect of Gal-3 downregulation on the *in vitro* tumor cell invasion ability (*p<0.01, NT shRNA control and Gal-3 shRNA tumors, respectively, Figure 33).

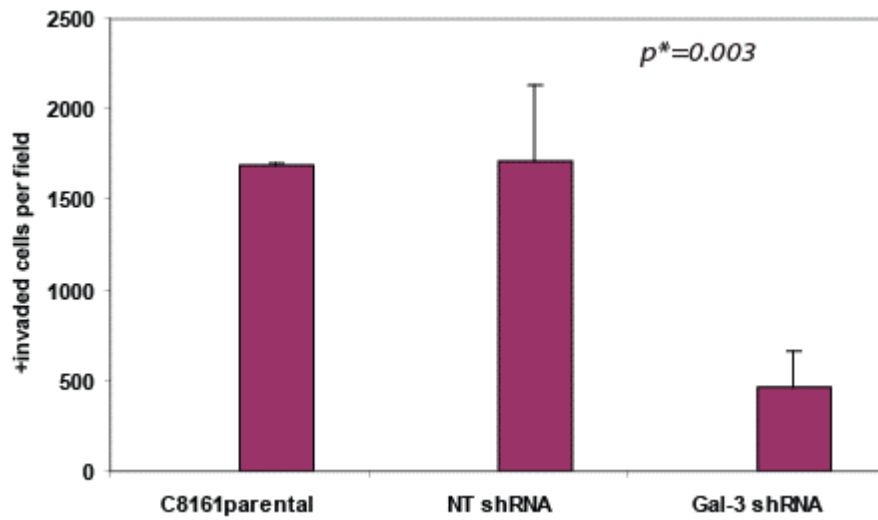


Figure 34 Quantitative measurement of in vitro tumor cell invasion before and after Gal-3 knockdown.

Tumor cell invasion through matrigel coated filters was performed as described in section 2.13. The results are presented as mean \pm STD of invaded tumor cells in 4 fields of duplicate chambers after 22 hours. Decrease in Gal-3 expression resulted in a highly-significant suppression of tumor cell invasion *in vitro* (* $p < 0.01$).

Overall, the analysis of Gal-3 downstream target genes reveals that:

- a) Gal-3 shRNA cells show a notable knockdown in expression of a group of endothelial and mesenchymal markers, including VE-Cadherin, EDG-1, Fibronectin-1 and Interleukin-8.
- b) Tube-like vasculogenic network formation was blocked in the Gal-3 knockdown cells in a three dimensional collagen gel environment.
- c) IL-8 expression was decreased in Gal-3 shRNA tumor specimens.
- d) ELISA studies show that *in vitro* secretion of IL-8 into the supernatant of Gal-3 knockdown cells was 3 fold decreased compared with parental cells.
- e) Gal-3 affects VE-Cadherin and IL-8 on the transcriptional level.
- f) A decrease in VE-Cadherin and IL-8 expression after Gal-3 knockdown was accompanied by a recruitment of the tumor suppressor transcription factor EGR-1 to the promoters of these genes.
- g) Transient overexpression of EGR-1 in C8161 parental cells lead to a downregulation of VE-Cadherin protein level.
- h) Overexpression of EGR-1 downregulated the VE-Cadherin promoter activity.
- i) Gal-3 knockdown resulted in a decrease in MMP-2 expression and secretion as well as a decrease in tumor cell invasion through matrigel-coated filters.

Chapter IV:

4. Discussion

In this dissertation, Gal-3 is proposed to play a major role in melanoma progression. Gal-3 is known to be associated with cell growth, cellular adhesion processes, cell proliferation, transformation, metastasis and apoptosis (Xu et al. 2000; Ellerhorst et al. 2002; Nakahara et al. 2005). Since Gal-3 is overexpressed in some types of cancers, it is therefore thought to be involved in tumorigenesis (Yoshii et al. 2001; Takenaka et al. 2003). In the presented work, the involvement of Gal-3 in melanoma tumor growth and metastatic progression has been studied.

First, the Gal-3 expression in human melanocytic lesions was investigated with the use of a progression- tissue microarray, which features melanocytic lesions from different stages of melanoma. It was found that Gal-3 expression correlated significantly with melanoma progression from the benign and dysplastic nevi toward primary and metastatic melanoma. A higher nuclear expression in lesions metastatic to viscera and lymph nodes was observed than in subcutaneous lesions. These analysis revealed that patients with lesions that express Gal-3 in the nucleus at the levels equal or higher than in the cytoplasm, have a shorter overall disease free survival.

Overall, it is proposed that Gal-3 may serve as a marker of progression in human melanoma. Supporting these findings, Vereecken et al. have recently observed a high serum level of Gal-3 in patients with metastatic melanoma (Vereecken & Heenen 2006; Vereecken et al. 2006). They proposed that Gal-3 was probably produced by the tumor cells themselves (Vereecken & Heenen 2006; Vereecken et al. 2006). Furthermore, Vereecken et al. have utilized an immunohistochemical study with monoclonal anti-Gal-3 antibody in a series of primary and metastatic melanoma lesions as well as benign skin

pigmented lesions to see if there was a possible correlation between Gal-3 expression and malignant potential in primary melanoma lesions (Vereecken et al. 2005). A xenograft melanoma model in nude mice with two melanoma cell lines (ATCC G-361 and ATCC HT-144) was established to assess staining with the Gal-3 antibody in the xenografts and the metastases. In the xenograft mouse model it was shown that Gal-3 expression was higher in thin primary melanoma lesions than in benign pigmented skin lesions or metastases and seemed to correlate inversely with the aggressiveness as estimated by the Breslow index. Therefore, it was concluded that Gal-3 expression in melanoma may act as a diagnostic and/or a prognostic parameter (Vereecken et al. 2005). Also a direct correlation has been reported between Gal-3 and the stage of tumor progression in colon, gastric, thyroid, breast, and head and neck carcinomas (Lotan et al. 1994; Schoeppner et al. 1995; Xu et al. 1995; Gillenwater et al. 1996; Fernandez et al. 1997; Bresalier et al. 1998; Nangia-Makker et al. 1998). For example, in gastric cancer, an unfavorable prognosis is a result of reduced Gal-3 expression (Okada et al. 2006). In advanced melanoma patients, however, serum Gal-3 gives rise to a possible responsibility in melanoma inflammation and progression (Vereecken & Heenen 2006). Furthermore, Gal-3 is considered to be also a possible molecular marker for thyroid malignancy (Weinberger et al. 2007). Krishnan et al. reported that b1,6 branched N-oligosaccharides participate in a metastasis-dependent manner in B16- melanoma cell lines in adhesion (Krishnan et al. 2005).

Also a correlation between the metastatic potential of mouse melanoma and fibrosarcoma cells and the level of Gal-3 expression on the cell surface in mice was shown by Raz et al. (Raz et al. 1987)

A history of severe sunburns early in life, together with intermittent UV exposure is implicated in the etiology of human melanoma (Prieto et al. 2006). However, the

mechanism by which UV radiation participates in melanoma formation is widely debated due to the lack of direct evidence for the UV-induced genetic mutations in melanoma. Nevertheless, recent analysis of a large group of primary melanomas revealed that melanoma subgroups develop by distinct mechanistic routes depending on the patterns of sun-exposure (Curtin et al. 2005). It was found that melanomas derived from body sites with chronic sun exposure had infrequent mutations in BRAF and frequent increases in the number of copies of the *cyclin D1* gene. On the other hand, melanomas on sites with intermittent sun-exposure revealed frequent mutations in *BRAF* or *N-RAS* oncogenes and frequent loss of phosphatase and tensin homologue deleted on chromosome 10, *PTEN*. In acral melanomas, which are normally not associated with sun exposure, a high degree of focal chromosomal amplifications and losses were observed (Curtin et al. 2005).

In this here presented study, the expression of Gal-3 in the nucleus was only found in chronically sun-exposed skin lesions. In addition, skin lesions with chronic and intermittent sun-exposure have high cytoplasmic expression of Gal-3, as compared to acral melanomas, which did not express Gal-3 at all. This strongly suggests that nuclear translocation of Gal-3 is associated with UV-induced damage.

In vitro, Gal-3 protein expression showed a strong correlation with metastatic potential of cultured melanoma cell lines in nude mice, with metastatic cells expressing high amounts of Gal-3 as compared to non-metastatic cells. A slight correlation between Gal-3 localization and metastatic potential in cultured cell lines was observed. This suggests that nuclear translocation of Gal-3 is an *in vivo* phenomenon that may be induced by the tumor microenvironment. Gal-3 facilitates cell-to-cell adhesions and cell-to-matrix contacts through binding with interstitial expressed markers like laminin, fibronectin and collagen IV (Iacobini et al. 2003) (Figure 4).

In order to further delineate the function of Gal-3 in melanoma, a knockdown of the Gal-3 expression in C8161 metastatic melanoma cells was performed using lentiviral delivery of small hairpin RNA (Stewart et al. 2003). Based on immunohistochemical staining and Western Blot analysis, Gal-3 expression was stably reduced by 90% compared to C8161 cells transduced with vector alone. Gal-3 knockdown exerted a major inhibitory effect on subcutaneous tumor growth and experimental lung metastasis of C8161 cells in nude mice. The decrease in tumor growth was accompanied by a 50% decrease in cell proliferation, as measured by PCNA expression, and an 80% increase in cell apoptosis as measured in an in situ TUNEL assay. Both of these effects could be associated with a dramatic decrease in tumor angiogenesis, as indicated by a 50% decrease in CD31 staining in C8161 Gal-3 knockdown tumors.

The complex, multistep process of angiogenesis is comprised of a series of events that enable neovascularization from the existing vascular bed. The process of angiogenesis can also be linked to processes such as inflammation, wound healing, tumor growth, and metastasis (Folkman 1995a, b; Lee et al. 1997; Pluda 1997). The microvessel density of a growing tumor has been recognized as a prognostic value predicting recurrence and survival in patients (Vartanian & Weidner 1994). Different groups of angiogenic factors include those that induce both epithelial cell proliferation and differentiation, such as bFGF, aFGF, VEGF, platelet-derived endothelial cell growth factor (PD-ECGF), and TGF β (Burgess & Maciag 1989; Conn et al. 1990) as well as angiogenic factors that only affect cell differentiation in vitro, such as angiogenin, TGF β , platelet-activating factor, soluble E-selectin, TNF α and Gal-3 (Folkman & Klagsbrun 1987; Muller et al. 1987; Roberts & Sporn 1989; Pepper et al. 1990; Meininger & Zetter 1992; Bussolino et al. 1997; Nangia-Makker et al. 2000). Inhibitors of angiogenesis, such as angiostatin (O'Reilly et al. 1994; Gately et al. 1996), thrombospondin (Good et al.

1990; DiPietro & Polverini 1993), and endostatin (O'Reilly et al. 1997), can also be secreted by tumors. The disaccharide lactose and modified citrus pectin, a competitive polysaccharide, have both been shown to behave as natural ligand recognition competitors by Gal-3 (Platt & Raz 1992; Inohara & Raz 1994; Pienta et al. 1995). This implies that angiogenesis occurs out of a balance between positive and negative regulators within the microenvironment (Folkman 1992; Iruela-Arispe & Dvorak 1997).

Nangia-Makker et al. transfected Gal-3 null human breast carcinoma BT-549 cells with human Gal-3 cDNA and showed that the established expressing cell clones could grow progressively and metastasized in nude mice (Nangia-Makker et al. 1998). Furthermore, it was demonstrated that Gal-3 is involved in tumor related angiogenesis (Nangia-Makker et al. 2000).

Soluble Gal-3 has also been shown to induce endothelial capillary tube formation *in vitro* and angiogenesis *in vivo*, which suggests that angiogenesis could be mediated by carbohydrate recognition (Nangia-Makker et al. 2000). Potentially, following secretion, Gal-3 could either be stored in bound form to its ECM ligands or interact directly with endothelial cells. Once it binds to its cell surface receptors, Gal-3 may induce overexpression of integrin $\alpha\beta3$, leading to endothelial cell migration and attachment (Nangia-Makker et al. 2000).

Indeed, no changes in the *in vitro* proliferation rate of the Gal-3 knockdown cells were observed, as measured by the MTT assay (data not shown).

The introduction of wild-type Gal-3 into nontumorigenic, Gal-3-null BT549 human breast epithelial cells conferred tumorigenicity and metastatic potential in nude mice, and that Gal-3 expressed by the cells was phosphorylated. In contrast, BT549 cells expressing Gal-3 incapable of being phosphorylated (Ser6-->Glu Ser6-->Ala) were nontumorigenic (Mazurek et al. 2005).

Interaction between the tumor-specific Thomsen-Friedenreich glycoantigen (TFAg) and Gal-3 resulted in carbohydrate-mediated metastatic cell adhesion. This is possible through both homotypic (between carcinoma cells) and heterophilic (between carcinoma cells and endothelium) interactions. Zhou et al. proposed that using synthetic peptides to blocking the Gal-3 carbohydrate recognition domain would reduce metastasis-associated carcinoma cell adhesion (Zhou et al. 1997). In forming organ specific metastasis the main adhesive determinant is the interaction between the molecules on the cancer cells and the target organ. In B16- melanoma cell lines, Krishnan et al. revealed that in adhesion, b1,6 branched N-oligosaccharides contribute in a metastasis-dependent manner (Krishnan et al. 2005). The lysosome associated membrane protein, LAMP1, is a major carrier of these oligosaccharides. In highly metastatic cell lines, LAMP1 is usually translocated to the cell surface and then substituted with poly N-acetyl lactosamine (polylacNAc). This results in expression of the high density of very high affinity ligands for Gal-3 on the cell surface and may therefore facilitate organ specific metastasis (Krishnan et al. 2005).

Deininger et al. suggested that in tumor cells, there is a positive correlation for Gal-3 expression and in endothelial cells, there is a negative correlation as a marker for poor prognosis and malignancy in oligodendroglioma patients. Low endothelial Gal-3 labeling in patients with primary oligodendrogliomas and anaplastic oligodendrogliomas was an indication for shorter time to progression and overall survival than patients with high endothelial Gal-3 labeling (Deininger et al. 2002).

It is known that Gal-3 binds to the non-integrin laminin (Woo et al. 1990). However, soluble Gal-3 on the cell surface makes it impossible for melanoma cells to adhere to laminin (van den Brule et al. 1995), whereas oligomerized Gal-3 induces melanoma cell spreading on laminin (van den Brule et al. 1998). Controversially,

adhesion of neutrophils to laminin is supported by exogenous expressed Gal-3, where the adhesion may result of the lectin induced activation of neutrophils (Kuwabara & Liu 1996). Warfield et al. support these findings in demonstrating that soluble Gal-3 inhibits melanoma, breast cancer, fibrosarcoma and prostate cancer cell adhesion to laminin (Warfield et al. 1997). Although Gal-3 can bind laminin, it is proven that it cannot mediate cell adhesion to laminin, whereas it may act indirectly by regulating other molecules such as integrins (Takenaka et al. 2004).

A form of apoptosis, which occurs by disruption of cell-matrix interaction, is called anoikis (Frisch & Francis 1994). In a study by Zhu et al. it was shown that a selection of melanoma cells for anoikis resistance resulted in an increase in their metastatic potential (Zhu et al. 2001). It was also observed that overexpression of Gal-3 resulted in the protection of cells from anoikis as well as other apoptotic stimuli (Akahani et al. 1997; Kim et al. 1999; Yoshii et al. 2002).

For cells to form emboli, they have to aggregate with other tumor cells or host cells, which enable the circulating cancer cells to form secondary tumors. Extravasation of tumor cells at secondary sites is only possible after the tumor cell aggregates, embolizes into microcapillaries and forms a tumor embolus. A study by Thompson H proved after tumor cells injection as aggregates, that only those cumulated tumor cells formed more lung colonies in mice than those injected as single cells (Thompson 1974). Also, Raz et al. demonstrated a strong correlation between the *in vitro* aggregation property and the *in vivo* metastatic potential (Raz et al. 1980). Furthermore, pH-modified citrus pectin showed inhibition of aialofetuin which induced homotypic aggregation of B16-F1 melanoma cells *in vitro* (Inohara & Raz 1994). Inohara et al. reported further that cell surface Gal-3 is able to mediate homotypic cell adhesion by bridging through branched, soluble complementary glycoconjugates (Inohara & Raz 1995).

After intravenous injection of B16-F1 melanoma cells with modified citrus pectin into syngeneic mice resulted in a significant decrease of lung colonization (Platt & Raz 1992). Taken together, Gal-3 induces homotypic aggregation, resulting in tumor embolism, which increases metastatic potential.

Iurisci et al. reported that circulating levels of Gal-3 reflect biological aspects of tumor behavior associated with a metastasizing phenotype due to the fact that circulating levels of Gal-3 in the sera of patients with breast, gastrointestinal, lung, or ovarian cancer, melanoma, and Hodgkin's lymphoma were increased (Iurisci et al. 2000).

Therefore expression of Gal-3 by tumor cells can lead to increased growth and metastasis formation through a variety of mechanisms.

To investigate the possible effect of Gal-3 on gene expression in melanoma, a cDNA microarray analysis was performed comparing Gal-3 knockdown cells and vector control cells. Overall, 794 genes were identified which showed significant differences in gene expression, in which 567 genes showed downregulation and 227 upregulation after Gal-3 knockdown. The validation of the cDNA microarray analysis demonstrated that silencing Gal-3 expression resulted in a loss of expression of a number of endothelial cell differentiation markers by melanoma cells (Vascular Endothelial (VE)-Cadherin (CDH5), Interleukin-8 (IL-8), Fibronectin-1 (FN-1) and Endothelial Differentiation, sphingolipid G-protein receptor-1 (EDG-1)). In contrast the Protein fucosyltransferase, nuclear receptor corepressor isoform-2 (NCOR1), hepatocyte growth factor (HGF) agonist/antagonist and WNTB2 were upregulated after Gal-3 knockdown. An inhibitory effect of Gal-3 knockdown on a group of endothelial marker genes led to the conclusion that Gal-3 may be implicated in the phenomenon of vasculogenic mimicry of highly aggressive melanoma cells.

In situ differentiation of mesodermal progenitor cells (hemangioblasts or angioblasts) to endothelial cells that organize to form primitive vascular networks occurs by vasculogenesis during embryogenesis (Carmeliet 2000). This is followed by angiogenesis, which results in the sprouting of new capillaries from a preexisting network to expand the primitive vascular network into a more sophisticated complex of functionally efficient vasculature (Risau 1997). A widely held belief is that during cancer progression, angiogenesis plays an important role to signal new blood vessel growth for a growing tumor mass. This progression of blood supply is important and necessary for tumors to grow, survive and ultimately metastasize (Folkman 1995a, b; Rak & Kerbel 1996; Risau 1997; Kumar & Fidler 1998). Maniotis et al. introduced the term ‘vasculogenic mimicry’ to describe the ability of highly aggressive uveal melanomas to form patterns of extracellular matrix-rich networks with red blood cell (RBC)- containing channels in many areas by tumor cells (Maniotis et al. 1999). In this way, melanoma tumor cells are able to mimic endothelial cells and form vasculogenic networks (Bissell 1999; Maniotis et al. 1999).

Failed organization of vascular- like structures in embryoid bodies gives further support for VE-Cadherin importance in vascular structure assembly, which was shown with the generated VE-cadherin-negative mouse embryonic stem cells (VE-cadherin-/- ES cells) by gene targeting (Vittet et al. 1997). Thoses studies have implicated VE-cadherin (CDH5) in the ability of the tumor cells to mimic endothelial cells and form embryonic-like, patterned, vasculogenic-like networks in 3-D cultures (Hendrix et al. 2001; Seftor et al. 2002; Hendrix et al. 2003b, a).

Indeed, the here presented experiments revealed that Gal-3 knockdown in C8161 cells resulted in a loss of their ability to form the tube-like structures when plated on a 3-dimensional type I collagen gel. This suggests that Gal-3 influences this stem cell-like

plasticity of melanoma cells, which is described as the ability of melanoma cells to resemble endothelial cells phenotypically and functionally, which helps them after acceptance of signals from their environment to transdifferentiate into endothelial cells (Seftor et al. 2002; Hendrix et al. 2003b).

In a study with cytotrophoblasts, other than endothelial cells, VE-cadherin has been found to help those cells to differentiate into human placental tissue and adopt a vascular phenotype called pseudovasculogenesis (Zhou et al. 1997), suggesting that melanoma cells can engage in vasculogenic mimicry through an embryonic-like phenotype reversion with potential stem cell plasticity. Furthermore, another study assessed aggressive human cutaneous melanoma tumor cells in their ability to revascularize an ischemic limb model. Green fluorescent- labeled aggressive melanoma cells were seen to participate in revascularization in the ischemic muscle together with the tumor cells to restore blood flow to the previously injured tissue (Schatteman et al. 2000; Seftor & Kirschmann 2001). This suggests a stem cell plasticity, similar to angioblasts, allowing these cells to resemble endothelial cells functionally and phenotypically. Furthermore it permits certain signaling cues from the environment to be accepted by aggressive tumor cells, which influences the transdifferentiation of melanoma cells to endothelial cells (Seftor et al. 2002; Hendrix et al. 2003b).

Microarray analysis comparing poorly to aggressive melanoma cells was initially used to identify the differential expression of genes that regulate melanoma vascular mimicry. This helped establish a molecular signature characteristic of aggressive melanoma cells, and revealed both the expression of the epithelial cell genotype (EphA2) and the endothelial genotype (VE-cadherin) (Bittner et al. 2000; Hendrix et al. 2003b). EphA2 is a receptor tyrosine kinase and a member of the Eph family of protein tyrosine kinases, which is important in angiogenesis. In both *in vitro* and *in vivo* angiogenesis

models, regulation of key processes controlling tumor neovascularization has been shown to be through EphA2 in combination with its membrane bound ligand, ephrin-A1 (Pandey et al. 1995; Ogawa et al. 2000; Brantley et al. 2002; Cheng et al. 2002).

A novel signaling pathway described by Hess et al., suggests that at cell-cell contact areas in aggressive cutaneous and uveal melanoma, both EphA2 and VE-cadherin colocalize. Furthermore, during the formation of vascular mimicry, VE-cadherin and EphA2 associate with each other (Hess et al. 2006).

Knocking out VE-cadherin or EphA2 resulted in an inability of the cells to form vasculogenic structures, which resulted in the redistribution of EphA2 from the cell-cell adhesion complexes into a more random distribution over the cell surface. Disruption of VE-cadherin expression resulted in a dephosphorylation of EphA2, suggesting that VE-cadherin facilitates relocation of EphA2 to cell-cell adhesion complexes and may potentiate its interaction with ephrin-A1 (EphA2's membrane-bound ligand), and its subsequent phosphorylation (Pandey et al. 1995; Carmeliet et al. 1999; Dejana et al. 1999; Ogawa et al. 2000; Hendrix et al. 2001; Hess et al. 2001). This might result in loosening the cell-cell-adhesion and therefore an increase in cell migration, invasion and vasculogenic mimicry (Hendrix et al. 2003b).

Elevated lipid phosphoinositide 3-Kinase (PI3K) activity in epithelial cells has been shown to mediate the processes of survival, cell motility, and tubulogenesis through effectors downstream of EphA2 and VE-cadherin (Bazzoni et al. 1999). It was reported by Chan et al. that small GTPases such as RAC1 and CDC42 can transduce signals to cause tyrosine phosphorylation activity of PI3K. This in turn results in the formation of vasculogenic-like networks (Chan et al. 2002). It was also found that the activity of CDC42 and RAC1 were more increased in highly aggressive melanoma cells during tubular network formation and therefore suggests that both may play a role in cell

migration and formation of lumens (Hendrix et al. 2003b). E-Cadherin can induce phosphorylation of EphA2 which results in its binding and subsequent activation of PI3K (Pandey et al. 1994; Zantek et al. 1999; Orsulic & Kemler 2000). An additional role for PI3K activity was found in promoting melanoma vasculogenic mimicry by regulating the expression and function of MT1-MMP and MMP-2, and consequently the cleavage of laminin 5 γ 2 chain (Seftor & Kirschmann 2001; Hess et al. 2003). By interacting with VE-cadherin through VEGFR2 and B-catenin, PI3K is able to contribute to the survival of endothelial cells (Carmeliet et al. 1999). Endothelial cell migration is dependent on the activation of PI3K, which occurs downstream of focal adhesion kinase (FAK) activation in VEGF-A stimulated cells expressing VEGFR-2 (Carmeliet 2000; Qi & Claesson-Welsh 2001). In prostate cancer cells (PC-3), an interaction between FAK and EphA2 has been reported (Miao et al. 2000). While in aggressive melanoma cells, phosphorylated FAK interacts with EphA2. These aggressive melanoma cells mimic endothelial vasculature (Hess et al. 2005).

Hendrix et al. proposed that in highly aggressive melanoma cells, VE-cadherin would promote the interaction between FAK and EphA2 through regulation of EphA2's ability to translocate to the membrane. Interaction between EphA2 and its membrane bound ligand, would result in phosphorylation of EphA2. Phosphorylated EphA2 could then form an interaction with FAK, which would lead to the phosphorylation and activation of FAK. The signal transduction pathways activated through VE-cadherin and EphA2 could converge resulting in the activation of PI3K. This could then lead to melanoma vasculogenic mimicry via activation of MMP-2 and finally resulting in the cleavage of the laminin 5 γ 2 chain (Hendrix et al. 2003b).

Tumor cell-secreted IL-8 has been recently shown to act directly on vascular endothelial cells and to serve as their survival factor (Yoshida et al. 1997). In the cDNA

microarray, it was found that the angiogenic chemokine IL-8 was downregulated after Gal-3 knockdown. This effect was validated by RT-PCR and ELISA *in vitro*. The latter assay examined the secretion of IL-8 into the supernatant of cultured cells. Furthermore, the decrease in IL-8 levels was confirmed by immunohistochemical staining of C8161 tumors before and after Gal-3 knockdown.

In melanoma cell variants, both non-metastatic and metastatic, it was found that constitutive IL-8 transcription activity directly correlates with the activation level of constitutive NF- κ B (Huang et al. 2000). Using deletion mutants to analyze the IL-8 promoter, it was shown that upstream of the transcription start site there is a 133 bp region that is necessary for constitutive IL-8 promoter activity. Furthermore, it was found that mutation of NF- κ B binding sites in A375 human melanoma cells eliminated the constitutive IL-8 promoter activity (Huang et al. 2000). Finally, a dominant-negative mutant I κ B α expression vector transfected into melanoma cells resulted in a significant decrease of expression of IL-8 and the level of constitutive NF- κ B activity. This demonstrates that in highly metastatic human melanoma cells, constitutive NF- κ B/relA activities can contribute to overexpression of IL-8 (Huang et al. 2000). A critical role for NF κ B in regulating IL-8 expression was further confirmed by the production of IL-8 in malignant melanoma cells through the induction with L-1 α and TNF- α (Patel et al. 2002). In highly metastatic A375SM, Liu et al. demonstrated that the proangiogenic TGF- β 1 selectively induced IL-8 expression. This was not observed in A375P non-metastatic parental cells (Liu et al. 2005). However, this expression of the IL-8 gene was transcriptionally mediated through binding of NF- κ B, AP-1, and C/EBP-like factor NF-IL6 to the promoter region.

The thrombin receptor (PAR-1) can further induce IL-8 upon activation by thrombin (Tellez & Bar-Eli 2003). In metastatic melanoma, overexpression of PAR-1

appears to be causally related to a loss of AP-2 expression, as in the case of MCAM/MUC18 (Tellez et al. 2003). This suggests that the gain in expression of both IL-8 and MCAM/MUC18 is due to the loss of the AP-2 transcription factor in metastatic melanoma. It was shown, that metastatic melanoma cells, which produce IL-8 or primary cutaneous melanoma (IL-8-negative), which are transfected with the IL-8 gene, resulted in the upregulation of MMP-2 expression and activity, and displayed an increased invasiveness through Matrigel-coated filters (Luca et al. 1997). IL-8 activation of MMP-2 led to metastasis through enhanced invasion of host stroma by tumor cells and increased angiogenesis. The metastatic melanoma cells producing IL-8 or primary cutaneous melanoma (IL-8-negative) transfected with the IL-8 gene upregulated the Matrix Metalloproteinase-2 (MMP-2) expression and activity, which increased invasiveness through Matrigel-coated filters

Therefore, it was hypothesized that since the loss of Gal-3 resulted in downregulation of IL-8 secretion, it would also result in a loss of its downstream target expression, that of MMP-2. Western Blot analysis, zymography assay and immunohistochemical staining in C8161 experimental tumors confirmed that Gal-3 knockdown resulted in a loss of MMP-2 expression and secretion, whereas no MMP-2 expression was detected in the cDNA microarray analysis after Gal-3 knockdown.

The multiple mechanisms (migration, angiogenesis, tumor and vascular endothelial cell proliferation) which appear to be involved in IL-8 action, offer a potentially unique target for immunotherapies against human melanomas. It has already been shown in melanoma cells that a human anti-IL-8 antibody (ABX-IL8, obtained from Abgenix) displayed a neutralizing affect on IL-8 secretion (Huang et al. 2002). In addition, ABX-IL8 displayed potent inhibition of both MMP-2 expression and activity, and was able to decrease invasion of metastatic melanoma cells (A375SM) through the

basement membrane. Finally, ABX-IL8 has been shown to suppress the metastatic potential and tumorigenicity of human melanoma TXM-13 and A375SM cells in nude mice (Huang et al. 2002). The suppression of subcutaneous tumor cell growth was associated with the decrease in MMP-2 expression and angiogenesis (Huang et al. 2002). The results above indicate that metastatic melanoma could be treated with ABX-IL8. Anti-IL-8 should be tested either alone or in combination with other chemotherapeutic therapies.

Furthermore, the mechanism of Gal-3-dependent expression of VE-cadherin and IL-8 was investigated. The analysis of the VE-cadherin and IL-8 promoter reporters showed that Gal-3 knockdown resulted in inhibition of promoter activity. When the VE-cadherin promoter sequence for the putative transcription factor binding sites was analyzed, it was found that the 600 base pair region upstream from the start sequence relative to the start of transcription contains putative binding sites for SP-1, NFkB, EGR-1, and Ap-2 transcription factors. The IL-8 promoter was found to contain putative EGR-1, NFkB, SP-1, and AP-2 transcription factor binding sites. Chromatin Immunoprecipitation (ChIP) analysis revealed an increase in EGR-1 transcription factor binding to the CDH5 and IL-8 promoters in the Gal-3 shRNA cell line compared to parental cells or non-targeting shRNA cells.

EGR-1, described as a tumor suppressor, is an 82 kDa phosphoprotein and a member of the immediate early gene family of transcription factors that includes EGR-1 to -4 and NGFI-B (nerve growth factor inducible factor IB) (Milbrandt 1987; Liu et al. 1996; Silverman & Collins 1999). It is involved in the regulation of growth and differentiation through regulation of transcription of target genes through GC-rich elements (Liu et al. 1996). EGR-1 serves as a bridge between extracellular stimulation from growth factors, cytokines, hormones and environmental stress, and the cellular

responses associated with differentiation, proliferation, apoptosis and tissue injury (Liu et al. 1998; Silverman & Collins 1999). Many human tumors express moderate to no EGR-1 in contrast to their normal counterparts (Calogero et al. 1996; Huang et al. 1997b; Liu et al. 2000). In small cell lung and human breast tumors (Levin et al. 1995; Huang et al. 1997a) EGR-1 expression is decreased or undetectable as well as in human gliomas (Calogero et al. 2001). Since EGR1 has been previously shown to occasionally act as a transcriptional repressor (Tan et al. 2003), it is suggested that its binding to CDH5 and IL-8 promoters in melanoma cells might repress their activity leading to a decrease in gene expression.

In addition to changes to EGR1, it might be expected that Gal-3 knockdown can modulate the recruitment of other transcription factors to the CDH5 promoter such as AP-2, NFkB and SP-1. Indeed AP-2 is lost in melanoma. It can act either as transcription activator or repressor. Therefore to gain complete knowledge about CDH5 promoter regulation experiments on additional transcription factors has to be conducted in the future.

EGR-1 binding was upregulated in the Gal-3 knockdown cells on Chip assay whereas no difference in expression in cytoplasm was detected using Western Blotting comparing Gal-3 knockdown cells with NTshRNA control cells. In this study an increase in EGR-1 binding was associated with the decrease in the CDH5 promoter activity. The knockdown of Gal-3 resulted in an increase of EGR-1 recruitment to the CDH5 promoter. On the other hand, the transfection experiments showed that overexpression of EGR-1 resulted in the inhibition of CDH5 expression as well as promoter activity. However no difference in EGR-1 expression has been found after Gal-3 knockdown (data not shown). This indicates that EGR-1 may act as a negative regulator of the CDH5 promoter and that Gal-3 acts upstream to prevent EGR-1 binding to the CDH5 promoter.

To understand the mechanism of EGR-1 mediated repression of CDH5 promoter activity the recruitment of Histone deacetylases (HDAC 1 and 2) and Histone acetylase (HAT) (p300) to the CDH5 promoter before and after Gal-3 knockdown will be analyzed in future studies. It is possible that more HDACs and/or less p300 may bind to the CDH5 promoter as a result of EGR-1 recruitment. Although EGR-1 typically acts as a transcriptional activator it can be hypothesized that it either acts as a repressor on the CDH5 promoter or that its binding results in a decreased recruitment of other strong activators like SP-1. Indeed, analysis of the CDH5 promoter for potential binding sites using the Genomatix software revealed that EGR1 binding sites overlapped with binding sites for SP-1.

Intracellularly, Gal-3 has been shown to suppress both anoikis and drug induced apoptosis. Conversely, it was shown that Gal-3 which was secreted by tumor cells induces T-cell apoptosis and played a role in the immune escape mechanism during tumor progression through induction of apoptosis of cancer infiltrating T-cells (Nakahara et al. 2005). Zubieta et al. correlated the expression of Gal-3 with the apoptosis of tumor-associated lymphocytes (Zubieta et al. 2006). Transcriptional repression of Gal-3 has been associated with p53-induced apoptosis. Phosphorylation at Ser46 of p53 is important for proapoptotic gene transcription and induction of apoptosis. Furthermore, the homeodomain-interacting protein kinase 2 (HIPK2) has been shown to be involved in these functions. Cecchinelli et al. reported that in Gal-3 repression, p53 and HIPK2 cooperate and that HIPK2 kinase activity is necessary for this cooperation. These results uncover a new apoptotic pathway in which the antiapoptotic factor Gal-3 is repressed through the interaction of HIPK2 and phosphorylated p53 (Cecchinelli et al. 2006). Gal-3 has also been shown to be involved with AKT in the ability to protect bladder carcinoma cells during TRAIL-induced apoptosis (Oka et al. 2005).

Gal-3 is also known to bind to activated K-Ras-GTP. Both of these antiapoptotic proteins are associated with cancer progression. Overexpression of Gal-3 in the human breast cancer cell line of BT-549/Gal-3, correlated with a loss in wt N-Ras-GTP and a significant increase in wild-type (wt) K-Ras-GTP. However the mutant, nononcogenic proteins of Gal-3, Gal-3(S6E) and Gal-3(G182A), did not induce the Ras isoform switch. During Gal-3's binding and activation of wt-K-Ras, several oncogenic functions were conferred in BT-549 cells suggesting that some of the molecular functions of Gal-3 are due in part to K-Ras activation (Shalom-Feuerstein et al. 2005).

Overexpression of Gal-3 has been shown to regulate expression levels of the Wnt pathway, including c-myc and cyclin D1. (Kim et al. 1999; Lin et al. 2000; Shimura et al. 2004; Shimura et al. 2005). It has also been shown to be structurally similar to β -catenin. Both β -catenin and Gal-3 contain the consensus sequence (S₉₂XXXS₉₆) which is necessary for glycogen synthase kinase-3 β (GSK-3 β) phosphorylation. β -catenin is a substrate of GSK-3 β , and phosphorylation of β -catenin by GSK-3 β is required for its nuclear import-export. β -catenin is targeted for ubiquitination and degradation through phosphorylation by a dual kinase system of CKI α and GSK-3 β (Yost et al. 1996; Ikeda et al. 1998; Kishida et al. 1998; Yamamoto et al. 1998; Kikuchi 1999). Similarly, as the consensus sequences suggests, nuclear import-export of Gal-3 is phosphorylation dependent via GSK-3 β (Yoshii et al. 2002; Shimura et al. 2004; Takenaka et al. 2004). Axin, a regulator protein of Wnt, that complexes with β -catenin, also binds Gal-3 using the same sequence motif identified by a deletion mutant analysis (Shimura et al. 2005). Mutations in the genes of axin, APC or β -catenin led to enhanced phosphorylation, which subsequently led to both their accumulation and accumulation of Gal-3 in the nucleus. This resulted in Wnt target genes being activated (Yost et al. 1996; Ikeda et al. 1998).

Furthermore, EGR-1 was found to be bound to the Fibronectin (FN) promoter in response to HGF (hepatocyte growth factor) via inhibition of B-RAF/MAP kinase pathway by dominant-negative mutants and by U0126-abrogated HGF-induced EGR-1, and chromatin immunoprecipitation (Gaggioli et al. 2005). Also the FN levels were found to be increased through exogenous EGR-1, whereas on the other hand through activation of the EGR1 corepressor NAB2, EGR-1 was blocked. This blockage showed an upregulation of FN synthesis, which is induced by HGF, and reveals that EGR-1 plays a pivotal role in FN expression in response to HGF. Upon these findings, Gaggioli et al. described the regulation of melanoma progression by autocrine HGF signaling or by constitutive activation of MAP kinase pathway (Gaggioli et al. 2005).

It is known that the B-Raf mutation mainly activates the extracellular signal-regulated (ERK)/mitogen-activated protein (MAP) kinase pathway. Gaggioli et al. further showed that high FN and EGR-1 levels were mostly found in cells expressing this oncogenic B-Raf mutation. On the other hand, FN expressed endogenously was found to be blocked by small interfering RNA (siRNA)- mediated depletion of B-Raf or EGR-1, which lead to decreased ability of melanoma cells to be invasive *in vitro*. However, FN could not be upregulated by stimulation of the ERK pathway in normal melanocytes (Greene; Gaggioli et al. 2007). That shows that FN is tumor-specific regulated by the constitutive ERK/MAP-Kinase pathway, which reveals a possible role for FN through its ability of self-production to intervene in melanoma tumorigenesis by promoting tumor cell invasion.

In summary, a shift of Gal-3 immunophenotype from Benign Nevi to Metastatic Malignant Melanoma was observed in the human specimens, which supports the theory of a progression model between nevus cells and metastatic melanoma cells. A different pattern of Gal-3 expression in different histologic types of primary melanomas, possibly

related to the pattern of sun exposure, and in different types of metastatic lesions, possibly associated with survival, was identified. The increase of Gal-3 protein expression correlated with the metastatic potential of melanoma cell lines. Furthermore, decreased Gal-3 expression resulted in reduced tumor growth, lung metastases, proliferation, angiogenesis and increased apoptosis *in vivo*. Validation of the cDNA microarray analysis demonstrated that silencing Gal-3 expression resulted in a loss of expression of endothelial cell differentiation markers by melanoma cells (CDH5, FN-1, EDG-1) as well as decrease of the angiogenic factor IL-8. Taken together, these results indicate that Gal-3 contributes to melanoma tumor growth and metastasis by inducing cell plasticity and aggressiveness (Figure 35). Finally, since Gal-3 also provides cancer cells with anti-apoptotic functions, targeting Gal-3 with shRNA helpfully proved its significance for treatment in melanoma.

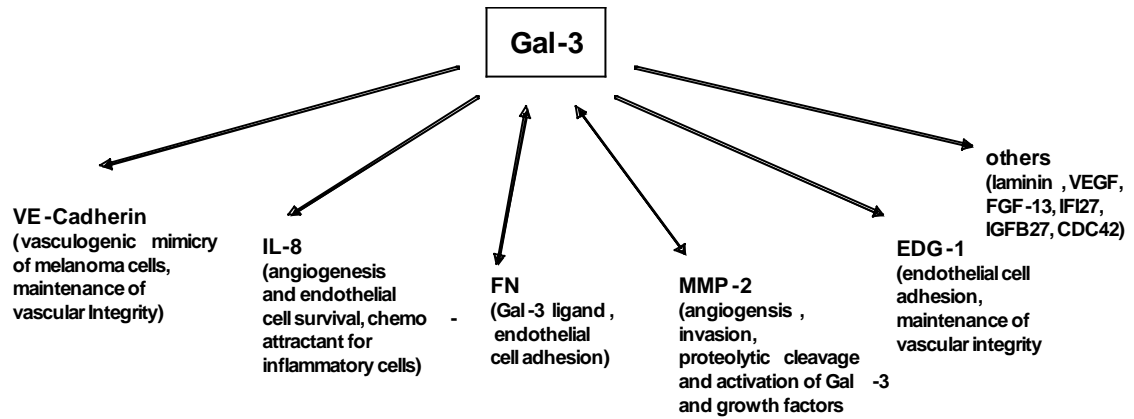


Figure 35 Gal-3 model.

Gal-3 participates in metastatic progression in melanoma by upregulating VE-cadherin, IL-8, FN, MMP-2, EDG-1 and others (laminin, VEGF, FGF-13, IFI27, IGFB27, CDC42). There has been found a repressor loop mechanism between Gal-3 and FN, and Gal-3 and MMP-2.

Summary

Galectin-3 (Gal-3) belongs to the lectin family of carbohydrate-binding proteins. Gal-3 is known to be involved in diverse biological processes including cell growth, differentiation, apoptosis, cell adhesion, malignant transformation and RNA processing. It is highly expressed in a variety of human cancers and therefore may play a putative role in carcinogenesis and cancer progression. In order to understand the role of Gal-3 in melanoma progression, Gal-3 expression in human melanocytic lesions was studied by utilizing a tissue microarray. Cytoplasmic and nuclear expression levels of Gal-3 increased as human melanoma lesions progress through the benign nevi to dysplastic nevi stages as well as from the primary melanoma to metastatic melanoma stages. Further melanocytic lesions from sun-exposed skin areas displayed high nuclear expression of Gal-3 versus low cytoplasmic expression levels. The analysis of metastatic lesions revealed that subcutaneous metastases display only cytoplasmic expression of Gal-3, whereas lymph node metastases showed higher nuclear Gal-3 expression. This indicates that Gal-3 levels may serve as a marker of metastatic progression in melanoma. Importantly, using clinical data, a near significant correlation was found between decreased patient survival and high nuclear-to-cytoplasmic Gal-3 expression ratio in tumor specimens. *In vitro*, Gal-3 expression showed correlation with an increase in metastatic potential of melanoma cell lines.

To further delineate the role of Gal-3 in tumor growth and metastasis, an RNA interference approach with lentiviral delivery technology was made to silence Gal-3 expression in the metastatic melanoma cell line C8161. A strong decrease in tumorigenic and metastatic potential of C8161 cells *in vivo* after knockdown of Gal-3 was observed. The decrease in tumorigenicity after Gal-3 knockdown was accompanied by a decrease in

tumor cell proliferation (revealed by staining for Proliferating Cell Nuclear Antigen, PCNA), increase in apoptosis (TUNEL assay), and decrease in vessel density (CD31 staining). In order to reveal potential gene targets downstream of Gal-3, an Affymetrix cDNA microarray analysis on C8161 melanoma cells following Gal-3 silencing was performed. The cDNA microarray analysis revealed that the expression of 567 genes was downregulated and in 227 genes upregulated after Gal-3 knockdown. Western blot analysis following Gal-3 knockdown confirmed the decrease in the expression of a group of endothelial and mesenchymal markers, like Vascular Endothelial (VE)-cadherin (CDH5), Interleukin-8 (IL-8), Fibronectin-1 (FN-1), and Endothelial Differentiation Sphingolipid G-protein receptor-1 (EDG-1). Since vascular endothelial cells usually express all these proteins, and since aberrant expression of VE-cadherin is known to induce vasculogenic mimicry of metastatic melanoma cells, it was hypothesized that Gal-3 mediates melanoma cell plasticity, a phenomenon associated with melanoma aggressiveness. Indeed, Gal-3 knockdown cells were unable to form tube-like structures in a three-dimensional growth model on collagen. IL-8 expression was decreased in Gal-3 shRNA tumor specimens and ELISA studies showed that the secretion of IL-8 into the media of Gal-3 knockdown cells was three fold decreased than in parental cells. Furthermore, Gal-3 downregulated the expression of VE-cadherin and IL-8 on the transcriptional level. Finally, the mechanism of downregulation of VE-cadherin and IL-8 expression following Gal-3 knockdown was analyzed and found that it was associated with an increase in binding of the early growth response-1 (EGR-1) transcription factor/tumor suppressor to the promoters of these genes, as revealed by chromatin immunoprecipitation assay. Transient overexpression of EGR-1 in C8161 parental cells led to the downregulation of VE-cadherin protein as shown by Western Blot analysis. Using VE-cadherin promoter/ luciferase reporter gene construct it was shown that

overexpression of EGR-1 downregulated the VE-cadherin promoter activity. Gal-3 knockdown resulted in a decrease in MMP-2 expression and secretion as well as a decrease in tumor cell invasion through matrigel-coated filters. Overall, the results presented here demonstrate that Gal-3 may play a critical role in melanoma tumor growth and metastasis, at least in part by mediating melanoma cell plasticity and vasculogenic mimicry and serves as a marker for melanoma progression.

Zusammenfassung

Galectin-3 (Gal-3) gehört zu der Familie der Lektine, welche Kohlenhydratbindende Proteine sind. Gal-3 hat eine grosse Bedeutung für verschiedene biologische Vorgänge, wie zum Beispiel (z.B.) Zellwachstum, Differenzierung, Apoptose, Zelladhäsion, maligne Transformation und RNA Prozessierung. Es ist in einer Reihe von malignen Tumoren / Karzinomen humanen Krebsformen stark exprimiert und spielt deshalb eine mögliche Rolle in der Karzinogenese und in der Progredienz des Karzinoms. Um die Rolle von Gal-3 beim Voranschreiten des Hautkrebses (Melanom) zu verstehen, wurde die Gal-3 Expression in humanen melanozytischen Gewebeproben mit Hilfe eines Gewebe-Microarrays untersucht. Der zytoplasmatische und nukleäre Expressionslevel von Gal-3 erhöhte sich im Verlaufe des Voranschreitens des Hautkrebses von dem Stadium des benignen Nevus zum dysplastischen Nevus, sowie auch vom primären zum metastatischen Melanomstadium.

Desweiteren zeigten Hautareale, die der Sonne ausgesetzt waren, eine erhöhte Expressionsrate von Gal-3 im Nukleus, im Gegensatz dazu war die Gal-3 Expressionsrate im Zytoplasma niedrig.

Die Analyse von Metastasen ergab, dass subkutane Metastasen Gal-3 nur im Zytoplasma exprimierten, wohingegen Lymphknotenmetastasen einen sehr hohen Gehalt an Gal-3 im Zellkern aufwiesen. Das bedeutet, dass der Gal-3 Gehalt in der Zelle als Marker für das Voranschreiten des metastatischen Melanoms benutzt werden könnte. Klinische Daten zeigten eine Korrelation zwischen einer geringeren Überlebenszeit von Patienten und einem erhöhten Verhältnis von nukleärer zu zytoplasmatischer Gal-3 Expressionsrate in Tumorgewebeproben. Ausserdem zeigte sich eine Korrelation

zwischen zytoplasmatischer und nukleärer Expressionrate in einer Serie von Melanomzelllinien mit aufsteigendem metastatischem Potential.

Um die Rolle von Gal-3 auf Tumorwachstum und Metastasenbildung weiter zu untersuchen, wurde ein RNA-Interferenzansatz gewählt, um mit Hilfe von lentiviraler Technologie die Expression von Gal-3 in der metastatischen Melanomzelllinie C8161 herunterzuregulieren. Ein starker Rückgang des tumorigenen und metastatischen Potentials der C8161 Zellen *in vivo* wurde nach Herunterregulierung von Gal-3 beobachtet. Neben der Abnahme in der Tumorigenität nach der Gal-3 Runterregulierung wurde gleichzeitig eine Abnahme des Tumorzellwachstums (gemessen mittels PCNA), eine erhöhte Apoptoserate (gemessen mittels TUNEL) und eine Abnahme in der Gefässdichte (gemessen mittels CD31) beobachtet.

Um Gene ausfindig zu machen, die unterhalb von Gal-3 auf molekularer Ebene liegen, wurde eine Affymetrix cDNA-Microarray Analyse von C8161 Melanomzellen vor und nach Herunterregulierung von Gal-3 durchgeführt. Die cDNA-Microarray Analyse ergab, dass nach der Runterregulierung von Gal-3 567 Gene herunter- und 227 Gene hochreguliert waren. Western Blot-Analysen bestätigten, dass nach Gal-3 Herunterregulierung die Expression einer Gruppe von endothelialen und mesenchymalen Markergenen, wie z.B. vaskuläres endotheliales (VE)-Cadherin (CDH5), Interleukin-8 (IL-8), Fibronectin-1 (FN-1) und der endotheliale Differenzierungssphingolipid G-Protein Rezeptor-1 (EDG-1) nach Gal-3 Herunterregulierung abnahmen. Da vaskuläre endotheliale Zellen gewöhnlich all diese Proteine exprimieren, und da bekannt ist, dass die anomale Expression von VE-Cadherin eine „vaskulogene Mimikry“ von metastatischen Melanomzellen induzieren kann, wurde angenommen, dass Gal-3 im Melanom Zellplastizität vermittelt, ein Phänomen, das mit Melanomaggressivität verbunden ist. Zellen, in denen Gal-3 herunterreguliert wurde, waren nicht in der Lage

tubulär-ähnliche Strukturen auf Kollagen in einem 3-dimensionalem Wachstumsmodell zu bilden.

Die Expression von IL-8 war in Gal-3 shRNA Tumorgewebeprobe herabgesetzt und ELISA Studien zeigten eine 3-fache Reduktion der Sekretion von IL-8 in das Medium von Gal-3 herunterregulierten Zellen im Vergleich zu den Ausgangszellen. Desweiteren herabregulierte Gal-3 die Transkriptionsrate von VE-Cadherin und IL-8.

Zum Schluss wurde der Mechanismus der Herabregulierung der Expression von VE-Cadherin und IL-8 nach Gal-3 Herunterregulierung untersucht und es wurde gefunden, dass die Herunterregulierung mit einer Zunahme in der Bindung des EGR-1 Transkriptionsfaktors/ Tumorsuppressors an die Promotoren dieser Gene assoziiert war, was durch ein Chromatinimmunoprecipitationsversuch gezeigt wurde.

Transiente Überexpression von EGR-1 in C8161 Ausgangszellen führte zu einer Herunterregulierung vom VE-Cadherinprotein, wie mittels Western Blot gezeigt wurde. Mit Hilfe eines VE-Cadherin Promoter/Luciferase Reporter-Konstruktes konnte gezeigt werden, dass die Überexpression von EGR-1 die Aktivität des VE-Cadherin Promoters herunterregulierte.

Weiterhin resultierte die Gal-3 Herunterregulierung in einer Abnahme der MMP-2 Expression und Sekretion sowie in der Abnahme der Fähigkeit von Tumorzellen in Matrigel-beschichteten Filter einzudringen.

Gal-3 spielt eine kritische Rolle im Fortschreiten des Melanoms und bei der Metastasenbildung zumindest teilweise dadurch, dass es Melanomzellplastizität und vaskulogene Mimikry vermittelt.

Zusammenfassend demonstriert die hier präsentierte Studie, dass die Gal-3 Expression als ein Marker für die Progredienz von Melanomen dienen kann.

List of Abbreviations

293 T	Human embryonal kidney cell line (HEK)
3-D	Three-dimensional
A	Assymetry, shape of melanoma lesion
A375P	Non-metastatic parental cell line
A375SM	Highly metastatic melanoma cell line
ABCDE	mnemotic guidance system
ABX-IL8	Abgenix-IL-8, fully humanized anti IL-8 antibody
AEC	3 Amino-Ethylcarbazole
AGE	Advanced glycosylation end product binding protein
Ala	Alanine
ALM	Acral-lentiginous melanoma
AP-2	Activator protein-2, transcription factor
Arg	Arginine
Asp	Asparagine
ATCC	American Type Culture Collection
ATF1	Activating transcription factor-1
ATF-2	Activating transcription factor-2
B	Border Irregularity of melanoma lesion
B16F1	Melanoma cell line
BAD	BCL associated death protein
Balb/C	nude mice
BCL-2	Anti-apoptotic protein
bFGF	Basic fibroblast growth factor

BH1	BCL-2 homology domain 1
BN	Benign nevus
BRAF	Small tyrosine kinase protein-encoding gene, protooncogene
BT-549	Human breast cancer cell line
C	Color Variations of melanoma lesion
C8161	Highly metastatic melanoma cell line
Ca ²⁺	Calcium ²⁺
cAMP	cyclic Adenosine Monophosphate
CD31	Micro vessel density marker
CDC42	GTPase, causes tyrosine phosphorylation activity of PI3K
CDH5	Vascular endothelial- Cadherin (VE-Cadherin, CD144)
cDNA	complementary DNA
CHIP	Chromatin Immunoprecipitation Assay
c-Kit	Tyrosine Kinase
CKI α	Dual kinase system
Cla1	Enzyme
cm	Centimeter
CO ₂	Carbondioxide
COOH	Carboxy- terminal end, binding to the carbohydrates
CRD	Carbohydrate recognition domain
CREB	cAMP reponse element binding protein, transcription factor
CXCR	Chemokine receptor
D	Diameter, Moles > than 5 mm
Da	Dalton
DAB	3,3' Diamine Benzadine Tetra Hydrochloride

DEPC	Diethylpyrocarbonate
DM-4	Low metastatic melanoma cell line
DMEM	Dulbeco's minimal essential medium
DMSO	Dimethyl sulfoxide
DN	Dysplastic nevus
DNA	Desoxyribonucleic acid
dNTP	Nucleotides
DTIC	Dacarbazine, alkylating chemotherapeutic agent
DX3	Low metastatic melanoma cell line
E	Evolving, defines mole changes in size, shape, surfaces, shades of color
E-Cadherin	Epithelial Cadherin, cell adhesion molecule
ECM	Extracellular membrane
EDG-1	Endothelial Differentiation Sphingolipid G-protein receptor-1
EGFR	Epidermal growth factor receptor
EGR-1	early growth response-1, transcription factor/ tumor suppressor
ELISA	Enzyme Linked Immunosorbent Assay
EPHA2	Ephrin A2, receptor tyrosine kinase
FACS	Fluorocytometry cell sorting assay
FAK	Focal adhesion kinase
FBS	Fetal bovine serum
FGF-13	Fibroblast growth factor-13
FN-1	Fibronectin-1
G-1	Growth phase 1 in cell cycle, Mitose
G-2	Growth phase 2 in cell cycle, Mitose
G-361	Melanoma cell line

Gal-3	Galectin-3, carbohydrate-binding protein, belongs to the lectin family
GAPDH	Glyceraldehydes-3 phosphate dehydrogenase
GC-rich	Glycine-Cystine rich
GFP	Green fluorescence protein
Gly	Glycine
GSK-3 β	Glycogen synthase kinase-3 β
H&E	Hematoxillin & Eosin staining
HAV	His-Ala-Val motif
HBSS	Hank's Balanced Salt Solution
HEK	Human embryonal kidney cell line (293 T)
HGF	Hepatocyte growth factor
Hind III	Enzyme
HIPK2	Homeodomain-interacting protein kinase 2
His	Histidine
HT-144	Melanoma cell line
HUVEC	Human umbilical vascular endothelial cells
i.p.	Intraperitoneal injection
i.v.	Intravenous injection
IACUC	Institutional Animal Care and Use Committee
IF127	Interferon-27, alpha inducible protein
IGFB27	Insulin-like growth factor binding protein 7
I κ B α	Inhibitor element of NF κ B complex
IL-2	Interferone-2
IL-5	Interleukin-5

IL-8	Interleukin-8
kDa	Kilo Dalton
Kpn1	Enzyme
LAMP1	Lysosome associated membrane protein 1
LDH	Lactat Dehydrogenase
Leu	Leucine
LOH	Loss of heterozygosity
MAC-2 BP	Gal-3 ligand
MAPK	Mitogen-activated protein kinase
MCAM	Melanoma cellular adhesion molecule (MUC18, Mel-CAM, CD146,A32 antigen, S-Endo-1)
MDG-2	Packaging plasmid
MEM	Eagle's minimal essential medium
MeWo	Highly metastatic melanoma cell line
Mg ²⁺	Magnesium ²⁺
MGAT-5	Mgat-5 modified N-glucans, Gal-3 ligand
Mlu1	Enzyme
MM	Primary melanoma
MMM	Metastatic melanoma
MMP	Matrix metalloproteinase
MMP-2	Matrix Metalloproteinase -2
MMP-9	Matrix metalloproteinase-9
mRNA	mitochondrial RNA
MT1-MMP	Membrane bound Matrix metalloproteinase-1
MVD	Micro vessel density

n	number
NaCl	Natrium Chloride
NADPH	Natriumdephosphohydroxyl
N-Cadherin	Neuronal Cadherin, cell adhesion molecule
NCOR-1	Nuclear correceptor-1
NFkB	Nuclear factor kappa B
NH ₂	Amino-terminal end, cellular targeting
NRAS	Small tyrosine kinase protein-encoding gene, protooncogene
NT shRNA	Nontargeting small hairpin RNA, control
NWGR	Asparagine-Trypsine-Glycine-Arginine anti-death motif
°C	Temperature
P16INK4A/P14ARF	Tumor suppressor gene
P21	Cyclin inhibitor
P27	Cyclin inhibitor
P53	Tumor suppressor gene
P60, p90	AGE- receptor complex
PACV	Polyvalent allogeneic whole-cell vaccine
PAR-1	Protease-activated receptor -1
PAX-2	Packaging plasmid
PBS	Phosphate balanced saline
PC3	Prostate cancer cell line
P-Cadherin	Placental Cadherin, cell adhesion molecule
PCNA	Proliferating cell nuclear antigen positive cells
PCR	Polymerize chain reaction
PD98059	ERK inhibitor

PD-ECGF	Platelet-derived endothelial cell growth factor
PDGF	Platelet derived growth factor, tyrosine kinase
PI3K	Phosphatidylinositol 3-kinase
pLVTHM	Vector, obtained from www.tronolab.com
polylacNAc	Poly N-acetyl lactosamine
pRL-CMV	Renilla Luciferase reporter plasmid
PTEN	Phosphatase and tensin homolog, tumor suppressor gene
RAC1	GTPase, causes tyrosine phosphorylation activity of PI3K
RAGE	Receptor for advanced glycosylation end product binding protein
Rb	Retinoblastoma
RBC	Red blood cell
RGP	Radial growth phase
RNA	Ribonucleic acid
rpm	centrifuge speed
s.c.	Subcutaneous injection
SB-2	Low metastatic melanoma cell line
SC35	Non- small nuclear ribonucleoprotein splicing factor
STD	Standard deviation
SDS	Sodium dodecyl sulfate
Ser46	Serine position 46
shRNA	small hairpin RNA
siRNA	small interfering RNA
SNAIL	Transcription factor
SP-1	Transcription factor
SSM	Superficial spreading melanoma

t ₅₀	tumor growth until death
Taq	Enzyme
T-cell	T(hymus) –cell, Immunsystem
TFAg	Thomsen- Friedenreich glycoantigen
TGFβ	Tumor growth factor beta
TIMP2	Matrix metalloproteinase Inhibitor-2
TMA	Tissue Microarray
TNFα	Tumor necrosis factor alpha
Trp	Trypsine
TUNEL	In situ terminal dUTP Nick End Labeling Assay
TXM-1	Median metastatic melanoma cell line
TXM-13	Median metastatic melanoma cell line
TXM-18	Median metastatic melanoma cell line
TXM-40	Low metastatic melanoma cell line
uPA	Urinary plasminogen activator
UV-B	Ultraviolet radiation light B
V600E	Single phosphomimetic substitution in the kinase activation domain (V599E) on exon 15
Val	Valine
VE-Cadherin	Vascular endothelial- Cadherin, cell adhesion molecule
VEGF	Vascular endothelial growth factor
VEGFR-2	Vascular endothelial growth factor receptor-2
VGP	Vertical growth phase
WM2664	Highly metastatic melanoma cell line
α5β1	Fibronectin receptor, integrin

$\alpha v\beta 3$	Vitronectin receptor, integrin
μg	Micro gramm
μm	Micro Milliliter
μM	Micro Molar

References

- Bar-Eli M 2001. Gene regulation in melanoma progression by the AP-2 transcription factor. *Pigment Cell Res* 14(2): 78-85.
- Bazzoni G, Dejana E, Lampugnani MG 1999. Endothelial adhesion molecules in the development of the vascular tree: the garden of forking paths. *Curr Opin Cell Biol* 11(5): 573-81.
- Bellett RE, Mastrangelo MJ, Laucius JF, Bodurtha AJ 1976. Randomized prospective trial of DTIC (NSC-45388) alone versus BCNU (NSC-409962) plus vincristine (NSC-67574) in the treatment of metastatic malignant melanoma. *Cancer Treat Rep* 60(5): 595-600.
- Bevona C, Goggins W, Quinn T, Fullerton J, Tsao H 2003. Cutaneous melanomas associated with nevi. *Arch Dermatol* 139(12): 1620-4; discussion 1624.
- Breslow A 1970. Thickness, cross-sectional areas and depth of invasion in the prognosis of cutaneous melanoma. *Ann Surg* 172(5): 902-8.
- Carmeliet P 2000. Mechanisms of angiogenesis and arteriogenesis. *Nat Med* 6(4): 389-95.
- Carter SK, Friedman MA 1972. 5-(3,3-dimethyl-1-triazeno)-imidazole-4-carboxamide (DTIC, DIC, NSC-45388)--a new antitumor agent with activity against malignant melanoma. *Eur J Cancer* 8(1): 85-92.
- Clark WH, Jr., Mihm MC, Jr. 1969. Lentigo maligna and lentigo-maligna melanoma. *Am J Pathol* 55(1): 39-67.

- Clark WH, Jr., Elder DE, Guerry Dt, Epstein MN, Greene MH, Van Horn M 1984. A study of tumor progression: the precursor lesions of superficial spreading and nodular melanoma. *Hum Pathol* 15(12): 1147-65.
- Cooper DN 2002. Galectinomics: finding themes in complexity. *Biochim Biophys Acta* 1572(2-3): 209-31.
- Cortegano I, del Pozo V, Cardaba B, de Andres B, Gallardo S, del Amo A, Arrieta I, Jurado A, Palomino P, Liu FT and others 1998. Galectin-3 down-regulates IL-5 gene expression on different cell types. *J Immunol* 161(1): 385-9.
- Dagher SF, Wang JL, Patterson RJ 1995. Identification of galectin-3 as a factor in pre-mRNA splicing. *Proc Natl Acad Sci U S A* 92(4): 1213-7.
- Deininger MH, Trautmann K, Meyermann R, Schluesener HJ 2002. Galectin-3 labeling correlates positively in tumor cells and negatively in endothelial cells with malignancy and poor prognosis in oligodendroglioma patients. *Anticancer Res* 22(3): 1585-92.
- Dennis LK 1999. Analysis of the melanoma epidemic, both apparent and real: data from the 1973 through 1994 surveillance, epidemiology, and end results program registry. *Arch Dermatol* 135(3): 275-80.
- Dhawan P, Singh AB, Ellis DL, Richmond A 2002. Constitutive activation of Akt/protein kinase B in melanoma leads to up-regulation of nuclear factor-kappaB and tumor progression. *Cancer Res* 62(24): 7335-42.
- Duffy MJ 1996. Proteases as prognostic markers in cancer. *Clin Cancer Res* 2(4): 613-8.

- Dumic J, Dabelic S, Flogel M 2006. Galectin-3: an open-ended story. *Biochim Biophys Acta* 1760(4): 616-35.
- Folkman J, Klagsbrun M 1987. Angiogenic factors. *Science* 235(4787): 442-7.
- Frisch SM, Francis H 1994. Disruption of epithelial cell-matrix interactions induces apoptosis. *J Cell Biol* 124(4): 619-26.
- Fukumori T, Takenaka Y, Yoshii T, Kim HR, Hogan V, Inohara H, Kagawa S, Raz A 2003. CD29 and CD7 mediate galectin-3-induced type II T-cell apoptosis. *Cancer Res* 63(23): 8302-11.
- Fukumori T, Oka N, Takenaka Y, Nangia-Makker P, Elsamman E, Kasai T, Shono M, Kanayama HO, Ellerhorst J, Lotan R and others 2006. Galectin-3 regulates mitochondrial stability and antiapoptotic function in response to anticancer drug in prostate cancer. *Cancer Res* 66(6): 3114-9.
- Griffiths L, Stratford IJ 1997. Platelet-derived endothelial cell growth factor thymidine phosphorylase in tumour growth and response to therapy. *Br J Cancer* 76(6): 689-93.
- Haluska FG, Hodi FS 1998. Molecular genetics of familial cutaneous melanoma. *J Clin Oncol* 16(2): 670-82.
- Harris CC, Hollstein M 1993. Clinical implications of the p53 tumor-suppressor gene. *N Engl J Med* 329(18): 1318-27.
- Hendrix MJ, Seftor EA, Hess AR, Seftor RE 2003a. Molecular plasticity of human melanoma cells. *Oncogene* 22(20): 3070-5.

- Hendrix MJ, Seftor EA, Hess AR, Seftor RE 2003b. Vasculogenic mimicry and tumour-cell plasticity: lessons from melanoma. *Nat Rev Cancer* 3(6): 411-21.
- Hess AR, Seftor EA, Gruman LM, Kinch MS, Seftor RE, Hendrix MJ 2006. VE-cadherin regulates EphA2 in aggressive melanoma cells through a novel signaling pathway: implications for vasculogenic mimicry. *Cancer Biol Ther* 5(2): 228-33.
- Hess AR, Postovit LM, Margaryan NV, Seftor EA, Schneider GB, Seftor RE, Nickoloff BJ, Hendrix MJ 2005. Focal adhesion kinase promotes the aggressive melanoma phenotype. *Cancer Res* 65(21): 9851-60.
- Hsu DK, Yang RY, Pan Z, Yu L, Salomon DR, Fung-Leung WP, Liu FT 2000. Targeted disruption of the galectin-3 gene results in attenuated peritoneal inflammatory responses. *Am J Pathol* 156(3): 1073-83.
- Hsueh EC, Essner R, Foshag LJ, Ollila DW, Gammon G, O'Day SJ, Boasberg PD, Stern SL, Ye X, Morton DL 2002. Prolonged survival after complete resection of disseminated melanoma and active immunotherapy with a therapeutic cancer vaccine. *J Clin Oncol* 20(23): 4549-54.
- Huang S, DeGuzman A, Bucana CD, Fidler IJ 2000. Level of interleukin-8 expression by metastatic human melanoma cells directly correlates with constitutive NF-kappaB activity. *Cytokines Cell Mol Ther* 6(1): 9-17.
- Huang S, Mills L, Mian B, Tellez C, McCarty M, Yang XD, Gudas JM, Bar-Eli M 2002. Fully humanized neutralizing antibodies to interleukin-8 (ABX-IL8) inhibit angiogenesis, tumor growth, and metastasis of human melanoma. *Am J Pathol* 161(1): 125-34.

- Iacobini C, Amadio L, Oddi G, Ricci C, Barsotti P, Missori S, Sorcini M, Di Mario U, Pricci F, Pugliese G 2003. Role of galectin-3 in diabetic nephropathy. *J Am Soc Nephrol* 14(8 Suppl 3): S264-70.
- Inohara H, Raz A 1994. Effects of natural complex carbohydrate (citrus pectin) on murine melanoma cell properties related to galectin-3 functions. *Glycoconj J* 11(6): 527-32.
- Inohara H, Raz A 1995. Functional evidence that cell surface galectin-3 mediates homotypic cell adhesion. *Cancer Res* 55(15): 3267-71.
- Inohara H, Akahani S, Kothe K, Raz A 1996. Interactions between galectin-3 and Mac-2-binding protein mediate cell-cell adhesion. *Cancer Res* 56(19): 4530-4.
- Ishikawa M, Dennis JW, Man S, Kerbel RS 1988. Isolation and characterization of spontaneous wheat germ agglutinin-resistant human melanoma mutants displaying remarkably different metastatic profiles in nude mice. *Cancer Res* 48(3): 665-70.
- Iurisci I, Tinari N, Natoli C, Angelucci D, Cianchetti E, Iacobelli S 2000. Concentrations of galectin-3 in the sera of normal controls and cancer patients. *Clin Cancer Res* 6(4): 1389-93.
- Kim HR, Lin HM, Biliran H, Raz A 1999. Cell cycle arrest and inhibition of anoikis by galectin-3 in human breast epithelial cells. *Cancer Res* 59(16): 4148-54.
- Kozlowski JM, Hart IR, Fidler IJ, Hanna N 1984. A human melanoma line heterogeneous with respect to metastatic capacity in athymic nude mice. *J Natl Cancer Inst* 72(4): 913-7.

- Kuwabara I, Liu FT 1996. Galectin-3 promotes adhesion of human neutrophils to laminin. *J Immunol* 156(10): 3939-44.
- Lev DC, Onn A, Melinkova VO, Miller C, Stone V, Ruiz M, McGary EC, Ananthaswamy HN, Price JE, Bar-Eli M 2004. Exposure of melanoma cells to dacarbazine results in enhanced tumor growth and metastasis in vivo. *J Clin Oncol* 22(11): 2092-100.
- Li G, Satyamoorthy K, Herlyn M 2001. N-cadherin-mediated intercellular interactions promote survival and migration of melanoma cells. *Cancer Res* 61(9): 3819-25.
- Li L, Price JE, Fan D, Zhang RD, Bucana CD, Fidler IJ 1989. Correlation of growth capacity of human tumor cells in hard agarose with their in vivo proliferative capacity at specific metastatic sites. *J Natl Cancer Inst* 81(18): 1406-12.
- Liu C, Calogero A, Ragona G, Adamson E, Mercola D 1996. EGR-1, the reluctant suppression factor: EGR-1 is known to function in the regulation of growth, differentiation, and also has significant tumor suppressor activity and a mechanism involving the induction of TGF-beta1 is postulated to account for this suppressor activity. *Crit Rev Oncog* 7(1-2): 101-25.
- Liu G, Zhang F, Lee J, Dong Z 2005. Selective induction of interleukin-8 expression in metastatic melanoma cells by transforming growth factor-beta 1. *Cytokine* 31(3): 241-9.
- Luca M, Xie S, Gutman M, Huang S, Bar-Eli M 1995. Abnormalities in the CDKN2 (p16INK4/MTS-1) gene in human melanoma cells: relevance to tumor growth and metastasis. *Oncogene* 11(7): 1399-402.

- Luca M, Huang S, Gershenwald JE, Singh RK, Reich R, Bar-Eli M 1997. Expression of interleukin-8 by human melanoma cells up-regulates MMP-2 activity and increases tumor growth and metastasis. *Am J Pathol* 151(4): 1105-13.
- Luu Y, Li G 2002. The p53-stabilizing compound CP-31398 enhances ultraviolet-B-induced apoptosis in a human melanoma cell line MMRU. *J Invest Dermatol* 119(5): 1207-9.
- Maniotis AJ, Folberg R, Hess A, Seftor EA, Gardner LM, Pe'er J, Trent JM, Meltzer PS, Hendrix MJ 1999. Vascular channel formation by human melanoma cells in vivo and in vitro: vasculogenic mimicry. *Am J Pathol* 155(3): 739-52.
- Mazurek N, Sun YJ, Price JE, Ramdas L, Schober W, Nangia-Makker P, Byrd JC, Raz A, Bresalier RS 2005. Phosphorylation of galectin-3 contributes to malignant transformation of human epithelial cells via modulation of unique sets of genes. *Cancer Res* 65(23): 10767-75.
- Melnikova VO, Bar-Eli M 2006. Bioimmunotherapy for melanoma using fully human antibodies targeting MCAM/MUC18 and IL-8. *Pigment Cell Res* 19(5): 395-405.
- Miao H, Burnett E, Kinch M, Simon E, Wang B 2000. Activation of EphA2 kinase suppresses integrin function and causes focal-adhesion-kinase dephosphorylation. *Nat Cell Biol* 2(2): 62-9.
- Nakahara S, Oka N, Raz A 2005. On the role of galectin-3 in cancer apoptosis. *Apoptosis* 10(2): 267-75.

- Nangia-Makker P, Sarvis R, Visscher DW, Bailey-Penrod J, Raz A, Sarkar FH 1998. Galectin-3 and L1 retrotransposons in human breast carcinomas. *Breast Cancer Res Treat* 49(2): 171-83.
- Nangia-Makker P, Honjo Y, Sarvis R, Akahani S, Hogan V, Pienta KJ, Raz A 2000. Galectin-3 induces endothelial cell morphogenesis and angiogenesis. *Am J Pathol* 156(3): 899-909.
- Ochieng J, Green B, Evans S, James O, Warfield P 1998. Modulation of the biological functions of galectin-3 by matrix metalloproteinases. *Biochim Biophys Acta* 1379(1): 97-106.
- Ochieng J, Fridman R, Nangia-Makker P, Kleiner DE, Liotta LA, Stetler-Stevenson WG, Raz A 1994. Galectin-3 is a novel substrate for human matrix metalloproteinases-2 and -9. *Biochemistry* 33(47): 14109-14.
- Okada K, Shimura T, Suehiro T, Mochiki E, Kuwano H 2006. Reduced galectin-3 expression is an indicator of unfavorable prognosis in gastric cancer. *Anticancer Res* 26(2B): 1369-76.
- Omholt K, Platz A, Kanter L, Ringborg U, Hansson J 2003. NRAS and BRAF mutations arise early during melanoma pathogenesis and are preserved throughout tumor progression. *Clin Cancer Res* 9(17): 6483-8.
- Oppenheim JJ, Zachariae CO, Mukaida N, Matsushima K 1991. Properties of the novel proinflammatory supergene "intercrine" cytokine family. *Annu Rev Immunol* 9: 617-48.

- Park JW, Voss PG, Grabski S, Wang JL, Patterson RJ 2001. Association of galectin-1 and galectin-3 with Gemin4 in complexes containing the SMN protein. *Nucleic Acids Res* 29(17): 3595-602.
- Patel PS, Varney ML, Dave BJ, Singh RK 2002. Regulation of constitutive and induced NF-kappaB activation in malignant melanoma cells by capsaicin modulates interleukin-8 production and cell proliferation. *J Interferon Cytokine Res* 22(4): 427-35.
- Platt D, Raz A 1992. Modulation of the lung colonization of B16-F1 melanoma cells by citrus pectin. *J Natl Cancer Inst* 84(6): 438-42.
- Pricci F, Leto G, Amadio L, Iacobini C, Romeo G, Cordone S, Gradini R, Barsotti P, Liu FT, Di Mario U and others 2000. Role of galectin-3 as a receptor for advanced glycosylation end products. *Kidney Int Suppl* 77: S31-9.
- Prieto VG, Mourad-Zeidan AA, Melnikova V, Johnson MM, Lopez A, Diwan AH, Lazar AJ, Shen SS, Zhang PS, Reed JA and others 2006. Galectin-3 expression is associated with tumor progression and pattern of sun exposure in melanoma. *Clin Cancer Res* 12(22): 6709-15.
- Ramachandran V, Arumugam T, Hwang RF, Greenson JK, Simeone DM, Logsdon CD 2007. Adrenomedullin is expressed in pancreatic cancer and stimulates cell proliferation and invasion in an autocrine manner via the adrenomedullin receptor, ADMR. *Cancer Res* 67(6): 2666-75.

- Raz A, Bucana C, McLellan W, Fidler IJ 1980. Distribution of membrane anionic sites on B16 melanoma variants with differing lung colonising potential. *Nature* 284(5754): 363-4.
- Raz A, Meromsky L, Zvibel I, Lotan R 1987. Transformation-related changes in the expression of endogenous cell lectins. *Int J Cancer* 39(3): 353-60.
- Risau W 1997. Mechanisms of angiogenesis. *Nature* 386(6626): 671-4.
- Rodolfo M, Daniotti M, Vallacchi V 2004. Genetic progression of metastatic melanoma. *Cancer Lett* 214(2): 133-47.
- Salomon D, Ayalon O, Patel-King R, Hynes RO, Geiger B 1992. Extrajunctional distribution of N-cadherin in cultured human endothelial cells. *J Cell Sci* 102 (Pt 1): 7-17.
- Shalom-Feuerstein R, Cooks T, Raz A, Kloog Y 2005. Galectin-3 regulates a molecular switch from N-Ras to K-Ras usage in human breast carcinoma cells. *Cancer Res* 65(16): 7292-300.
- Shen SS, Zhang PS, Eton O, Prieto VG 2003. Analysis of protein tyrosine kinase expression in melanocytic lesions by tissue array. *J Cutan Pathol* 30(9): 539-47.
- Shimura T, Takenaka Y, Fukumori T, Tsutsumi S, Okada K, Hogan V, Kikuchi A, Kuwano H, Raz A 2005. Implication of galectin-3 in Wnt signaling. *Cancer Res* 65(9): 3535-7.
- Silva-Monteiro E, Reis Lorenzato L, Kenji Nihei O, Junqueira M, Rabinovich GA, Hsu DK, Liu FT, Savino W, Chammas R, Villa-Verde DM 2007. Altered expression

- of galectin-3 induces cortical thymocyte depletion and premature exit of immature thymocytes during *Trypanosoma cruzi* infection. *Am J Pathol* 170(2): 546-56.
- Soengas MS, Capodici P, Polsky D, Mora J, Esteller M, Opitz-Araya X, McCombie R, Herman JG, Gerald WL, Lazebnik YA and others 2001. Inactivation of the apoptosis effector Apaf-1 in malignant melanoma. *Nature* 409(6817): 207-11.
- Spatz A, Giglia-Mari G, Benhamou S, Sarasin A 2001. Association between DNA repair-deficiency and high level of p53 mutations in melanoma of Xeroderma pigmentosum. *Cancer Res* 61(6): 2480-6.
- Stewart SA, Dykxhoorn DM, Palliser D, Mizuno H, Yu EY, An DS, Sabatini DM, Chen IS, Hahn WC, Sharp PA and others 2003. Lentivirus-delivered stable gene silencing by RNAi in primary cells. *Rna* 9(4): 493-501.
- Strieter RM 2001. Chemokines: not just leukocyte chemoattractants in the promotion of cancer. *Nat Immunol* 2(4): 285-6.
- Strongin AY, Marmer BL, Grant GA, Goldberg GI 1993. Plasma membrane-dependent activation of the 72-kDa type IV collagenase is prevented by complex formation with TIMP-2. *J Biol Chem* 268(19): 14033-9.
- Suzuki S, Sano K, Tanihara H 1991. Diversity of the cadherin family: evidence for eight new cadherins in nervous tissue. *Cell Regul* 2(4): 261-70.
- Takenaka Y, Fukumori T, Yoshii T, Oka N, Inohara H, Kim HR, Bresalier RS, Raz A 2004. Nuclear export of phosphorylated galectin-3 regulates its antiapoptotic activity in response to chemotherapeutic drugs. *Mol Cell Biol* 24(10): 4395-406.

- Tan L, Peng H, Osaki M, Choy BK, Auron PE, Sandell LJ, Goldring MB 2003. Egr-1 mediates transcriptional repression of COL2A1 promoter activity by interleukin-1beta. *J Biol Chem* 278(20): 17688-700.
- Tellez C, Bar-Eli M 2003. Role and regulation of the thrombin receptor (PAR-1) in human melanoma. *Oncogene* 22(20): 3130-7.
- Tellez C, McCarty M, Ruiz M, Bar-Eli M 2003. Loss of activator protein-2alpha results in overexpression of protease-activated receptor-1 and correlates with the malignant phenotype of human melanoma. *J Biol Chem* 278(47): 46632-42.
- Thompson SC 1974. The colony forming efficiency of single cells and cell aggregates from a spontaneous mouse mammary tumour using the lung colony assay. *Br J Cancer* 30(4): 332-6.
- van 't Veer LJ, Burgering BM, Versteeg R, Boot AJ, Ruiter DJ, Osanto S, Schrier PI, Bos JL 1989. N-ras mutations in human cutaneous melanoma from sun-exposed body sites. *Mol Cell Biol* 9(7): 3114-6.
- van den Brule FA, Liu FT, Castronovo V 1998. Transglutaminase-mediated oligomerization of galectin-3 modulates human melanoma cell interactions with laminin. *Cell Adhes Commun* 5(6): 425-35.
- van den Brule FA, Buicu C, Sobel ME, Liu FT, Castronovo V 1995. Galectin-3, a laminin binding protein, fails to modulate adhesion of human melanoma cells to laminin. *Neoplasia* 42(5): 215-9.

- Varney ML, Johansson SL, Singh RK 2006. Distinct expression of CXCL8 and its receptors CXCR1 and CXCR2 and their association with vessel density and aggressiveness in malignant melanoma. *Am J Clin Pathol* 125(2): 209-16.
- Vartanian RK, Weidner N 1994. Correlation of intratumoral endothelial cell proliferation with microvessel density (tumor angiogenesis) and tumor cell proliferation in breast carcinoma. *Am J Pathol* 144(6): 1188-94.
- Veierod MB, Weiderpass E, Thorn M, Hansson J, Lund E, Armstrong B, Adami HO 2003. A prospective study of pigmentation, sun exposure, and risk of cutaneous malignant melanoma in women. *J Natl Cancer Inst* 95(20): 1530-8.
- Vereecken P, Heenen M 2006. Serum galectin-3 in advanced melanoma patients: a hypothesis on a possible role in melanoma progression and inflammation. *J Int Med Res* 34(1): 119-20.
- Vereecken P, Debray C, Petein M, Awada A, Lalmand MC, Laporte M, Van Den Heule B, Verhest A, Pochet R, Heenen M 2005. Expression of galectin-3 in primary and metastatic melanoma: immunohistochemical studies on human lesions and nude mice xenograft tumors. *Arch Dermatol Res* 296(8): 353-8.
- Villa-Verde DM, Silva-Monteiro E, Jasiulionis MG, Farias-De-Oliveira DA, Brentani RR, Savino W, Chammas R 2002. Galectin-3 modulates carbohydrate-dependent thymocyte interactions with the thymic microenvironment. *Eur J Immunol* 32(5): 1434-44.

- Vittet D, Buchou T, Schweitzer A, Dejana E, Huber P 1997. Targeted null-mutation in the vascular endothelial-cadherin gene impairs the organization of vascular-like structures in embryoid bodies. *Proc Natl Acad Sci U S A* 94(12): 6273-8.
- Vleminckx K, Kemler R 1999. Cadherins and tissue formation: integrating adhesion and signaling. *Bioessays* 21(3): 211-20.
- Vyakarnam A, Lenneman AJ, Lakkides KM, Patterson RJ, Wang JL 1998. A comparative nuclear localization study of galectin-1 with other splicing components. *Exp Cell Res* 242(2): 419-28.
- Wang L, Inohara H, Pienta KJ, Raz A 1995. Galectin-3 is a nuclear matrix protein which binds RNA. *Biochem Biophys Res Commun* 217(1): 292-303.
- Warfield PR, Makker PN, Raz A, Ochieng J 1997. Adhesion of human breast carcinoma to extracellular matrix proteins is modulated by galectin-3. *Invasion Metastasis* 17(2): 101-12.
- Weinberger PM, Adam BL, Gourin CG, Moretz WH, 3rd, Bollag RJ, Wang BY, Liu Z, Lee JR, Terris DJ 2007. Association of nuclear, cytoplasmic expression of galectin-3 with beta-catenin/Wnt-pathway activation in thyroid carcinoma. *Arch Otolaryngol Head Neck Surg* 133(5): 503-10.
- Woo HJ, Shaw LM, Messier JM, Mercurio AM 1990. The major non-integrin laminin binding protein of macrophages is identical to carbohydrate binding protein 35 (Mac-2). *J Biol Chem* 265(13): 7097-9.
- Wu H, Goel V, Haluska FG 2003. PTEN signaling pathways in melanoma. *Oncogene* 22(20): 3113-22.

- Yamaoka A, Kuwabara I, Frigeri LG, Liu FT 1995. A human lectin, galectin-3 (epsilon bp/Mac-2), stimulates superoxide production by neutrophils. *J Immunol* 154(7): 3479-87.
- Zhang H 2006. p53 plays a central role in UVA and UVB induced cell damage and apoptosis in melanoma cells. *Cancer Lett* 244(2): 229-38.
- Zhou Y, Fisher SJ, Janatpour M, Genbacev O, Dejana E, Wheelock M, Damsky CH 1997. Human cytotrophoblasts adopt a vascular phenotype as they differentiate. A strategy for successful endovascular invasion? *J Clin Invest* 99(9): 2139-51.
- Zhu Z, Sanchez-Sweatman O, Huang X, Wiltrout R, Khokha R, Zhao Q, Gorelik E 2001. Anoikis and metastatic potential of cloudman S91 melanoma cells. *Cancer Res* 61(4): 1707-16.
- Zubieta MR, Furman D, Barrio M, Bravo AI, Domenichini E, Mordoh J 2006. Galectin-3 expression correlates with apoptosis of tumor-associated lymphocytes in human melanoma biopsies. *Am J Pathol* 168(5): 1666-75.
- Zucker S, Cao J, Chen WT 2000. Critical appraisal of the use of matrix metalloproteinase inhibitors in cancer treatment. *Oncogene* 19(56): 6642-50.

Lebenslauf

Persönliche Daten:

Name: Alexandra Anastasia Mourad-Zeidan

Anschrift: P.O. Box 20682, Houston, Texas 77225, USA/
Winzererstr. 50 , 80797 Muenchen, Deutschland

Telefon: 001-832-205-6001 (USA), 089-1292241, (DE)

Geburtsdatum: 12.19.1976

Geburtsort: München, Deutschland

Eltern: Josef S. Mourad, ehemaliger Professor für Physik an
der Technischen Universität München,
Afaf C. Mourad, geb. Deen, Juristin, Diplomatin

Staatsangehörigkeit: Deutsch

Familienstand: geschieden

Schulbildung:

1984-1998: Grundschule an der Dachauerstrasse, München

1998-1992: Maximiliansgymnasium, München

1992-1998: Oscar-von- Millergymnasium, München

Abschluß: Abitur

Studium:

1998-2002: Studium der Biologie an der Ludwig-Maximilians
Universität München

Abschluß: Diplom

11/2000-08/2002: Diplomarbeit an der Ludwig-Maximilians
Universität München, Abteilung

Autoimmunbiologie unter der Leitung von Dr. Gerhild Wildner,

Thema: „Die Untersuchung von pathologischen und/oder regulatorischen T-Zell Epitopen im Model der experimentellen autoimmunen Uveitis (EAU)“

seit 05/2003:

Doktorandin an der Medizinischen Fakultät der Ludwig-Maximilians Universität München in der Abteilung der Immunologie unter der Leitung von Prof. Dr. Judith Johnson, in Zusammenarbeit mit Dr. Menashe Bar-Eli, in der Abteilung „Cancer Biology“ an der University of Texas, MD Anderson Cancer Center, Houston, Texas, USA

Thema: „Role of Galectin-3 in Melanoma progression“

wissenschaftliche Tätigkeit:

01/2000-03/2000:

Praktikum im Rot-Kreuz Krankenhaus, München in der Abteilung der Inneren Medizin unter der Leitung von Prof. Dr. Neuhann

05/2001-04/2002:

Tätigkeit als technische studierte Hilfskraft in der Abteilung der Autoimmunbiologie der Augenklinik der Ludwig-Maximilians Universität München, unter der Leitung von Dr. Gerhild Wildner

praktische Tätigkeit:

05/1998-03/2002

Tutor der lateinischen Sprache in der Schülerhilfe, München

09/2003-04/2006

Lehrerin der deutschen Sprache in der Deutschen Samstagschule in Houston, Texas, USA

Fremdsprachen:

Englisch, Latein, Französisch, Arabisch und Italienisch

Veröffentlichungen:

1. **Mourad-Zeidan AA**, Melnikova VO, Wang H, Raz A, Bar-Eli M. Expression Profiling of Galectin-3-Depleted Melanoma Cells Reveals its Major Role in Melanoma Cell Plasticity and Vasculogenic Mimicry. *AM J Pathol.* 2008 Nov 6:173:1838-1851

2. Melnikova VO, **Mourad-Zeidan AA**, Lev DC, Bar-Eli M. Platelet-activating factor mediates MMP-2 expression and activation via phosphorylation of cAMP-response element-binding protein and contributes to melanoma metastasis. *J Biol Chem*. 2006 Feb 3; 281(5):2911-22.
3. Prieto VG, **Mourad-Zeidan AA**, Melnikova V, Johnson MM, Lopez A, Diwan AH, Lazar AJ, Shen SS, Zhang PS, Reed JA, Gershenwald JE, Raz A, Bar-Eli M. Galectin-3 expression is associated with tumor progression and pattern of sun exposure in melanoma. *Clin Cancer Res*. 2006 Nov 15;12(22):6709-15
4. Schwartz B, Melnikova VO, Tellez C, **Mourad-Zeidan A**, Blehm K, Zhao YJ, McCarty M, Adam L, Bar-Eli M. Loss of AP-2alpha results in deregulation of E-cadherin and MMP-9 and an increase in tumorigenicity of colon cancer cells in vivo. *Oncogene*. 2007 Jun 14; 26(28):4049-58.
5. **Mourad-Zeidan AA**, Prieto VG, Melnikova VO, Wang H, Raz A and Bar-Eli M. Identification of endothelial and mesenchymal associated markers in melanoma cells following Galectin-3 silencing: Relevance to tumor growth and metastasis (in Vorbereitung).

Poster:

1. **Mourad-Zeidan AA**, Prieto VG, Melnikova VO, Wang H, Raz A and Bar-Eli M. Identification of endothelial and mesenchymal associated markers in melanoma cells following Galectin-3 silencing: Relevance to tumor growth and metastasis. *98th Annual meeting of American Association for Cancer Research*, April 14-18, 2007 Los Angeles, CA
2. **Mourad-Zeidan AA**, Melnikova VO, Wang H, Raz A and Bar-Eli M. Expression Profiling of Gal-3-depleted melanoma cells reveals its major role in melanoma cell plasticity and vasculogenic mimicry *99th Annual meeting of American Association for Cancer Research*, April 12-16, 2008 San Diego, CA

12. 15. 2008, Alexandra Anastasia Mourad-Zeidan

Acknowledgement

It is with sincerest gratitude that I acknowledge the contribution of the following people to this body of work, my education, and my research experience:

I would like to express my utmost appreciation to my PhD advisor, Prof. Dr. Judith Johnson, for giving me the opportunity to work with the caliber scientists at the Immunology Department of Ludwig-Maximilians University, Munich, Germany. Prof. Dr. Johnson enabled collaboration with the University of Texas MD Anderson Cancer Center and encouraged my entry into the laboratory of Dr. Menashe Bar-Eli, my PhD supervisor in the Department of Cancer Biology.

I thank especially Dr. Bar-Eli for the guidance he has provided throughout my entire education, which has been instrumental in the compilation of this dissertation.

I am very grateful for the opportunities both my supervisors have given me; opportunities that undoubtedly have provided me with a strong scientific foundation onto which I can build my career.

I am grateful to Dr. Vladislava Melnikova and Dr. Hua Wang for their support and encouragement throughout my training. Finally, I am very grateful to have had the opportunity to work with excellent colleagues at MD Anderson, particularly Laura K Nolden and Mollianne McGahren Murray.

My heartfelt appreciation is extended to all the members and students of the Immunology Department in Munich, Germany and of the MDACC Cancer Biology Department Houston, Texas.